Introduction to Electrodynamics for Microwave Linear Accelerators

David H. Whittum

Stanford Linear Accelerator Center, Stanford University,
Stanford, California 94309

This collection of notes and exercises is intended as a workbook to introduce the principles of microwave linear accelerators, starting with the underlying foundation in electrodynamics. We review Maxwell's equations, the Lorentz force law, and the behavior of fields near a conducting boundary. We go on to develop the principles of microwave electronics, including waveguide modes, circuit equivalence, shunt admittance of an iris, and voltage standing-wave ratio. We construct an elementary example of a waveguide coupled to a cavity, and examine its behavior during transient filling of the cavity, and in steady-state. We go on to examine a periodic line. We then turn to examine the problem of acceleration in detail, studying first the properties of a single cavity-waveguide-beam system and developing the notions of wall Q, external Q, [R/Q], shunt impedance, and transformer ratio. We examine the behavior of such a system on and off resonance, on the bench, and under conditions of transient and steady-state beam-loading. This work provides the foundation for the commonly employed circuit equivalents and the basic scalings for such systems. Following this we examine the coupling of two cavities, powered by a single feed, and go on to consider structures constructed from multiple coupled cavities. The basic scalings for constant impedance and constant gradient travelling-wave structures are derived, including features of steady-state beam-loading, and the coupled-circuit model. Effects of uniform and random detuning are derived. These notes conclude with a brief outline of some problems of current interest in accelerator research.

Introduction

The *accelerator* is the instrument on which all intellectual life in high-energy physics depends. Without accelerators, the great physicists of our time and decades past would have been reduced to inspection of cosmic ray dribble, atomic spectra corrections, and mathematics of uncertain pedigree. Happily, there were physicists who loved to tinker, and from their sketches and machine shops sprang the *klystron*,[1] and in the fog of their musings appeared the microwave *linear accelerator*,[2] finally cut in copper and called the *Mark III*.[3] Today, when Physics has dwindled in the popular imagination, and 80,000 patients are treated each day

by S-Band linacs, it is easy to forget that there is a field called High-Energy Physics, that Man's ultimate reach into the sub-atomic world has yet to be decided, that it depends on invention, and possibly your invention.

Historically, the kinds of inventions that have helped can be seen in the story of the Two-Mile Accelerator,[4] the evolution of the 25-MW "XK-5" klystron to the 60-MW "5045" model,[5] the invention of "SLED" pulse compression,[6] and the transformation of the 20-GeV Two-Mile Linac to the 50-GeV Stanford Linear Collider.[7] To reach still higher energies, the *collider scalings*[8] indicate that shorter wavelength is required, and this observation has resulted in ten years of research and development, culminating in the 50-MW "X-Band" klystron, "SLED-II" pulse compression, and new "damped detuned structures" designed to pass beams of extraordinary charge and current.[9] It is now thought possible that a 1-TeV collider could be engineered based on these and other inventions.Yet to reach much higher energies, 5 TeV and beyond, the collider scalings indicate that the linac would be of enormous size, probably larger than society would care to support. Beyond 5 TeV there is no technology adequate to the task, and inventions are required.

These notes are intended as a primer for those who are new to linacs and are taken with the idea of exploration into the farthest realms of the universe. If the desire is to invent the machine for tomorrow, let us review here what has shaped the machines of today.

In its simplest form, the problem is to increase the energy of a particle, and this requires applying a force. There are a handful of known Forces of the Universe, and only one of them appears to be of much use for acceleration, and that is the electromagnetic interaction. Electromagnetic acceleration in empty space, we will find, is rather ineffective, and so material boundaries are favored to shape the electromagnetic fields. Materials are lossy and so power, needed to establish accelerating fields, is dissipated. Power dissipation in the end appears to be the ultimate limit on terrestrial accelerators. But what this limit is no one knows.

These notes provide an elementary introduction to the theory of electromagnetic accelerators. Appendix A summarizes the math we will be using, and Appendix B, the low-frequency electronics concepts often relied on for circuit analogies. In Sec. 1, electrodynamics is reviewed, and in Sec. 2 electrodynamics with material boundaries---microwave electronics---is developed. In Sec. 3, driven on by the logic of Sections 1 and 2, we construct the simplest of accelerators, consisting of a single cavity powered via waveguide, and perturbed by a beam. We go on to couple such cavities together to fashion standing-wave linacs. Appendix C is included to provide more detail on the five formal calculations underpinning this work. In Sec. 4 the extension to travelling-wave linacs is developed.

We omit quite a lot that one needs to construct and operate an accelerator: techniques for fabrication and assembly, the klystrons, magnets, beam dynamics, vacuum, radiation shielding, personnel protection, and operational know-how. However, all one really needs in this field is a new idea that works; let us consider then what works.

1. Electrodynamics

To accelerate particles, for best results, the particles should be charged, and electric fields should be applied. In fields, energy is stored, and in media, energy is dissipated. These features of accelerator mechanics we review from the beginning.

1.1 Lorentz Force Law

The force $\vec{F}$ acting on a charge q with velocity $\vec{V}$ takes the form

$$\vec{F} = q\left(\vec{E} + \vec{V} \times \vec{B}\right) \tag{1.1}$$

where $\vec{E}$ is the electric field with units of force per unit charge, newtons per coulomb = volts per meter. The quantity $\vec{B}$ is the magnetic flux density or magnetic induction, with units of newtons per ampere-meter = tesla = weber/meter^2. Eq. (1.1) describes the forces acting on charged particles. Implicitly, it *defines* what these fields are and it abstracts them from the sources that produced them.

With only the Lorentz force law we can determine how charges respond to fields, but we are left wondering how the fields themselves are determined. One may take some comfort in the observation that this problem is easily solved *in principle* if one knows the fields arising from a single charged particle in motion, for then the fields would be simply a superposition of each individual particle's fields. In practice, we may have to account for enormous numbers of such charges---all the charges composing the conductors and dielectrics in the system. A proper accounting for the evolution of the motion of an N-particle system by this method must then track the microscopic motions of the constituents of the media involved, and the N^2 interactions taking place. In practice, with $\ln N \approx 50$, this approach is quite inefficient. Happily, one can make do by tracking the fields directly, and the N interactions with the field. In fact, for many media, one needn't even track the response of the medium directly, and one may confine attention only to charges external to the medium. Oftentimes one may consider just one such external charge, and reason by superposition to obtain a complete description of the system's evolution. This approach relies however on an understanding of *media*, summarized in the notions of *permittivity* and *permeability*.

Exercise 1.1 A charged particle has a kinetic energy of 50 keV. You wish to apply as large a force as possible. You may choose either an electric field of 500 kV/m or a magnetic induction of 0.1 T. Which should you choose (a) for an electron, (b) for a proton? In each case, compute also the gravitational force.

1.2 Permittivity and Permeability

In considering ensembles of charge, it is helpful to distinguish between "free" charge or externally controllable charge, and "bound" charge, charge that is a constituent of a medium in the system. An example would be a capacitor consisting of two plates, filled with oil. The circuit attached to the plates is controllable; the

electrical behavior of the oil is not. We are free to place charge on the plates if we don't mind doing some work. However, the response of the oil to the applied field is not ours to specify. Specifically, the atomic electrons in the oil will be perturbed by any applied field, and their motions will be distorted, resulting in a dipole moment proportional to the applied field. This dipole moment contributes to the electric field in the gap.

To account for the response of media, we have two choices. We may attempt to calculate the response of the medium from first principles or we may consult the known response of the medium as determined from experiment. To take the latter, simpler approach however, we first must know the language folks use to describe the response of media. Let us introduce the notion of electric displacement and magnetic field.

In vacuum, the electric displacement is $\vec{D} = \varepsilon_0 \vec{E}$, and the magnetic field is $\vec{H} = \vec{B}/\mu_0$, where $\varepsilon_0 = 8.85 \times 10^{-12}$ farad/m and $\mu_0 = 4\pi \times 10^{-7}$ henry/m. As is, this is just a change of units, not cause for great excitement. In media, however, the relation takes the form

$$\vec{D} = \varepsilon_0 \vec{E} + \vec{P}, \tag{1.2}$$

$$\vec{H} = \vec{B}/\mu_0 - \vec{M} \tag{1.3}$$

where $\vec{P}$ is the electric dipole moment density of the medium and $\vec{M}$ is the magnetic dipole moment density. These moment densities are the result of polarization or magnetization of the medium by the very fields we are trying in the end to determine, $\vec{E}$ and $\vec{B}$. In the frequency domain, for a linear medium, they may be expressed as

$$\tilde{P} = \chi_e \varepsilon_0 \tilde{E}, \tag{1.4}$$

$$\tilde{M} = \chi_m \tilde{H}, \tag{1.5}$$

where χ_e and χ_m are the electric and magnetic susceptibilities of the medium. In terms of fields, these expressions take the form $\tilde{D} = \varepsilon \tilde{E}$, and $\tilde{B} = \mu \tilde{H}$, where $\varepsilon = \varepsilon_0 (1 + \chi_e)$ is the electrical permittivity, and $\mu = \mu_0 (1 + \chi_m)$ is the magnetic permeability. Thus ε and μ are frequency-domain quantities, and, in general, they are tensors. Note particularly that $\vec{H}$ and $\vec{D}$ depend on how one chooses to distinguish an external circuit. One could guess this by noticing that $\vec{H}$ and $\vec{D}$ do not appear in the Lorentz force law, $\vec{E}$ and $\vec{B}$ do.

1.3 Maxwell's Equations

Maxwell's equations are four; we review each in turn. The first and the oldest is *Gauss's law* stating that at the end of a line of electric force one will find charge. In differential form,

$$\vec{\nabla} \bullet \vec{D} = \rho, \tag{1.6}$$

with ρ the density of externally imposed charge, *i.e.*, whatever charge is not accounted for in the electrical permittivity ε that has been used to define $\vec{D}$. Like each of Maxwell's equations, this can also be stated in integral form,

$$\oint_{\partial V} \vec{D} \bullet d\vec{S} = \int_V \rho \, dV,$$

so that the flux of $\vec{D}$ through a surface ∂V bounding a volume V is proportional to the charge enclosed. It is often useful to have the corollary boundary condition at the interface between two media, on the normal component of electric displacement. This can be determined by integrating Eq. (1.6) over the small volume depicted in Fig. 1.1 to relate the discontinuity in electric displacement across an interface to the surface charge density

$$\left(\vec{D}_2 - \vec{D}_1\right) \bullet \hat{n} = \Sigma. \tag{1.6a}$$

Evidently the units for $\vec{D}$ are the same as surface charge density, coulomb/meter^2.

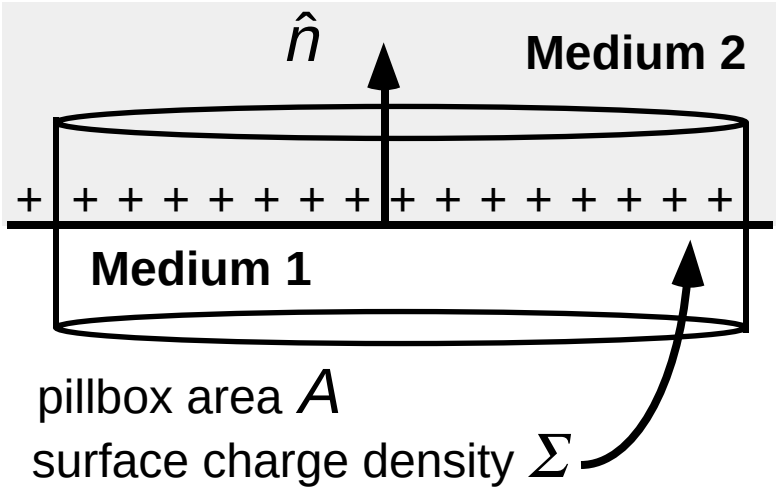

FIGURE 1.1. Sketch for application of Gauss's law to a thin pillbox at the interface between two media.

Next we have *Ampere's law*

$$\vec{\nabla} \times \vec{H} = \vec{J} + \frac{\partial \vec{D}}{\partial t}, \tag{1.7}$$

or, in integral form,

$$\underbrace{\oint_{\partial S} \vec{H} \bullet d\vec{l} = \int_{S} \vec{J} \bullet d\vec{S}}_{pre-Maxwell} + \underbrace{\int_{S} \frac{\partial \vec{D}}{\partial t} \bullet d\vec{S}}_{displacement\ current},$$

so that the circulation of magnetic field strength around a closed path ∂S bounding a surface S is proportional to the current enclosed. (Note that care is required in applying integral forms to moving surfaces.) The displacement current term implies that the magnetic induction is equally happy to circulate around a transient bundle of electric field lines.

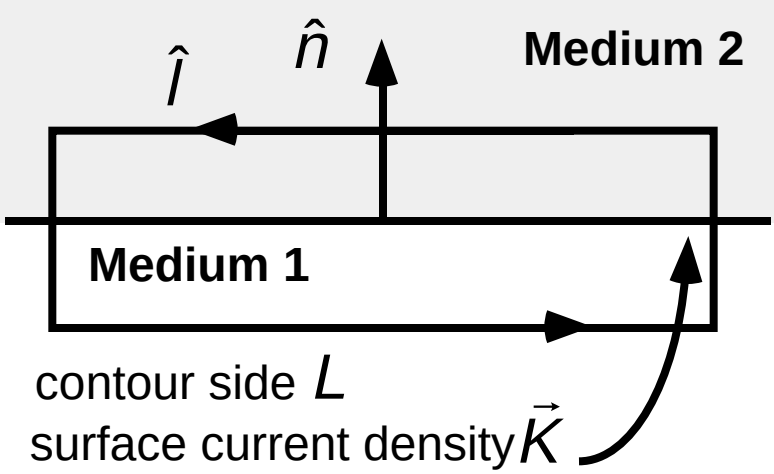

FIGURE 1.2. Sketch for application of Ampere's law to a thin loop at the interface between two media.

The boundary condition accompanying Ampere's law is illustrated in Fig. 1.2 for a thin loop placed across the interface between two media. For this geometry and in the limit that the loop width goes to zero, Ampere's law takes the form

$$\left(\vec{H}_2 - \vec{H}_1\right) \bullet \hat{l} = \vec{K} \times \hat{n} \bullet \hat{l}, \tag{1.7a}$$

and states that a discontinuity in tangential magnetic field arises if any surface current $\vec{K}$ is present. Evidently the units for $\vec{H}$ are those of surface current, ampere/meter.

Gauss's law and Ampere's law together describe the response of the fields to media; but electric fields don't depend solely on charge. According to *Faraday's law*,

$$\vec{\nabla} \times \vec{E} = -\frac{\partial \vec{B}}{\partial t}, \tag{1.8}$$

circumferential electric field lines are induced around any magnetic flux varying in time. In integral form,

$$\oint_{\partial S} \vec{E} \bullet d\vec{l} = -\int_S \frac{\partial \vec{B}}{\partial t} \bullet d\vec{S}.$$

Thus a voltage drop will develop around a closed path ∂S bounding a surface S, proportional to the time-rate of change of the magnetic flux enclosed by the path. Applying Faraday's law to the geometry of Fig. 1.2, one finds,

$$\hat{n} \times \left(\vec{E}_2 - \vec{E}_1 \right) = 0, \tag{1.8a}$$

i.e., the tangential component of the electric field is continuous at the interface between two media.

The last of our four equations states that there is no magnetic charge,

$$\nabla \bullet \vec{B} = 0, \tag{1.9}$$

or in integral form, the flux of $\vec{B}$ through a closed surface ∂V vanishes,

$$\int_{\partial V} \vec{B} \bullet d\vec{S} = 0.$$

Thus one will never find $\vec{B}$ field lines terminating anywhere; they form closed loops. Applying this condition in the geometry of Fig. 1.1 yields the boundary condition on normal magnetic induction,

$$\left(\vec{B}_2 - \vec{B}_1 \right) \bullet \hat{n} = 0, \tag{1.9a}$$

and corresponds to the absence of any magnetic charge layer.

1.4 Charge Conservation

Naturally, to get these equations named after him, Maxwell had to contribute more than mere mathematical trickery; he contributed in particular the displacement current. The first consequence of this term is the relation between current and charge. Charge conservation as we now know it states that the time rate of change of charge enclosed in a volume is equal to the flux of charge out of the volume,

$$\frac{\partial}{\partial t} \int_V \rho \, dV = -\oint_{\partial V} \vec{J} \bullet d\vec{S}$$

or, in differential form,

$$\frac{\partial \rho}{\partial t} + \nabla \bullet \vec{J} = 0. \tag{1.10}$$

Ampere's law without displacement current implies

$$\frac{\partial \rho}{\partial t} = -\nabla \bullet \vec{J} = -\nabla \bullet \nabla \times \vec{H} = 0,$$

i.e., that charge density is constant in time. This is not a bad approximation in conductors, or a dense plasma; it is exact for electrostatics, magnetostatics. However, considered as a law of nature, Ampere's law was, before Maxwell, inconsistent with conservation of charge. One could describe the situation somewhat differently by saying that it hadn't been established that the current determining $\vec{B}$ was in fact the flux of charge determining $\vec{E}$. In this view, Maxwell unified $\vec{E}$ and $\vec{B}$, proposing that they were in fact two aspects of the same phenomenon, electromagnetism. We will see shortly that displacement current permits the fields to propagate on their own, in vacuum, without any local charge to support the field lines. Charge conservation, a "symmetry" of nature, implied the existence of a field with an identity of its own, that could propagate freely in vacuum, and, as we will see, carry energy and momentum with it.

To appreciate Maxwell's contribution one can compare electrodynamics *before* Maxwell, and *after*. In the centuries prior, it was gradually understood that charges repel or attract, a property shared by current-carrying wires. Time-varying currents can induce currents in their surroundings. Action at a distance could be understood via lines of force. However, the unified equations Maxwell set down contained in them features that were to revolutionize our understanding of physics: **(1)** light is an electromagnetic phenomenon, **(2)** nature is not Galilean, **(3)** thermodynamics applied to electromagnetic fields gives rise to divergences (*i.e.*, nonsense), **(4)** matter must be unstable, **(5)** Newtonian gravitation is inconsistent with electrodynamics. In short, two solid predictions, two paradoxes, and one conundrum, all with one very reasonable looking term! The resolution of the second item was to be found in special relativity. The resolution of the third item commenced with the introduction of Planck's constant, and the notion that electromagnetic energy comes in discrete packets called *photons*. This development and the fourth item eventually precipitated the development of *quantum mechanics*. The fifth item led Einstein to develop his theory of *general relativity*.

1.5 Accelerators According to Maxwell

One can immediately discern in Maxwell's equations the three principle methods of acceleration. The first employed by Man was electrostatic acceleration. This is the limit $\partial / \partial t \approx 0$, so that $\vec{\nabla} \times \vec{E} = 0$, implying that the electric field may be represented as the gradient of an electrostatic potential, $\vec{E} = -\nabla \varphi$. In this case, Maxwell's equations reduce to Gauss's law, which in turn may be expressed as Poisson's equation $\nabla^2 \varphi = -\rho / \varepsilon_0$. If the beam is of sufficiently low charge, this is approximately just Laplace's equation, $\nabla^2 \varphi = 0$, and fields are determined by electrode shapes alone. Otherwise, one must solve self-consistently for the particle motion, and the fields together, a nonlinear problem. Probably the most common accelerator design activities today are the solution of this problem for an electron source (gun design), and the closely related problem of solving for the magnetostatic fields due to a configuration of magnetic materials and current-carrying coils (magnet design).

Somewhat less frequently one encounters a problem which requires the induction effect embodied in Faraday's law, but for which the displacement current

is small. Such *magneto-inductive* effects are the operating principle for the *betatron* and *induction linacs*. In such problems, a magnetic field is driven to a good approximation, exclusively by external currents. With the help of magnetic materials ($\mu >> \mu_0$) the magnetic induction is shaped, and the corresponding magnetic flux drives an electric field.

The foregoing acceleration techniques require media of one kind or another to be exposed to large persistent fields, and for this reason are limited in the net accelerating voltage they can impart. Somewhat more robust, though still subject to material damage, is the fully electromagnetic (*microwave*) accelerator. Here all terms in Maxwell's equations are important; however, unless one is modelling the microwave power source, one can frequently do without the source terms, in the first approximation. This is because the fully electromagnetic solutions of Maxwell's equations are capable of propagating on their own to their place of business, being at most guided, shaped, and perhaps slowed down by material boundaries. When intense beams are present (and they often are) one must consider them as well, in the final accounting.

In the electromagnetic accelerator, the logical algorithm for time-advance of the fields is based on Faraday's law and Ampere's law,

$$\frac{\partial \vec{B}}{\partial t} = -\vec{\nabla} \times \vec{E}, \quad \frac{\partial \vec{D}}{\partial t} = \vec{\nabla} \times \vec{H} - \vec{J},$$

while the remaining two equations are simply constraints that magnetic induction be solenoidal, and Gauss's law. If these constraints are satisfied by the initial state of the system, they will be satisifed by the evolved state. In practice the discretization of space (the use of a "grid") in a numerical simulation introduces a numerical error in the electric displacement. This error corresponds to an erroneous charge that the numerical fields will see on the next time step, and respond to. As a result, errors can quickly become compounded. To avoid this, one enforces Gauss's law at each time-step by solution for an error potential and correction of the electric displacement obtained from Ampere's law.

1.6 Scalar and Vector Potentials

In all these cases there is an instructive alternative to solving for the fields directly. Instead we may express them in terms of potentials, and solve for the potentials. Since magnetic induction is solenoidal, we may express it as the curl of a vector

$$\vec{B} = \vec{\nabla} \times \vec{A}, \tag{1.11}$$

so that $\vec{\nabla} \bullet \vec{B} = \vec{\nabla} \bullet \vec{\nabla} \times \vec{A} = 0$. $\vec{A}$ is referred to as the *vector potential*. From Faraday's law then,

$$\vec{\nabla} \times \vec{E} + \frac{\partial \vec{B}}{\partial t} = \vec{\nabla} \times \left\{ \vec{E} + \frac{\partial \vec{A}}{\partial t} \right\} = 0,$$

and this suggests that we express $\vec{E}$ as

$$\vec{E} = -\frac{\partial \vec{A}}{\partial t} - \vec{\nabla}\varphi, \tag{1.12}$$

for some function φ, referred to as the *scalar potential*. Note that the fields are invariant *(gauge invariance)* under a change of potentials,

$$\vec{A} \to \vec{A} - \vec{\nabla}\psi, \quad \varphi \to \varphi + \frac{\partial \psi}{\partial t}, \tag{1.13}$$

where ψ is any well-behaved function. Thus $\vec{A}$ and φ are not yet uniquely defined. Let us determine what equations the potentials must satisfy. Ampere's law implies

$$\vec{\nabla} \times \mu\vec{H} = \vec{\nabla} \times \left(\vec{\nabla} \times \vec{A}\right) = \vec{\nabla}\left(\nabla \bullet \vec{A}\right) - \nabla^2 \vec{A}$$

$$= \mu\vec{\nabla} \times \vec{H} = \mu \frac{\partial \varepsilon \vec{E}}{\partial t} + \mu\vec{J} = \mu\varepsilon \frac{\partial}{\partial t}\left(-\frac{\partial \vec{A}}{\partial t} - \vec{\nabla}\varphi\right) + \mu\vec{J}$$

or

$$\nabla^2 \vec{A} - \mu\varepsilon \frac{\partial^2 \vec{A}}{\partial t^2} = -\mu\vec{J} + \vec{\nabla}\left(\nabla \bullet \vec{A} + \mu\varepsilon \frac{\partial \varphi}{\partial t}\right).$$

Gauss's law implies

$$\vec{\nabla} \bullet \vec{D} = \vec{\nabla} \bullet \varepsilon\vec{E} = \varepsilon\vec{\nabla} \bullet \left(-\frac{\partial \vec{A}}{\partial t} - \vec{\nabla}\varphi\right) = \rho,$$

or

$$\nabla^2 \varphi - \mu\varepsilon \frac{\partial^2 \varphi}{\partial t^2} = -\frac{1}{\varepsilon}\rho - \frac{\partial}{\partial t}\left(\nabla \bullet \vec{A} + \mu\varepsilon \frac{\partial \varphi}{\partial t}\right).$$

Since there are infinitely many gauge choices, one is free to pick one's own unique, personal gauge. In the meantime, two are quite popular. The *Lorentz gauge* is defined by

$$\nabla \bullet \vec{A} + \mu\varepsilon \frac{\partial \varphi}{\partial t} = 0. \qquad \textit{(Lorentz gauge condition)} \tag{1.14}$$

In the Lorentz gauge, Maxwell's equations reduce to wave equations for each component of the potential,

$$\nabla^2 \vec{A} - \mu\varepsilon \frac{\partial^2 \vec{A}}{\partial t^2} = -\mu\vec{J}, \qquad \textit{(Lorentz gauge)} \tag{1.15}$$

$$\nabla^2 \varphi - \mu\varepsilon \frac{\partial^2 \varphi}{\partial t^2} = -\rho/\varepsilon. \qquad \textit{(Lorentz gauge)} \tag{1.16}$$

Evidently the characteristic speed of propagation in the medium is $V = (\mu\varepsilon)^{-1/2}$.

However, the Lorentz gauge is by no means a unanimous choice, and often

one encounters the Coulomb gauge,

$$\vec{\nabla} \bullet \vec{A} = 0, \qquad \textit{(Coulomb gauge condition)}$$

in which Maxwell's equations take the form

$$\nabla^2 \vec{A} - \mu\varepsilon \frac{\partial^2 \vec{A}}{\partial t^2} = -\mu \vec{J} + \mu\varepsilon \vec{\nabla} \frac{\partial \varphi}{\partial t}, \qquad \textit{(Coulomb gauge)}$$

$$\nabla^2 \varphi = -\rho / \varepsilon. \qquad \textit{(Coulomb gauge)}$$

We won't try here to promote one gauge over the other, as the question of gauge is really a personal decision each researcher must make on his own.

1.7 Energy Conservation

Usually the best-sounding ideas for accelerators fail one of two tests: (a) they require excessive amounts of unobtainium or (b) they don't conserve energy. Let's consider (b). The rate of work per unit volume done by the fields is just $\vec{J} \bullet \vec{E}$, and this may be evaluated by substitution from Ampere's law,

$$-\vec{J} \bullet \vec{E} = \left\{ \frac{\partial \vec{D}}{\partial t} - \vec{\nabla} \times \vec{H} \right\} \bullet \vec{E} = \frac{\partial \vec{D}}{\partial t} \bullet \vec{E} \underbrace{- \vec{\nabla} \times \vec{H} \bullet \vec{E} + \vec{\nabla} \times \vec{E} \bullet \vec{H}}_{\vec{\nabla} \bullet \left(\vec{E} \times \vec{H} \right)} - \vec{\nabla} \times \vec{E} \bullet \vec{H}$$

$$= \frac{\partial \vec{D}}{\partial t} \bullet \vec{E} + \vec{\nabla} \bullet \left(\vec{E} \times \vec{H} \right) + \frac{\partial \vec{B}}{\partial t} \bullet \vec{H} = \frac{\partial \vec{D}}{\partial t} \bullet \vec{E} + \frac{\partial \vec{B}}{\partial t} \bullet \vec{H} + \vec{\nabla} \bullet \vec{S}$$

where in the last line we introduce the Poynting flux,

$$\vec{S} = \vec{E} \times \vec{H}, \tag{1.17}$$

with units of watts/meter^2. In vacuum we may write this as

$$-\vec{J} \bullet \vec{E} = \vec{\nabla} \bullet \vec{S} + \frac{\partial u}{\partial t}, \tag{1.18}$$

where the quantity

$$u = \frac{1}{2} \left(\vec{E} \bullet \vec{D} + \vec{B} \bullet \vec{H} \right), \tag{1.19}$$

may be interpreted as the density of energy stored in the fields. This is a statement of energy conservation. Work done on charges in some volume is balanced by a loss of the energy stored in the fields in that volume, and/or a flux of energy into the volume through the surface. Eq. (1.19) is usually sufficient for the most commonly encountered problems.

Exercise 1.2 Consider a geometry consisting of two wide parallel plates of area A, separated by a gap of length d, filled with dielectric of permittivity ε. Suppose a charge Q

has been placed on one plate. Compute the steady-state electric field and the voltage V between the plates. Show that the capacitance of the circuit $C=Q/V$ is given by $C=\varepsilon A/d$, and that the energy stored is $W_e=CV^2/2$.

Exercise 1.3 Consider a long helical coil of radius a, occupying a length d, with n turns per meter, carrying current I, filled with material of magnetic permeability μ. Compute the magnetic induction inside the coil, show that the stored energy is $W_m=LI^2/2$, with $L=\mu\pi a^2 n^2 d$, the inductance. Considering a time-varying current, show that the voltage drop along the coil $V=LdI/dt$.

1.8 Momentum Conservation

Consider a collection of particles in vacuum, enclosed by a volume V, and acted on by electromagnetic fields. The Lorentz force law implies that the rate of change of particle momentum is given by

$$\frac{d\vec{P}_{mech}}{dt} = \int_V dV\left(\rho\vec{E} + \vec{J}\times\vec{B}\right).$$

One expects this momentum gain or loss to be balanced by a momentum associated with the fields. To determine this field momentum, we may re-express the relation above, using Maxwell's equations. First,

$$\rho\vec{E} + \vec{J}\times\vec{B} = \vec{E}\,\nabla\bullet\vec{D} + \left(\vec{\nabla}\times\vec{H} - \frac{\partial\vec{D}}{\partial t}\right)\times\vec{B}.$$

Next we apply the chain rule, followed by Faraday's law,

$$\frac{\partial\vec{D}}{\partial t}\times\vec{B} = \frac{\partial}{\partial t}\left(\vec{D}\times\vec{B}\right) - \vec{D}\times\frac{\partial\vec{B}}{\partial t} = \frac{\partial}{\partial t}\left(\vec{D}\times\vec{B}\right) + \vec{D}\times\left(\vec{\nabla}\times\vec{E}\right),$$

so that

$$\rho\vec{E} + \vec{J}\times\vec{B} = \vec{E}\,\nabla\bullet\vec{D} + \left(\vec{\nabla}\times\vec{H}\right)\times\vec{B} - \vec{D}\times\left(\vec{\nabla}\times\vec{E}\right) - \frac{\partial}{\partial t}\left(\vec{D}\times\vec{B}\right).$$

Finally, we make use of the identities

$$\left\{\vec{E}\,\nabla\bullet\vec{E} - \vec{E}\times\left(\vec{\nabla}\times\vec{E}\right)\right\}^a = E^a\partial^b E^b - E^b\partial^a E^b + E^b\partial^b E^a = \partial^b\left(E^a E^b - \tfrac{1}{2}\vec{E}\bullet\vec{E}\,\delta_{ab}\right),$$

$$\left\{\left(\vec{\nabla}\times\vec{B}\right)\times\vec{B}\right\}^a = \left\{\vec{B}\underbrace{\nabla\bullet\vec{B}}_{0} - \vec{B}\times\left(\vec{\nabla}\times\vec{B}\right)\right\}^a = \partial^b\left(B^a B^b - \tfrac{1}{2}\vec{B}\bullet\vec{B}\,\delta_{ab}\right).$$

From this one has

$$\left\{\rho\vec{E}+\vec{J}\times\vec{B}\right\}^a$$

$$=\varepsilon_0\partial^b\left(E^aE^b-\tfrac{1}{2}\vec{E}\bullet\vec{E}\delta_{ab}\right)+\mu_0\partial^b\left(B^aB^b-\tfrac{1}{2}\vec{B}\bullet\vec{B}\delta_{ab}\right)-\varepsilon_0\frac{\partial}{\partial t}\left(\vec{E}\times\vec{B}\right)^a.$$

or

$$\frac{dP^a_{mech}}{dt}=\int_V dV\partial^bT^{ab}-\varepsilon_0\int_V dV\frac{\partial}{\partial t}\left(\vec{E}\times\vec{B}\right)^a,$$

with the tensor

$$T^{ab}=\varepsilon_0\left(E^aE^b-\tfrac{1}{2}\vec{E}\bullet\vec{E}\delta_{ab}\right)+\mu_0\left(B^aB^b-\tfrac{1}{2}\vec{B}\bullet\vec{B}\delta_{ab}\right).$$

This relation equates the time-rate of change of momentum within a volume, to a surface flux,

$$\left(\frac{d\vec{P}_{mech}}{dt}+\frac{d\vec{P}_{em}}{dt}\right)^a=\int_{\partial V}T^{ab}dS_b, \tag{1.20}$$

where the momentum carried by the electromagnetic fields is simply

$$\vec{P}_{em}=\varepsilon_0\vec{E}\times\vec{B}=\frac{1}{c^2}\vec{E}\times\vec{H}=\frac{\vec{S}}{c^2}, \tag{1.21}$$

with $\vec{S}$ the Poynting flux. The rate of convection in the direction *b*, of field momentum oriented along *a* is evidently given by T^{ab}, thus referred to as the electromagnetic stress tensor. A useful alternative expression is

$$T^{ab}=D^aE^b+H^aB^b-\frac{1}{2}\left(\vec{D}\bullet\vec{E}+\vec{H}\bullet\vec{B}\right)\delta_{ab}=D^aE^b+H^aB^b-u\delta_{ab}, \tag{1.22}$$

with *u* the energy density stored in electromagnetic fields. The symmetry of the stress tensor (and the simplicity of the derivation) is insured by the assumption that the particles are in vacuum. In general, in media, anisotropy may be present.

1.9 The Problem of Electromagnetic Acceleration

Equipped with the mechanics of fields, let us reconsider the problem of accelerating charged particles. We require an electric field, $\vec{E}$, to produce any change in particle energy, ε, and energy transfer is governed by

$$\frac{d\varepsilon}{dt}=q\vec{E}\bullet\vec{V},$$

where $\vec{V}$ is the particle velocity and *q* is the charge. Let us suppose the particle is already relativistic, so that $V\approx c$ is constant. Denote the direction of particle motion $\hat{s}$, and parameterize the motion by length traversed, *s*, with $ds=Vdt$. Then the particle coordinates may be expressed as

$$\vec{r} = s\hat{s}, \qquad t = t_0 + \frac{s}{V},$$

where t_0 is the time at which the particle reaches s=0. Energy gain takes the form

$$\frac{d\varepsilon}{ds} = qE_s(\vec{r},t) = qE_s\left(s\hat{s}, t_0 + \frac{s}{V}\right),$$

where E_s is the electric field component parallel to the particle motion.

To ascertain the form of the electric field, note that in an infinite unbounded time-independent medium a well-behaved function may be expanded as a superposition of plane-waves. This implies that at linear order we may consider fields of the form

$$\vec{E} = \Re\left\{\tilde{E}\exp\left(j\omega t - j\vec{k}\bullet\vec{r}\right)\right\},\ \vec{H} = \Re\left\{\tilde{H}\exp\left(j\omega t - j\vec{k}\bullet\vec{r}\right)\right\}.$$

Gauss's law requires that the polarization of the electric field be transverse to the direction of propagation, $\tilde{E}\bullet\vec{k} = 0$, implying two independent polarizations. Faraday's Law requires that the magnetic field polarization be transverse to both the direction of propagation and the electric field, $Z_0\tilde{H} = \tilde{E}\times\hat{k}$. The quantity $Z_0 = \sqrt{\mu_0/\varepsilon_0} \approx 377\,\Omega$ we will refer to as the wave impedance of free-space. Evidently amplitude, propagation direction, polarization and frequency exhaust the fundamental attributes of plane electromagnetic waves in free-space.

With this we can compute the energy imparted to the particle in passing through any finite region $s_0 < s < s_1$,

$$\Delta\varepsilon = \Re q\tilde{E}_s\int_{s_0}^{s_1} ds\exp\left(j\omega t_0 + j\left[\frac{\omega}{V} - k_s\right]s\right) = \Re q\tilde{V}e^{j\omega t_0},$$

and we introduce the *accelerating voltage* phasor $\tilde{V}$. In free-space, we extend the limits to infinity to obtain

$$\tilde{V} = 2\pi\tilde{E}_s\delta\left(\frac{\omega}{V} - k_s\right).$$

The dispersion relation $\vec{k}^2 = \omega^2/c^2$, and transverse polarization, imply that for $E_s \neq 0$, $\omega/k_s > c$, so that $\omega/k_s > V$, and therefore $\tilde{V} = 0$. In accelerator jargon, we say that this concept starts to look *iffy*.

This observations suggests that useful acceleration should take place either (1) in a terminated region of space, or (2) over an extended region, but with a wave whose phase-velocity $\omega/k_s = c$. These two possibilities correspond to *standing-wave* and *travelling-wave* accelerators.

There is a second problem of equal importance: how to produce the electromagnetic wave? One needs a power converter drawing low-frequency power from the wall-plug, and transforming it into high-frequency electromagnetic power. In free space, a *high* peak power is required to produce a *high* electric field. In structures, we will find that a high field can be obtained with *lower* peak power than in free-space. This is because, with the help of material boundaries, we may

store energy by resonant excitation. How much energy we may store, or how long we may store it, depends on dissipation in the medium. Thus we require not only a material medium, but one with low loss.

Exercise 1.4 The law of energy conservation has $\vec{J} \bullet \vec{E}$ on one side, and expressions *quadratic* in the fields on the other. How is it that the energy gain of a particle traversing an accelerator might include a term proportional to the *first power* of the applied field?

1.10 Conductors

For engineering purposes there are four kinds of materials: *metals*, *ceramics*, *semiconductors*, and *plastics*. From a more elementary point of view, there are *solids*, *liquids*, *gases* and *plasma*. All have been proposed for accelerating structures. However, let us not be distracted at the outset by the diversity of media from which one could build accelerators. Any linac concept can be compared to and judged against the conventional linac built of normal conductor.

The behavior of conductors with steady applied voltage was first noted in the lab notebooks of Cavendish, but is usually associated with the name of Ohm, since Cavendish failed to publish. It wasn't until 1900 that the first microscopic picture of resistivity was developed, by Paul Drude,[10] whose model of a conductor consisted of a gas of electrons in an array of ions. In the presence of an applied field, electrons are accelerated but they tend to collide with ions on some characteristic collision time-scale τ. A simple model of this motion takes the form

$$m\frac{d\vec{V}}{dt} = q\vec{E} - m\frac{\vec{V}}{\tau},$$

and when the fields vary slowly on the time-scale τ, the solution is simply

$$\vec{V} = \frac{q\tau}{m}\vec{E}.$$

The current density flowing through the metal is then

$$J = nq\vec{V} = \frac{nq^2\tau}{m}\vec{E} = \sigma\vec{E}, \tag{1.23}$$

where σ is the conductivity.

To appreciate the effect of a conducting boundary, consider first a perfect conductor, $\sigma \to \infty$. The boundary conditions on fields are two. (1) If electric field lines terminate on a surface, they do so normal to the surface, for any tangential component would quickly be neutralized by lateral motion of charge within the surface. (2) Magnetic field lines avoid surfaces, for if they did not they would terminate, since the magnetic field is zero within the conductor. These rules can be employed to sketch rough solutions of Maxwell's equations in a copper structure.

The correction to the approximation $\sigma \to \infty$ is quite small, in the sense that it results in dissipation that is slow on the time-scale of an rf period. However, this "small" correction in the end dominates the scalings for accelerators. To appreciate

this slow dissipation, we start from Maxwell's equations, in a conducting medium, assuming a single frequency excitation, so that fields are proportional to exp*(jωt)*. Using phasor notation, Ampere's law takes the form

$$\vec{\nabla}\times\tilde{H} = j\omega\tilde{D} + \tilde{J} \approx \tilde{J} = \sigma\tilde{E},$$

and we neglect displacement current in the limit of high-conductivity, since in this limit, currents in the media are much larger than the displacement current. Faraday's law takes the form $\vec{\nabla}\times\tilde{E} = -j\omega\tilde{B}$. In the limit of high-conductivity, the electrons inside the conductor respond quickly to the applied field, so that inside the conductor there is no bulk charge separation. In this case, Gauss's law takes the form $\vec{\nabla}\bullet\tilde{E} = 0$. We can reduce this system to a single equation for $\tilde{H}$,

$$\vec{\nabla}\times\left(\vec{\nabla}\times\tilde{H}\right) = \vec{\nabla}\left(\vec{\nabla}\bullet\tilde{H}\right) - \nabla^2\tilde{H} = -\nabla^2\tilde{H} = \vec{\nabla}\times\left(\sigma\tilde{E}\right) = -j\omega\sigma\tilde{B} = -j\mu\omega\sigma\tilde{H}$$

so that,

$$\nabla^2\tilde{H} - j\,\mathrm{sgn}\,\omega\frac{2}{\delta^2}\tilde{H} = 0$$

where we have introduced the *skin-depth*, δ, a quantity with units of length,

$$\delta = \left(\frac{2}{\mu\sigma|\omega|}\right)^{1/2}. \tag{1.24}$$

Next, let's solve for the fields in the conductor, consulting the sketch in Fig. 1.3. Choosing the coordinate ξ to measure displacement into the surface along the unit normal, we have

$$\frac{d^2}{d\xi^2}\tilde{H}_t - j\,\mathrm{sgn}\,\omega\frac{2}{\delta^2}\tilde{H}_t = 0,$$

and the solution is

$$\tilde{H}_t(\xi) = \tilde{H}_t(0)\exp\left\{-\frac{\xi}{\delta}(1 + j\,\mathrm{sgn}\,\omega)\right\}, \tag{1.25}$$

$$\tilde{E} = \frac{1}{\sigma}\vec{\nabla}\times\tilde{H} \approx \frac{1}{\sigma}\hat{n}\times\frac{\partial\tilde{H}}{\partial\xi} = -Z_s\hat{n}\times\tilde{H}_t. \tag{1.26}$$

Evidently a conductor of finite conductivity does not satisfy exactly the condition that transverse electric field should vanish on the surface. Instead, the transverse electric field satisfies an *impedance boundary condition* with surface impedance,

$$Z_s = \frac{1 + j\,\mathrm{sgn}\,\omega}{\sigma\delta} = R_s(1 + j\,\mathrm{sgn}\,\omega), \tag{1.27}$$

and *surface resistance*, a quantity with units of ohms,

$$R_S = \frac{1}{\sigma\delta}. \tag{1.28}$$

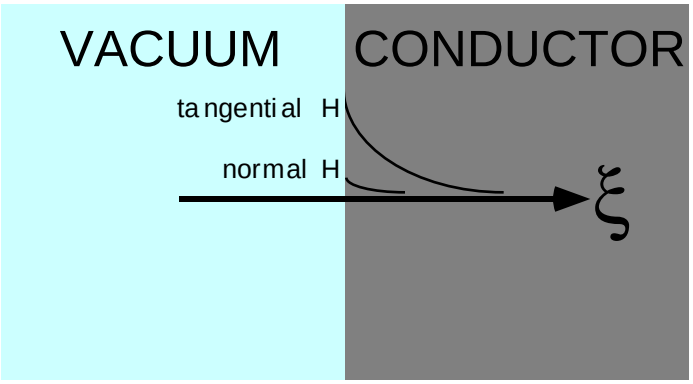

FIGURE 1.3. Sketch of the geometry for calculation of rf field penetration into a conductor.

Due to the collisions of conduction electrons, a non-zero power per unit area is deposited in the conductor on average,

$$\bar{S} \bullet \hat{n} = \frac{1}{2}\Re\left(\tilde{E} \times \tilde{H}^* \bullet \hat{n}\right) = -\frac{1}{2}\Re\left(Z_s\left(\hat{n} \times \tilde{H}_t\right) \times \tilde{H}^* \bullet \hat{n}\right)$$
$$= \frac{1}{2}\Re\left(Z_s\left|\hat{n} \times \tilde{H}_t\right|^2\right) = \frac{1}{2}R_s\left|n \times \tilde{H}\right|^2 = \frac{1}{2}R_s\left|\tilde{K}\right|^2$$

where in the last line we have expressed the Ohmic power deposition in terms of the surface current density,

$$\tilde{K} = \int_0^\infty \tilde{J} d\xi = -\hat{n} \times \tilde{H}(0).$$

This relation states that, in order to cancel out the magnetic field within the bulk of the conductor, wall currents must flow. These currents should flow in the conductor, and hence be perpendicular to the normal, $\hat{n}$. In addition, Ampere's law implies the currents must be perpendicular to the magnetic field, otherwise, the currents will produce an additional uncompensated field component. Hence the cross-product of $\hat{n}$ and $\tilde{H}$.

With the help of the foregoing analysis, and inspecting Table 1.1 we can see why most linacs are built of copper. Copper is cheaper than silver, and just about as good. Because of this, the facts of life for the material boundaries of a normal-conducting microwave linac are just those for copper,

$$\delta \approx \frac{2.1\mu\text{m}}{\sqrt{f(\text{GHz})}}, \qquad R_S \approx 8.3\text{m}\Omega\sqrt{f(\text{GHz})}.$$

The skin-depth and surface resistance will appear frequently in our discussions, as losses limit the efficiency of accelerators and set their characteristic length and time

scales. Ohmic heating appears today to set the limit on achievable gradient in conducting structures, although no one is quite sure what the limiting gradient is. At a more mundane level, Ohmic heating can cause cavity dimensions to change, and requires temperature stabilization.

Table 1.1. Conductivity of some common materials, in units of mho/m.

silver	6.2×10^7
copper	5.8×10^7
gold	4.1×10^7
aluminum	3.8×10^7
brass	1.5×10^7
solder	0.7×10^7
stainless steel	0.1×10^7

Equipped then with Maxwell's equations, conservation laws (charge, energy, momentum), and the skin-effect, we are almost ready to sketch out an accelerator. However, we will require some mechanism of power *feed* to the interaction region, and in practice this is accomplished with waveguide. Waveguide falls under a well-developed subject-heading called *microwave electronics,* to which we turn in the next section. Before proceeding, it might be useful to take a look at Appendix B where there is a brief summary of *"low-frequency"* electronics.

Exercise 1.5 Show that a magnetic field in a uniform conductor satisfies the difffusion equation, $\partial\vec{H}/\partial t = D\nabla^2\vec{H}$, and determine the diffusion coefficient D in terms of the conductivity, σ and the permeability, μ . Argue from this result, that the time scale for diffusion through a depth d is $T \approx d^2/D$, and explain the scaling with d^2 on intuitive grounds, referring to your experience with the random walk problem. Go on to justify the scaling of rf penetration depth with $\omega^{-1/2}$.

Exercise 1.6 Solve the collisional equation of motion subject to an electric field,

$$\vec{E} = \Re\left(\tilde{E}e^{j\omega t}\right) = \frac{1}{2}\left(\tilde{E}e^{j\omega t} + \tilde{E}^* e^{-j\omega t}\right),$$

with $\Re$ denoting the real part. Show that the electron current takes a similar form, with

$$\tilde{J} = \frac{\sigma}{(1+ j\omega\tau)}\tilde{E}.$$

Apply charge conservation to compute charge density from the current density. Show that

$$\nabla\bullet\varepsilon_0\tilde{E} = \tilde{\rho} = -\frac{1}{j\omega}\nabla\bullet\tilde{J} = -\frac{1}{j\omega}\nabla\bullet\frac{\sigma}{(1+ j\omega\tau)}\tilde{E}.$$

and conclude that an electron gas in an array of infinitely massive ions has permittivity

$$\varepsilon = \varepsilon_0 + \frac{1}{j\omega}\frac{\sigma}{(1+ j\omega\tau)}.$$

What form does this take in the collisionless limit? Express this in terms of the plasma frequency $\omega_p^2 = nq^2/m\varepsilon_0$. Note that one may view the problem treating the plasma as a medium: $\nabla \bullet \varepsilon\, \tilde{E} = \tilde{\rho}_{ext}$, $\tilde{D} = \varepsilon\, \tilde{E}$ or not: $\nabla \bullet \varepsilon_0 \tilde{E} = \tilde{\rho}_{plasma} + \tilde{\rho}_{ext}$, $\tilde{D} = \varepsilon_0 \tilde{E}$. Taking the former view, show that polarization as a function of time is given by

$$\vec{P}(t) = \varepsilon_0 \int_{-\infty}^{+\infty} dt' G(t-t')\vec{E}(t')$$

with

$$G(t) = \frac{1}{2\pi}\int_{-\infty}^{+\infty} d\omega\, e^{j\omega t}\chi_e(\omega) = \omega_p^2 \tau\left(1 - e^{-t/\tau}\right)H(t)$$

where H is the step-function.

Exercise 1.7 Considering a current source in free-space, confirm that in the frequency domain the Lorentz gauge vector potential satisfies, $\left(\nabla^2 + k^2\right)\tilde{A} = -\mu_0 \tilde{J}$, with $k=\omega/c$ and ω the angular frequency. Derive the solution for a point source, $\tilde{J} = \delta^3(\vec{r})$, and argue by superposition that the general solution is

$$\tilde{A}(\vec{r},k) = \frac{\mu_0}{4\pi}\int d^3\vec{r}\,' \frac{e^{-jk|\vec{r}-\vec{r}\,'|}}{|\vec{r}-\vec{r}\,'|}\tilde{J}(\vec{r}\,',k).$$

You will want to make use of causality, the result for the Coulomb field, $\nabla^2(1/r) = -4\pi\delta^3(\vec{r})$, and the Laplacian in spherical coordinates. Argue that the scalar potential satisfies,

$$\tilde{\varphi}(\vec{r},k) = \frac{1}{4\pi\varepsilon_0}\int d^3\vec{r}\,' \frac{e^{-jk|\vec{r}-\vec{r}\,'|}}{|\vec{r}-\vec{r}\,'|}\tilde{\rho}(\vec{r}\,',k),$$

and show that this is consistent with the Lorentz Gauge condition.

Exercise 1.8 Consider a plane-polarized wave propagating in the z-direction,

$$\vec{A} = \hat{x}\frac{mc}{e}\Re\left\{\tilde{a}(\vec{r}_\perp, z, t)e^{j(\omega t - kz)}\right\}.$$

Suppose that the $\tilde{a}$ varies slowly on the time-scale $1/\omega$, and slowly in space on the length scale $1/\beta$. Starting from the wave-equation for the vector potential, in the Lorentz gauge in free-space, and changing variables to $\tau=ct$, and $\xi=z-c^2kt/\omega$, show that the phasor $\tilde{a}$ satisfies

$$\left\{\nabla_\perp^2 - 2j\frac{\omega}{c}\frac{\partial}{\partial\tau}\right\}\tilde{a} = 0.$$

Check that the Poynting flux is given approximately by $\vec{S} \approx P_0\left(\frac{\omega}{c}k\right)|\tilde{a}|^2\hat{z}$, with P_0~8.7GW.

2. MICROWAVE ELECTRONICS

It wasn't until 1888 that Heinrich Rudolf Hertz at the age of 31, provided the experimental confirmation of Maxwell's displacement current, demonstrating electromagnetic wave propagation in his lab using a spark-gap. Nine years later Guglielmo Marconi, at the age of 23, demonstrated sending and receiving of signals over a two-mile range. Prior to this time, speed of light communication had been available only by telegraph. While radio was vulnerable to eavesdropping, it required no cable, and, for the first time, permitted communication over the horizon with *ships at sea*. The navies of the world were not slow to notice this and the first application of radio in war occurred on 14 April 1904, during the bombardment of Port Arthur.[11] The advent of bomber aircraft added some urgency to the quest for reliable radar systems. The US Army conducted its first field tests of a pulse radar system in 1936, and deployed its first operational system, the SCR-268 (3 GHz) in 1938.[12] By the end of World War II, the MIT Radiation Laboratory had developed some 150 radar systems. The subject of *microwave electronics* was developed largely as a result of such military demands during the period 1900-1950.

The work of this section is to describe the foundations of microwave electronics, while somehow managing not to derive it in all its detail. We introduce the notion of *voltage*, *V*, and *current*, *I*, as they are used in waveguide and cavity systems, and indicate how they may be employed in circuit equivalent models for accelerators.

2.1 Waveguide Modes

All high-power microwave systems have connected to them a length of *waveguide*. Waveguide is used to transport energy, and is favored over free-space transport because it is compact and is immune to cross-talk from the surroundings. It can also be temperature-stabilized to preserve phase-information in a diurnally reliable fashion. It can be filled with a high-pressure electronegative gas or evacuated to inhibit breakdown. The two most common types of waveguide are depicted in Fig. 2.1. One of these is rectangular waveguide, referred to as "WRXX", where *XX* is the inner dimension (*a* in Fig 2.1) in hundredths of an inch.[13] Thus *WR90* is rectangular waveguide, with a=0.90". Coaxial waveguide comes in many sizes corresponding to the many different frequency ranges in which it is employed. For work in *S-Band* (2-4 GHz) it is not uncommon to use *RG-214/U* with *Type-N* connectors.[14] Such practices can be understood starting from Maxwell's equations, but the reader will be spared that.

We start with uniform conducting waveguide, *i.e.*, an arrangement of conductors that is uniform in some direction, call it *z*. Since the geometry is constant in time, and uniform in *z*, we are free to consider a single angular frequency ω and a single wavenumber β. Let the fields take the form

$$\vec{E}(\vec{r},t) = \Re\left\{\tilde{E}(\vec{r}_\perp,\omega)e^{j(\omega t-\beta z)}\right\}, \qquad \vec{H}(\vec{r},t) = \Re\left\{\tilde{H}(\vec{r}_\perp,\omega)e^{j(\omega t-\beta z)}\right\}.$$

The coordinate $\vec{r}_\perp = \hat{x}x + \hat{y}y$ is the position relative to the axis of the waveguide.

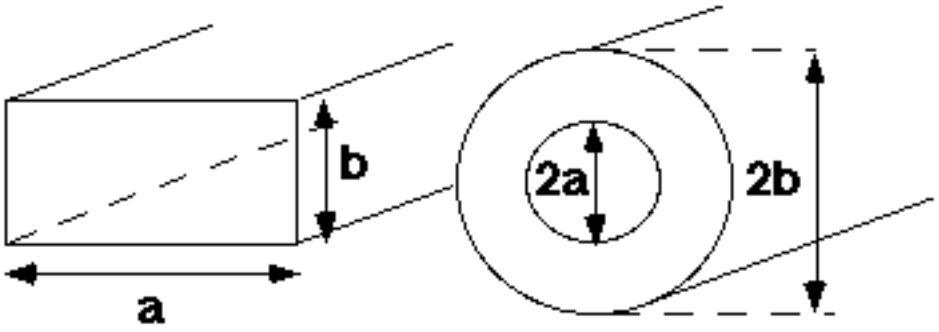

FIGURE 2.1. The most commonly used waveguides are rectangular and coaxial.

We assume in the following discussion that $\omega \neq 0$, and that the boundaries are perfectly conducting. Wall losses will be incorporated later as a perturbation.

We write out Maxwell's equations assuming no external source terms and a uniform medium present in the waveguide,

$$-j\beta\tilde{E}_z + \vec{\nabla}_\perp \bullet \tilde{E}_\perp = 0, \qquad \text{(Gauss's law)}$$

$$-j\beta\tilde{H}_z + \vec{\nabla}_\perp \bullet \tilde{H}_\perp = 0. \qquad \text{(solenoidal condition)}$$

Here the subscript $\perp$ denotes transverse components, thus

$$\tilde{E}_\perp = \hat{x}\tilde{E}_x + \hat{y}\tilde{E}_y,$$

$$\vec{\nabla}_\perp = \hat{x}\frac{\partial}{\partial x} + \hat{y}\frac{\partial}{\partial y},$$

$$\vec{\nabla} = \hat{x}\frac{\partial}{\partial x} + \hat{y}\frac{\partial}{\partial y} - \hat{z}j\beta = \vec{\nabla}_\perp - \hat{z}j\beta.$$

The last definition we make for convenience to simplify the expression of Ampere's law and Faraday's law,

$$\vec{\nabla} \times \tilde{H} = j\omega\varepsilon\tilde{E}, \qquad \vec{\nabla} \times \tilde{E} = -j\omega\mu\tilde{H}.$$

We can reduce these coupled first-order equations to second-order equations for $\tilde{E}$ and $\tilde{H}$, separately, in the form of wave equations,

$$\vec{\nabla} \times \left(\vec{\nabla} \times \tilde{H}\right) = -\nabla^2\tilde{H} = j\omega\varepsilon\vec{\nabla} \times \tilde{E} = j\omega\varepsilon\left(-j\omega\mu\tilde{H}\right) = \omega^2\varepsilon\mu\tilde{H}$$

and similarly for $\tilde{E}$. The results then are two vector Helmholtz equations,

$$\left(\nabla_\perp^2 + \beta_c^2\right)\tilde{H} = 0, \qquad \left(\nabla_\perp^2 + \beta_c^2\right)\tilde{E} = 0,$$

where we have introduced

$$\beta_c^2 = \beta_0^2 - \beta^2, \qquad \beta_0^2 = \omega^2\varepsilon\mu.$$

We will refer to β_c as the *cutoff wavenumber*, since frequencies lower than $\omega < \beta_c / \sqrt{\varepsilon\mu}$ correspond to evanescent waves (*i.e.*, β is imaginary). The divergence conditions may be used to express the longitudinal field components in terms of the transverse components

$$\tilde{E}_z = \frac{1}{j\beta}\nabla_\perp \bullet \tilde{E}_\perp, \qquad \tilde{H}_z = \frac{1}{j\beta}\nabla_\perp \bullet \tilde{H}_\perp.$$

In addition,we may write the curl equations

$$\tilde{E} = \frac{1}{j\beta_0}\vec{\nabla} \times Z_0\tilde{H}, \qquad Z_0\tilde{H} = -\frac{1}{j\beta_0}\vec{\nabla} \times \tilde{E},$$

where we make use of the *wave impedance* for free propagation in this medium,

$$Z_0 = \sqrt{\frac{\mu}{\varepsilon}}. \qquad \text{(wave impedance)}$$

These last results may be written more explicitly using the expression for the gradient operator,

$$j\beta_0 Z_0 \tilde{H}_\perp = \hat{z} \times \left(\vec{\nabla}_\perp \tilde{E}_z + j\beta\tilde{E}_\perp\right), \tag{2.1}$$

$$j\beta_0 \tilde{E}_\perp = -\hat{z} \times \left(\vec{\nabla}_\perp Z_0\tilde{H}_z + j\beta Z_0\tilde{H}_\perp\right). \tag{2.2}$$

We proceed to enumerate the three kinds of solutions (*modes*) to Maxwell's equations in uniform conducting guide. Notice that solutions of these equations in guide may be represented as superpositions of plane-waves.

Exercise 2.1 Conducting boundary conditions require that tangential electric field $\hat{n} \times \tilde{E} = \hat{n} \times \tilde{E}_\perp = 0$, and that normal magnetic field, $\hat{n} \bullet \tilde{H} = \hat{n} \bullet \tilde{H}_\perp = 0$, with $\hat{n}$ the normal to the bounding surface. Making use of the last results, and taking dot and cross products with $\hat{n}$, confirm that a necessary condition for the vanishing of $\hat{n} \times \tilde{E}_\perp$ is $\partial\tilde{H}_z / \partial n = \hat{n} \bullet \vec{\nabla}_\perp \tilde{H}_z = 0$, and then that $\partial\tilde{H}_z / \partial n = \tilde{E}_z = 0$ are both *necessary* and *sufficient* conditions for *all* components of the boundary conditions.

Exercise 2.2 Express $\tilde{E} = \hat{y}\sin(\beta_c x)\exp(j\omega t - j\beta z)$ as a superposition of plane-waves. Compute the corresponding $\tilde{H}$. Determine conditions on β_c such that these fields are a solution of Maxwell's equations in an infinite medium of permeability μ and permittivity ε. Show that at the planes $x=0$, $x=\pi/\beta_c$, $y=0$, and $y=b$ conducting boundary conditions are satisfied. Assuming $\beta=3^{1/2}\beta_c$, sketch the constant phase fronts in the x-z plane for each plane-wave in the superposition. What angle do the plane-wave components make with the z-axis? If these signals were being generated at the $z=0$ plane, and the signal generator were turned off, how long would it take for the signals to begin to die off at a plane $z=L$ in the waveguide?

2.2 Modes With Zero Cutoff

First we consider a special case, $\beta_c = 0$. We know, from the work of Sec. 1, that the solution will be a superposition of plane-waves with $\beta_c = 0$---which is to say, propagating in the *z*-direction. Since the plane-waves are transverse, the *z*-components for the superposition must also vanish. Let us check this. For such a mode, we have, from the Helmholtz equation,

$$\nabla_\perp^2 \tilde{E}_z = \nabla_\perp^2 \tilde{H}_z = 0.$$

Green's theorem then implies

$$0 = \oint \tilde{H}_z \frac{\partial \tilde{H}_z}{\partial n} dl = \int \left(\tilde{H}_z \nabla_\perp^2 \tilde{H}_z + \vec{\nabla}_\perp \tilde{H}_z \bullet \vec{\nabla}_\perp \tilde{H}_z \right) d^2 r_\perp = \int \left| \vec{\nabla}_\perp \tilde{H}_z \right|^2 d^2 r_\perp ,$$

and thus $\tilde{H}_z$ is a constant throughout the waveguide cross-section. On the other hand, if $\tilde{H}_z$ is a constant then the circulation of $\tilde{E}$ about a closed loop ∂S, bounding an area *S*, with normal $\hat{z}$ is proportional, by this constant, to the area enclosed.

$$\oint_{\partial S} \tilde{E} \bullet d\vec{l} = \int_S \vec{\nabla} \times \tilde{E} \bullet d\vec{S} = -j\beta_0 Z_0 \int_S \tilde{H}_z dS = -j\beta_0 Z_0 \tilde{H}_z \int_S dS,$$

Taking the loop ∂S along the waveguide periphery, we see that tangential electric field vanishes there, and the circulation integral must therefore vanish. Thus $\tilde{H}_z = 0$. A similar argument can be employed to show that $\tilde{E}_z = 0$. Thus a mode with zero cutoff is a *transverse electromagnetic mode* or *TEM mode*, with vanishing longitudinal fields. This accords with our intuition that $\beta_c = 0$ corrresponds to $\beta = \omega\sqrt{\mu\varepsilon}$, having the appearance of a plane-wave in an unbounded medium propagating in the $\hat{z}$ direction. Plane electromagnetic waves are inherently transverse, polarized perpendicular to the direction of propagation.

Since the circulation integral of $\tilde{E} = \tilde{E}_\perp$ about any closed loop lying in the transverse plane vanishes, we may express $\tilde{E}_\perp$ in terms of a potential function, defined according to a line integral,

$$\psi(\vec{r}_\perp) = \int_{\vec{r}_{\perp 0}}^{\vec{r}_\perp} d\vec{l} \bullet \tilde{E}_\perp ,$$

where the choice of the reference point $\vec{r}_{\perp 0}$ corresponds to the choice of a constant of integration, and might as well be placed on a conducting surface. This definition is independent of the path connecting $\vec{r}_\perp$ and $\vec{r}_{\perp 0}$ since the circulation integral about any closed loop in the transverse plane vanishes. With this definition for ψ, it follows that $\tilde{E}_\perp = \vec{\nabla}_\perp \psi$, and Gauss's law implies $\vec{\nabla}_\perp^2 \psi = 0$. Boundary conditions

require $0 = n \times \tilde{E}_\perp = n \times \vec{\nabla}_\perp \psi$. Since the geometric meaning of $\vec{\nabla}_\perp \psi$ is the *normal to a surface of constant* ψ, it follows that each conductor is an *equipotential*. Upon reflection one sees that ψ is just a solution of the ω=0 electrostatics problem in the waveguide. Thus for example, if we have one conducting boundary (one equipotential) then Green's theorem implies that the potential is a constant and the electric field is zero. In this case, there is no TEM mode. If we have two conducting boundaries, then we may have one TEM mode.

Exercise 2.3 (**TEM Mode of Coaxial Line**) The most commonly used mode is TEM mode of coaxial cable. Considering the geometry of Fig. 2.1, and starting from $\tilde{E}_\perp = \vec{\nabla}\psi$ and $Z_0 \tilde{H}_\perp = \hat{z} \times \tilde{E}_\perp$, argue that $\partial\psi / \partial\phi = 0$. Show that the solution takes the form

$$\psi = k \ln\left(\frac{r}{a}\right), \qquad Z_0 \tilde{H}_\perp = \hat{\phi}\frac{k}{r}, \qquad \tilde{E}_\perp = \hat{r}\frac{k}{r}$$

where k is a constant. Confirm that the choice $k^{-2} = 2\pi \ln(b/a)$ corresponds to the normalization $\int d^2\vec{r}_\perp \tilde{E}_\perp \bullet \tilde{E}_\perp = 1$. Make a sketch of the field lines and wall currents.

2.3 Modes With Finite Cutoff

To treat the case $\beta_c \neq 0$, we return to Eqs. (2.1) and (2.2). Writing these equations out component-wise we find that the transverse fields can be determined in terms of the longitudinal fields,

$$\tilde{E}_\perp = \frac{\beta_0}{j\beta_c^2}\left(\hat{z} \times \vec{\nabla}_\perp Z_0 \tilde{H}_z - \frac{\beta}{\beta_0}\vec{\nabla}_\perp \tilde{E}_z\right), \tag{2.3}$$

$$Z_0 \tilde{H}_\perp = \frac{\beta_0}{j\beta_c^2}\left(\hat{z} \times \vec{\nabla}_\perp \tilde{E}_z + \frac{\beta}{\beta_0}\vec{\nabla}_\perp Z_0 \tilde{H}_z\right). \tag{2.4}$$

Of the modes with $\beta_c \neq 0$, the first are *transverse electric modes*, or *TE* modes, with E_z=0 (also called *H*-modes) for which the transverse fields may be determined from H_z,

$$Z_0 \tilde{H}_\perp = \frac{\beta}{j\beta_c^2}\vec{\nabla}_\perp Z_0 \tilde{H}_z, \tag{2.5}$$

$$\tilde{E}_\perp = -\frac{\beta_0}{j\beta_c^2}\hat{z} \times \vec{\nabla}_\perp Z_0 \tilde{H}_z = -\frac{\beta_0}{\beta}\hat{z} \times Z_0 \tilde{H}_\perp, \tag{2.6}$$

and $\tilde{H}_z$ satisfies

$$\left(\nabla_\perp^2 + \beta_c^2\right)\tilde{H}_z = 0, \qquad \text{(TE)} \tag{2.7}$$

with boundary condition

$$0 = \hat{n} \bullet Z_0 \tilde{H}_\perp = \frac{\beta}{j\beta_c^2} \hat{n} \bullet \vec{\nabla}_\perp Z_0 \tilde{H}_z,$$

or

$$\frac{\partial \tilde{H}_z}{\partial n} = 0, \tag{2.8}$$

where n is the unit normal to the conducting boundary. Pictorially, a TE mode is one for which the lines of electrical field, when viewed in cross-section, close on themselves.

Of the modes with $\beta_c \neq 0$, the second kind of mode is the *transverse magnetic mode* or *TM* mode, with $H_z=0$, (also called an *E*-mode) for which the transverse fields may be determined from $\tilde{E}_z$,

$$\tilde{E}_\perp = \frac{\beta}{j\beta_c^2} \vec{\nabla}_\perp \tilde{E}_z, \tag{2.9}$$

$$Z_0 \tilde{H}_\perp = \frac{\beta_0}{j\beta_c^2} \hat{z} \times \vec{\nabla}_\perp \tilde{E}_z = \frac{\beta_0}{\beta} \hat{z} \times \tilde{E}_\perp, \tag{2.10}$$

and the longitudinal field satisfies

$$\left(\nabla_\perp^2 + \beta_c^2\right) \tilde{E}_z = 0, \qquad \text{(TM)} \tag{2.11}$$

with boundary condition

$$\tilde{E}_z = 0. \tag{2.12}$$

For a TM mode the lines of magnetic field form closed loops in the transverse plane.

Note that if $\tilde{E}_z$ is a solution to this problem, then so is $\Re \tilde{E}_z$, and similarly for $\tilde{H}_z$. Evidently then one may choose longitudinal fields to be real for either TE or TM modes. On the other hand, the transverse fields for these travelling waves are in phase with each other, and always 90° out of phase with the longitudinal field. We will employ the convention that both transverse fields are real, with the result that longitudinal fields are imaginary.

Exercise 2.4 (**TE_{10} Mode of Rectangular Guide**) The second most commonly used mode is TE_{10} mode of rectangular waveguide. Consider the rectangular geometry of Fig. 2.1, with $a>b$. Starting from the TE mode equation, Eq. (2.7) and considering the most general solution $\exp(jk_x x)\exp(jk_y y)$, show that boundary conditions require solutions of the form $\tilde{H}_z(x,y) \propto \cos(n\pi x/a)\cos(m\pi y/b)$, with $k_x = n\pi/a$, and $k_y = m\pi/b$ (TE_{nm} mode). Compute the cutoff wavenumber and confirm that TE_{10} mode has the lowest cutoff ("fundamental mode of rectangular guide") and the fields take the form

$$\tilde{E}_\perp = E_0 \sin(\beta_c x)\hat{y}, \quad Z_c \tilde{H}_\perp = E_0 \sin(\beta_c x)\hat{x}, \quad Z_0 \tilde{H}_z = -j\frac{\beta_c}{\beta_0} E_0 \cos(\beta_c x),$$

and determine Z_c. Confirm that the choice $E_0 = (2/ab)^{1/2}$ corresponds to the normalization $\int d^2\vec{r}_\perp \tilde{E}_\perp^2 = 1$.

To summarize the foregoing analysis, boundary conditions restrict the permissible values of cut-off wavenumber β_c to a discrete set. Each mode has a corresponding minimum wavelength $\lambda_c = 2\pi/\beta_c$, the cut-off wavelength; for longer wavelengths, the solution for β is imaginary and the field evanesces in the waveguide. The *guide wavelength* is $\lambda_g = 2\pi/\beta = \lambda_0/\sqrt{1-\lambda_0^2/\lambda_c^2}$, where the wavelength in the absence of boundaries is $\lambda_0 = 2\pi/\beta_0$. In general for a given mode we have

$$Z_c \tilde{H}_\perp = \hat{z} \times \tilde{E}_\perp, \tag{2.13}$$

where the *characteristic impedance* associated with the mode is

$$Z_c = Z_0 \begin{cases} \dfrac{\beta_0}{\beta} = \dfrac{\lambda_g}{\lambda_0} & \text{TE mode} \\ \dfrac{\beta}{\beta_0} = \dfrac{\lambda_0}{\lambda_g} & \text{TM mode} \\ 1 & \text{TEM mode} \end{cases} . \tag{2.14}$$

This is a function of frequency for TE and TM modes. We choose the sign of Z_c positive for positive β.

2.4 Circuit Equivalence

Supposing that we have determined all the modes for our geometry, and their eigenvalues, β_c, let us form a list (an infinite list) of all these modes, and tally them with index a. A general solution for a vacuum oscillation in a given geometry may then be represented as a sum over all these modes:

$$\tilde{E}_t = \sum_a E_{\perp a}(\vec{r}_\perp)\, V_a(z,\omega), \tag{2.15}$$

$$\tilde{H}_t = \sum_a H_{\perp a}(\vec{r}_\perp) I_a(z,\omega) Z_{ca}(\omega) \tag{2.16}$$

where

$$Z_{ca} H_{\perp a} = \hat{z} \times E_{\perp a}. \tag{2.17}$$

We adopt the normalization

$$\int d^2 r_\perp E_{\perp a}(\vec{r}_\perp) \bullet E_{\perp a}(\vec{r}_\perp) = 1, \qquad \text{(Slater normalization)} \tag{2.18}$$

where the integral is over the waveguide cross-section. We have chosen the transverse field components in this normalization to be real. The coefficients V,I take the forms

$$V_a(z,\omega) = V_a^+ e^{-j\beta_a z} + V_a^- e^{j\beta_a z}, \tag{2.19}$$

$$Z_{ca} I_a(z,\omega) = V_a^+ e^{-j\beta_a z} - V_a^- e^{j\beta_a z}. \tag{2.20}$$

The longitudinal fields may be determined using Eqs. (2.4) and (2.5), the conditions that the fields be solenoidal in the source-free waveguide,

$$\tilde{E}_z = \sum_a E_{za}(\vec{r}_\perp)\left\{V_a^+ e^{-j\beta_a z} - V_a^- e^{j\beta_a z}\right\}, \tag{2.21}$$

$$\tilde{H}_z = \sum_a H_{za}(\vec{r}_\perp)\left\{V_a^+ e^{-j\beta_a z} + V_a^- e^{j\beta_a z}\right\}. \tag{2.22}$$

As defined, V and I are nothing more than mode coefficients, phasors that represent the amplitude and phase of excitation of each and every waveguide mode. Most typically one employs waveguide at a frequency below cut-off for all but one mode, the *fundamental mode* or *dominant mode*---just the mode with the lowest β_c. In this case one may rightly expect that only the coefficients for the fundamental mode are non-negligible. Even so, we leave in all the coefficients for the time being. We will find in later work that the usefulness of V and I arises in coupled systems, where one waveguide is joined to another, or to a cavity, or where an obstacle or aperture has been placed in the waveguide. At waveguide junctions, discontinuities or obstacles, evanescent modes play an important role, even while their spatial extent is limited.

Next we develop the circumstances that motivate and justify the terminology "voltage" and "current," and form the basis for the microwave electronics circuit analogy for waveguide systems. Let us consider each mode as consisting of two *channels*, corresponding to right- and left-going waves. From Eqs. (2.19) and (2.20) voltage and current in each channel are proportional by a constant with units of impedance,

$$Z_{ca}(\omega) I_a^\pm = \pm V_a^\pm, \qquad \text{(characteristic mode impedance)} \tag{2.23}$$

where $\pm$ denotes the wave flowing in the $\pm\hat{z}$ direction. Evidently these channels are uncoupled in smooth waveguide, insofar as the forward-channel or forward-going current is determined only by the forward-going voltage. To make further progress, we must make a brief digression into *mode orthogonality*.

A number of integral relations can be established demonstrating the independence of each mode as a channel of communication through the waveguide. To demonstrate these relations one calls on the eigenvalue equations for $\tilde{H}_z$ and $\tilde{E}_z$, the boundary conditions, Green's theorem, and, in the case of degenerate modes, Gram-Schmidt orthogonalization. We will simply list the results, assuming orthogonalized modes,

$$\int d^2 r_\perp E_{\perp a}(\vec{r}_\perp) \bullet E_{\perp b}(\vec{r}_\perp) = \delta_{ab}. \tag{2.24}$$

$$\int H_{\perp a} \bullet H_{\perp b} d^2 r_\perp = \frac{\delta_{a,b}}{Z_{ca}^2}, \tag{2.25}$$

$$\int d^2 r_\perp \hat{z} \bullet \left(E_{\perp a} \times H_{\perp b}\right) = \delta_{ab} Z_{ca}^{-1}. \tag{2.26}$$

It is also helpful to note the orthogonality and norm of the full fields,

$$\int \tilde{E}_a \bullet \tilde{E}_b^* d^2 r = \frac{\beta_0^2}{\beta_a^2} \delta_{a,b}\ , \qquad \text{(TM Mode)} \tag{2.27}$$

$$\int \tilde{H}_a \bullet \tilde{H}_b^* d^2 r = \frac{\beta_0^2}{\beta_a^2} \frac{1}{Z_{ca}^2} \delta_{a,b}. \qquad \text{(TE Mode)} \tag{2.28}$$

(Note that from our choice of normalization the longitudinal fields are pure imaginary).

With these results in hand we can derive the basic relations that constrain the circuit-equivalent description of a microwave system. Let us first compute the power flowing in a particular channel in terms of voltage and current. Using Eq. (2.25), one may express the power flow in the waveguide in terms of V and I according to

$$\begin{aligned} P &= \tfrac{1}{2} \Re \int d^2 r\, \tilde{E}_t \times \tilde{H}_t^* \\ &= \tfrac{1}{2} \Re \sum_a \sum_b V_a(z,\omega) I_b^*(z,\omega) Z_{cb}(\omega) \int d^2 r\, E_{\perp a}(\vec{r}_\perp) \times H_{\perp a}(\vec{r}_\perp) \\ &= \tfrac{1}{2} \Re \sum_a \sum_b V_a(z,\omega) I_b^*(z,\omega) Z_{cb} \delta_{ab} Z_{ca}^{-1} = \tfrac{1}{2} \Re \sum_a V_a I_a^* \end{aligned} \tag{2.29}$$

In addition, given the orthogonality relations, one can determine V and I uniquely from the transverse fields at a point z,

$$V_a(z,\omega) = \int d^2 r_\perp \tilde{E}_t(\vec{r}_\perp, z) \bullet E_{\perp a}(\vec{r}_\perp), \tag{2.30}$$

$$I_a(z,\omega) = Z_{ca} \int d^2 r_\perp \tilde{H}_t(\vec{r}_\perp, z) \bullet H_{\perp a}(\vec{r}_\perp), \tag{2.31}$$

and this is enough to determine the solution everywhere in the uniform guide, since this fixes the right- and left-going amplitudes. Moreover it shows that V and I in any particular mode are functionally indepedent of the the other V's and I's. Given the uniqueness of V and I, their relation to power, and the units (volts, amperes) it is natural to refer to them as *voltage* and *current*. It is important to keep in mind however that they appear as complex mode amplitudes, not work done on a charge or time rate of change of charge.

Let us also take account of stored energy. The energy stored per unit volume in electric fields is $w_e = \tfrac{1}{4} \varepsilon_0 \tilde{E} \bullet \tilde{E}^*$, and in magnetic fields $w_m = \tfrac{1}{4} \mu_0 \tilde{H} \bullet \tilde{H}^*$. It is natural to associate w_e with capacitance and w_m with inductance. This can be made precise by means of the complex Poynting theorem. We return to Maxwell's equations in the frequency domain,

$$\vec{\nabla}\times\tilde{E}=-j\omega\mu\tilde{H},\qquad \vec{\nabla}\times\tilde{H}=j\omega\varepsilon\tilde{E}+\tilde{J},$$

considering a current source term, for example, $\tilde{J}=\sigma\tilde{E}$ within some region. Next we make use of the vector identity,

$$\vec{\nabla}\bullet\left(\tilde{E}\times\tilde{H}^{*}\right)=\tilde{E}\bullet\left(\vec{\nabla}\times\tilde{H}^{*}\right)-\tilde{H}^{*}\bullet\left(\vec{\nabla}\times\tilde{E}\right),$$

and combine it with Maxwell's equations to produce

$$\vec{\nabla}\bullet\left(\tilde{E}\times\tilde{H}^{*}\right)=j\omega\left(\tilde{D}^{*}\bullet\tilde{E}-\tilde{B}\bullet\tilde{H}\right)-\tilde{J}^{*}\bullet\tilde{E}.$$

This we integrate over any volume *V*, with the result

$$\oint_{\partial V}\tilde{E}\times\tilde{H}^{*}\bullet d\vec{S}=\omega\int_{V}dV\left(\varepsilon^{*}\left|\tilde{E}\right|^{2}-\mu^{*}\left|\tilde{H}\right|^{2}\right)-\int_{V}dV\tilde{J}^{*}\bullet\tilde{E}.$$

In vacuum this takes the form

$$\frac{1}{2}\int_{\partial V}\tilde{E}\times\tilde{H}^{*}\bullet d\vec{S}=-\frac{1}{2}\int_{V}\tilde{E}\bullet\tilde{J}^{*}+2j\omega\int_{V}\left(w_{e}-w_{m}\right)dV. \tag{2.32}$$

Employing this result together with the formulation of waveguide modes in terms of voltage and current, we can describe a cavity's response in terms of an impedance, as seen in the next exercise.

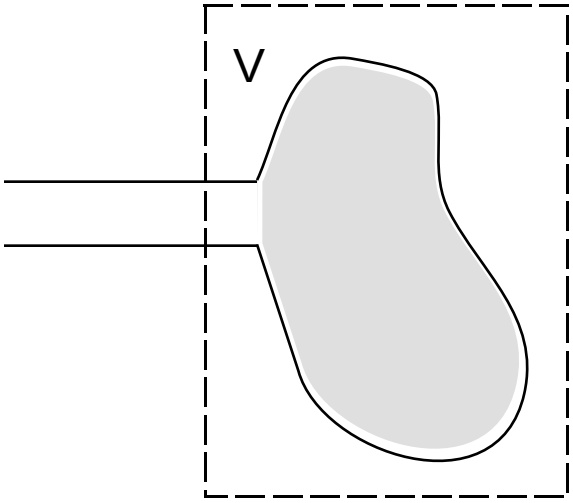

FIGURE 2.2. Sketch for application of the complex Poynting theorem to formulate the notion of impedance of a cavity.

Exercise 2.5 Consider a waveguide operated in fundamental mode, attached to a cavity, all encased in a perfect conductor, as illustrated in Fig. 2.2. Show that the "impedance looking into the cavity" $Z=V_1/I_1$ (with V_1 and I_1 the fundamental mode voltage and current coefficients) takes the form

$$Z = \frac{1}{|I_1|^2}\left\{\int_V \tilde{E}\bullet\tilde{J}^* + 4j\omega\int_V (w_m - w_e)\,dV\right\}. \tag{2.33}$$

Expressing this as $Z=R+jX$, identify the equivalent resistance and reactance.

2.5 Phase and Group Velocity

In the midst of the single-frequency circuit analogy, transient phenomena should not be forgotten. Let us consider, in the time-domain, the manner in which signals may propagate in a waveguide mode. Suppose that by some external means, a narrow-band signal is imposed at z=0,

$$V(t,0) = f(t)e^{j\omega_0 t},$$

where the phasor f may be slowly modulated in time. In the frequency domain we have

$$\tilde{V}(\omega,0) = \int_{-\infty}^{\infty}\frac{dt}{\sqrt{2\pi}} f(t)e^{j(\omega_0-\omega)t},$$

and the modulation may be expressed as

$$f(t) = \int_{-\infty}^{\infty}\frac{d\omega}{\sqrt{2\pi}}\tilde{V}(\omega,0)e^{j(\omega-\omega_0)t}.$$

Let us compute the voltage at a location z,

$$V(t,z) = \int_{-\infty}^{\infty}\frac{d\omega}{\sqrt{2\pi}}\tilde{V}(\omega,0)e^{j\omega t-j\beta z} \approx \int_{-\infty}^{\infty}\frac{d\omega}{\sqrt{2\pi}}\tilde{V}(\omega,0)e^{j\omega t-j\beta(\omega_0)z-j\frac{d\beta}{d\omega}(\omega_0)(\omega-\omega_0)z}$$

$$\approx e^{j\omega_0 t-j\beta(\omega_0)z}\int_{-\infty}^{\infty}\frac{d\omega}{\sqrt{2\pi}}\tilde{V}(\omega,0)e^{j(\omega-\omega_0)\left(t-\frac{d\beta}{d\omega}(\omega_0)z\right)t} \approx e^{j\omega_0\left(t-z/V_\varphi\right)} f\left(t-z/V_g\right).$$

We can see that constant phase-fronts travel at the *phase-velocity*

$$V_\varphi = \frac{\omega}{\beta} \tag{2.34}$$

while any modulation in f travels at the *group-velocity*

$$V_g = \frac{d\omega}{d\beta}. \tag{2.35}$$

For a mode in uniform guide,

$$V_\varphi = \frac{\omega}{\sqrt{\beta_0^2-\beta_c^2}} = \frac{1}{\sqrt{\mu\varepsilon}}\frac{1}{\sqrt{1-\beta_c^2/\beta_0^2}} \geq \frac{1}{\sqrt{\mu\varepsilon}},$$

$$V_g = \frac{1}{\sqrt{\mu\varepsilon}}\frac{\beta}{\beta_0} = \frac{1}{\sqrt{\mu\varepsilon}}\sqrt{1-\beta_c^2/\beta_0^2} \le \frac{1}{\sqrt{\mu\varepsilon}}.$$

Thus in straight guide the phase-velocity is never less than the speed of light in the medium. The group velocity is never more. Equality results only if β_c=0 and, as we know, that requires a TEM mode. None of this is too mysterious in the picture of the waveguide mode as a superposition of plane waves. The plane waves are individually propagating at the speed of light in the medium---however, unless the mode is a TEM mode, they are propagating at an angle to the *z*-axis. For this reason it takes longer for amplitude modulations to make their way from one point to another in the guide. Phase-velocity is larger than the speed of light simply because the phase-fronts are propagating at an angle, so that crests sweep down the *z*-axis at superluminal speeds. A similar phenomenon can be seen at a beach with long breakers incident on the beach at a slight angle. The point of wave-breaking may move at very high speed along the beachfront. For a surfer on the wave-crest, however, the speed of motion along the beachfront can be quite small.

2.6 Attenuation

In the foregoing discussions we considered lossless waveguide. Let us now consider the effect of finite wall resistivity, as indicated in Fig. 2.3. Taking the real part of Eq. (2.32) we obtain the change in forward-going power in the waveguide, from entrance to exit of the volume,

$$\Delta P = \tfrac{1}{2}\Re\oint_{\partial V}\tilde{E}\times\tilde{H}^*\bullet d\vec{S} = \tfrac{1}{2}\omega\int_V dV\left(\Im(\varepsilon)\left|\tilde{E}\right|^2 - \Im(\mu)\left|\tilde{H}\right|^2\right) - \tfrac{1}{2}\int_{V'} dV\sigma\left|\tilde{E}\right|^2,$$

where the volume *V′* is the region inside the conductor. Let us consider the case where losses in the bulk medium are negligible, $\Im\varepsilon = \Im\mu = 0$, and take over the result from Sec. 1 for the field profile within a conductor,

$$\tilde{E} \approx \frac{1}{\sigma}\vec{\nabla}\times\tilde{H} = -Z_s\hat{n}\times\tilde{H}_0\exp\left\{-\frac{\xi}{\delta}(1+j\,\mathrm{sgn}\,\omega)\right\},$$

where $\tilde{H}_0$ is the tangential magnetic field at the conducting surface, which is to a good approximation just the magnetic field one computes by assuming a perfectly conducting surface. With this expression, the integral over *V′* can be reduced to an area integral over the inner conducting face of the waveguide. Taking now the length of the volume Δz to be small, the area integral can be reduced to a line integral around the inner circumference of the waveguide cross-section,

$$\Delta P = -\tfrac{1}{2}\int_{V'} dV\sigma\left|\tilde{E}\right|^2 = -\frac{1}{2}R_s\oint_{\partial S} dl\left|\tilde{H}\right|^2\Delta z = \frac{dP}{dz}\Delta z.$$

The path ∂S bounds the cross-section *S* of the waveguide. Observing that the integral is quadratic in the fields, and therefore proportional to power, we may introduce the *attenuation parameter*, α,

$$\frac{dP}{dz} = -2\alpha P, \tag{2.36}$$

where

$$\alpha = \frac{1}{2} R_s \frac{\oint_{\partial S} dl \left| \tilde{H} \right|^2}{\Re \int d\vec{S} \bullet \tilde{E} \times \tilde{H}^*}. \qquad \text{(independent of norm)} \tag{2.37}$$

Thus in the presence of losses, the propagation constant takes on a small imaginary part, $j\beta \to \gamma = j\beta - \alpha$. With the Slater normalization, we may also express Eq. (2.40) as

$$\alpha = \frac{1}{4}\left(\frac{R_s}{Z_c} \right) \oint_{\partial S} dl \left| Z_c \tilde{H} \right|^2. \qquad \text{(Slater norm)}$$

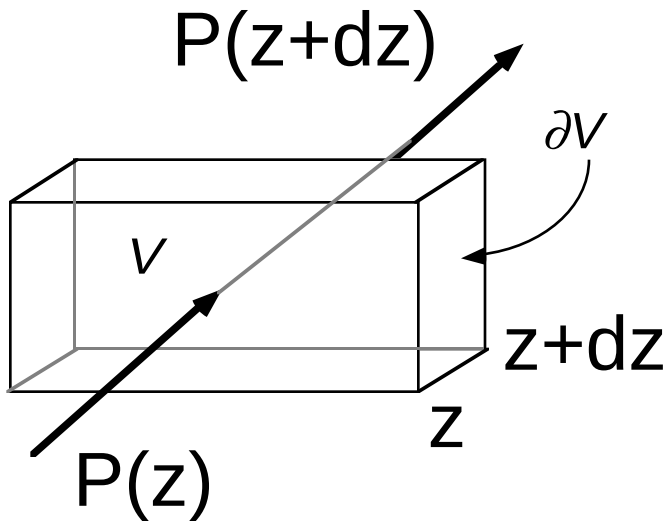

FIGURE 2.3. Geometry for calculation of attenuation in waveguide.

Exercise 2.6 Show that the attenuation constant for the TE_{10} mode of rectangular guide is given by

$$\alpha = \frac{R_S}{Z_0}\left[\frac{\omega^2}{c^2}\frac{1}{b} + 2\frac{\beta_c^2}{a} \right] \frac{c}{\omega}\left(\frac{\omega^2}{c^2} - \beta_c^2 \right)^{-1/2}. \tag{2.38}$$

Sketch the result as a function of frequency and explain the high and low frequency behavior in words. Why is WR90 operated in the frequency range of 8-12 GHz? Consulting Table 2.1, and the TE_{10} mode attenuation formula, confirm that the operating ranges and attenuations quoted are reasonable.

Table 2.1 Examples of standard rectangular waveguide.

Designation	*a* (inch)	*b* (inch)	*f* (GHz)	Attenuation (dB/100 ft)
WR650	6.50	3.25	1.1 - 1.7	0.3-0.2 (copper)
WR284	2.84	1.34	2.6 - 4.0	1.1-0.8 (copper)
WR90	0.90	0.4	8.2 -12.4	6.5-4.5 (copper)
WR62	0.62	0.31	12.4 - 18	9.5-8.3 (copper)
WR28	0.28	0.14	26.4 - 40	22-15 (silver)
WR10	0.10	0.05	75 - 110	>100 (silver)

Exercise 2.7 Show that the attenuation constant for TEM mode in coaxial cable with $\varepsilon \approx \varepsilon_0$ takes the form,

$$\alpha = \frac{1}{2}\left(\frac{R_S}{Z_c}\right)\frac{\left(\frac{1}{a}+\frac{1}{b}\right)}{\ln\left(\frac{b}{a}\right)}. \tag{2.39}$$

Most coax makes use of polyethylene dielectric, and attenuation occurs due not only to the "skin-effect" losses accounted for in the result above, but to those in the bulk of the dielectric. Starting from the dispersion relation $\beta = \omega\sqrt{\mu\varepsilon}$, argue that in general the attenuation constant should consist of two terms, $\alpha = \alpha_{skin}\sqrt{f} + \alpha_{bulk} f$, depending on the frequency *f*.

2.7 Impedance is a Many-Splendored Thing

The case of TEM mode in coaxial cable is illuminating for it provides a simple working example of the differences between low-frequency and high-frequency electronics. We may see an analogy between low-frequency circuits and microwave circuits for hollow waveguide, but it is at best an analogy, since hollow waveguide does not support a zero-frequency mode. For coaxial cable one can compare directly the microwave circuit notions, and the ordinary low-frequency concepts. In most engineering texts on the subject, the example of TEM mode is discussed at length for this reason.[15] Consider the solution as derived in a previous exercise, with voltage coefficient as in our circuit analogy,

$$\psi = k\ln\left(\frac{r}{a}\right)\tilde{V}(z,\omega), \quad \tilde{E}_\perp = \hat{r}\frac{k}{r}\tilde{V}(z,\omega), \qquad \tilde{H}_\perp = \hat{\phi}\frac{k}{r}\tilde{I}(z,\omega).$$

The coefficients take the form of forward and reverse waves,

$$\tilde{V}(z,\omega) = V_+(\omega)e^{-j\beta z} + V_-(\omega)e^{j\beta z}, \qquad Z_0\tilde{I}(z,\omega) = V_+(\omega)e^{-j\beta z} - V_-(\omega)e^{j\beta z},$$

and the propagation constant is $\beta = \omega\sqrt{\mu\varepsilon}$. Some observations are in order. First, the coefficient $\tilde{V}$ is not the line integral of the electric field between the conductors,

$$V_0 = \psi(b) = \left(\frac{\ln\left(\frac{b}{a}\right)}{2\pi}\right)^{1/2} \tilde{V}(z,\omega).$$

Nor for that matter does $\tilde{I}$ correspond to the physical current that the inner conductor would need to provide in order to support the magnetic field,

$$I_0 = \oint \tilde{H}_\perp \bullet d\vec{l} = \int_0^{2\pi} d\phi\, r\, \tilde{H}_\phi = \left(\frac{2\pi}{\ln\left(\frac{b}{a}\right)}\right)^{1/2} \tilde{I}(z,\omega).$$

As a result, the characteristic TEM mode impedance Z_c=Z_0 is not the same entity as the cable impedance used at low frequency,

$$Z_{cable} = \frac{V_0}{I_0} = \frac{1}{2\pi}\ln\left(\frac{b}{a}\right) Z_0. \tag{2.40}$$

As described this is simply a matter of normalization, but it is good to be aware of the ambiguity in the notion of impedance. Actually, the ambiguity is deeper than this. One very sensible definition of impedance is

$$Z = \frac{\tilde{V}(z,\omega)}{\tilde{I}(z,\omega)} = Z_0 \frac{V_+(\omega)e^{-j\beta z} + V_-(\omega)e^{j\beta z}}{V_+(\omega)e^{-j\beta z} - V_-(\omega)e^{j\beta z}}, \tag{2.41}$$

referred to as the "*impedance looking into the plane at z*." The implication is that as long as one thinks that impedance should be a ratio of voltage and current, then, regardless of the normalization, the impedance depends on where one looks (on z). One can also see how this problem was escaped at low frequency. The z-dependence is significant only if one is working over a range of z such that $\beta z \approx 1$. This motivates a simple definition of a microwave circuit: a circuit comparable to a wavelength in size. In such a circuit, effects of spatial phase-shifts and interference become noticeable.

This discussion helps to clarify that one may encounter many useful definitions of impedance, wave impedance of the medium, characteristic impedance of a mode (in a waveguide filled with this medium), cable impedance, and terminal impedance. Later we will develop also the notion of "impedance seen by the beam." It is best to remember that the notion of "impedance" is a tool we use, and in general one has to ask what definition of impedance is being used and why.

Having contemplated the wonders of waveguide, let us connect it to a thing or two.

Exercise 2.8 (**Impedance Transformation**) Consider a transmission line with characteristic impedance Z_c, and a signal with wavenumber β on the line. Show that the impedance looking into terminal #1, Z_1=V_1/I_1, may be related to the impedance looking into terminal #2, Z_2=V_2/I_2, according to

$$\frac{Z_2}{Z_c} = \frac{\frac{Z_1}{Z_c} - j\tan(\beta L)}{1 - j\frac{Z_1}{Z_c}\tan(\beta L)}. \tag{2.42}$$

2.8 Shunt Admittance of an Iris

Up to this point our treatment of waveguide propagation may have seemed a bit artificial, insofar as we have considered a reverse and a forward wave with no particular discussion of what caused the waves in the first place. In general we will be interested in a waveguide connected to a cavity, perhaps itself attached to other cavities. We may be interested in intersecting waveguides. Our primary tool for understanding these systems will be the notion of impedance introduced in Eq. (2.43). We consider the simplest of examples, as illustrated in Fig. 2.4, consisting of straight waveguide operated "in fundamental mode" (*i.e.*, below cutoff for all higher modes), with a thin, perfectly conducting obstacle placed transversely to the wave. This could by a symmetric iris, for example.

Let us consider the solution for the fields in this geometry, for a wave V_F incident from $z\rightarrow-\infty$. We know that the fields are completely specified once the transverse components are known. A general solution in uniform guide must take the form

$$\tilde{E}_t = \sum_a E_{\perp a}(\vec{r}_\perp)\left(V_a^+ e^{-j\beta_a z} + V_a^- e^{j\beta_a z}\right),\ \ \tilde{H}_t = \sum_a H_{\perp a}(\vec{r}_\perp) Z_{ca}(\omega)\left(I_a^+ e^{-j\beta_a z} + I_a^- e^{j\beta_a z}\right),$$

where $Z_{ca} I_a^\pm = \pm V_a^\pm$. However, this is only a "general solution" in *uniform guide*, and, having introduced an obstacle, we have split the guide into *two* lengths of uniform guide that are coupled. Thus the coefficients in the mode sum may take different values to the left and the right of the obstacle, for any obstacle worth its salt. Note that only the fundamental mode, call it mode 1, is propagating. Other modes evanesce with attenuation per unit length of

$$\gamma_a = -j\beta_a = \sqrt{\beta_{ca}^2 - \beta_0^2}\ .$$

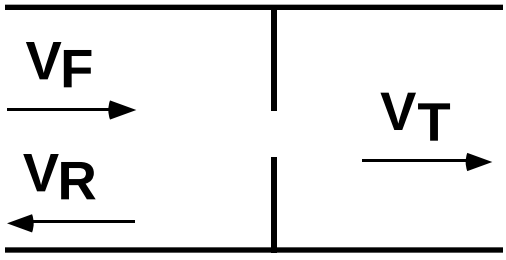

FIGURE 2.4. The "forward" wave V_F is incident from large negative z, and results in a reverse wave V_R reflected toward negative z and a wave V_T transmitted to positive z.

Their effect in this problem is to provide field matching; as a consequence of their presence, some energy is stored in the vicinity of the obstacle. If this energy is stored primarily in electric fields, we may say the obstacle is *capactive*; if primarily in magnetic fields, the obstacle is *inductive* in character. Since these fields should evanesce away from the obstacle, and not grow without bound, we exclude from the solutions the growing exponential terms.

Taking into account the foregoing comments, we may write out our mode sums more explicitly, for $z<0$,

$$\tilde{E}_t = E_{\perp 1}(\vec{r}_\perp)\left(V_F e^{-j\beta_a z} + RV_F e^{j\beta_a z}\right) + \sum_{a\neq 1} E_{\perp a}(\vec{r}_\perp) V_a^+ e^{\gamma_a z},$$
$$\tilde{H}_t = H_{\perp 1}(\vec{r}_\perp)\left(V_F e^{-j\beta_a z} - RV_F e^{j\beta_a z}\right) + \sum_{a\neq 1} H_{\perp a}(\vec{r}_\perp) V_a^+ e^{\gamma_a z},$$

and for $z>0$,

$$\tilde{E}_t = E_{\perp 1}(\vec{r}_\perp) TV_F e^{-j\beta_a z} + \sum_{a\neq 1} E_{\perp a}(\vec{r}_\perp) V_a^- e^{-\gamma_a z},$$
$$\tilde{H}_t = H_{\perp 1}(\vec{r}_\perp) TV_F e^{-j\beta_a z} + \sum_{a\neq 1} H_{\perp a}(\vec{r}_\perp) V_a^- e^{-\gamma_a z}.$$

In these expressions, we have introduced the *reflection coefficient*,

$$R(\omega) = \frac{V_R}{V_F},$$

the ratio of reverse to incident forward *voltage*, a quantity that is complex in general. We have also introduced the transmission coefficient,

$$T(\omega) = \frac{V_T}{V_F},$$

the ratio of transmitted to incident forward voltage. To solve this problem explicitly, one would like to match the fields across the plane $z=0$ and this requires some knowledge of the iris geometry. However, one can make some general statements independent of such details.

First, the transverse electric field must vanish on either side of the obstacle, since it is assumed to be a perfect conductor, and is placed transversely to the direction of propagation. Second, in the port, the tangential electric field must be continuous, a consequence of Faraday's law, or if one likes, the case of matching the field at a boundary between two identical media. Thus the transverse electric field must be continuous at $z=0$, as illustrated in Fig. 2.5. Thus $\tilde{E}_t\left(z=0^-\right) = \tilde{E}_t\left(z=0^+\right)$, or

$$E_{\perp 1}(\vec{r}_\perp) V_F (1+R) + \sum_{a\neq 1} E_{\perp a}(\vec{r}_\perp) V_a^+ = E_{\perp 1}(\vec{r}_\perp) V_F T + \sum_{a\neq 1} E_{\perp a}(\vec{r}_\perp) V_a^-.$$

Taking the dot product of both sides of this expression with $E_{\perp 0}(\vec{r}_\perp)$ and integrating over the waveguide cross-section, we obtain, from mode orthogonality,

$$1 + R = T, \qquad \text{(continuity of transverse electric field)} \qquad (2.43)$$

Next, let's consider the transverse magnetic field. According to Ampere's law, in the port the magnetic field will be continuous since there are no current sources there. However, it need not vanish at the conducting obstacle, for there wall currents may flow in such a way as to cancel out the field within the conductor. Thus there are no grounds for declaring that transverse magnetic field is continuous across the entire waveguide cross-section. In terms of current coefficients,

$$Z_{c1}I_F = V_F, \qquad Z_{c1}I_R = -V_R, \quad Z_{c1}I_T = V_T .$$

This discontinuity of the magnetic field amounts to some "missing current," $I_F + I_R \neq I_T$. We may say that some current, $I_S = I_F + I_R - I_T$, has been *shunted* to ground, and we may adopt a circuit picture, as illustrated in Fig. 2.6. Wall current is flowing through the iris and modifying the fields. This shunt current arises to cancel the longitudinal H field at the iris. Therefore, recalling Eq. (2.22), shunt current is proportional to the voltage at the iris, $V_T = V_F + V_R$. Thus we may define a *shunt admittance*,

$$Y_S = \frac{I_S}{V_T},$$

that depends only on the geometry of the iris, the mode, and the frequency, but not on the incident signal amplitude.

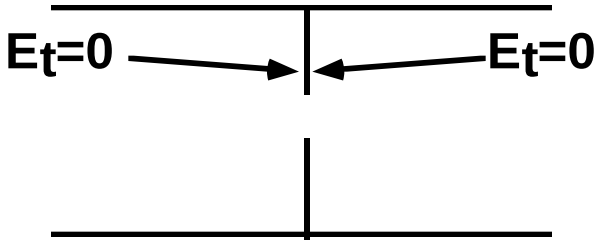

FIGURE 2.5. The transverse electric field is continuous across a thin obstacle.

Combining the foregoing, one may show that

$$Y_S(\omega) = \frac{-2R(\omega)}{1+R(\omega)} Y_{c1}(\omega), \tag{2.44}$$

where

$$Y_{c1} = \frac{1}{Z_{c1}} = \frac{1}{Z_0} \times \begin{cases} \dfrac{\beta}{\beta_0} & TE \text{ mode} \\ 1 & TEM \text{ mode} \end{cases} \tag{2.45}$$

is the *characteristic admittance* of this waveguide mode. Thus the shunt admittance is determined once the reflection coefficient is known, and vice versa.

Some common language is helpful to know. One often employs the *normalized shunt admittance*

$$\hat{Y}_S = \frac{Y_S}{Y_{c1}} = Y_S Z_{c1} = \frac{-2R}{1+R}. \tag{2.46}$$

In addition, one may express admittance in terms of real and imaginary parts, $Y_s = G_s + jB_s$, where G_s is called the *conductance* and B_s the *susceptance*. In the case of a thin, lossless obstacle, one has simply a shunt susceptance. A fair body of literature is available on the calculation of shunt susceptance of a mode---typically

the fundamental mode---for obstacles of various geometries. Starting with the earliest, Marcuvitz[16] provides a catalog of results, Montgomery, Dicke and Purcell[17] provide examples of its use, and Jackson[18] provides a very readable introduction to the variational technique. Modern works include textbooks by Collin,[19] and Felsen and Marcuvitz.[20]

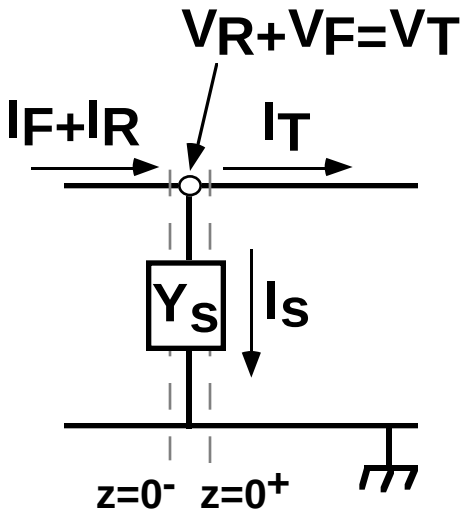

FIGURE 2.6. Equivalent circuit for a thin iris on a waveguide operated in a single mode.

2.9 VSWR

The reflection coefficent on a line is quantified by the *voltage-standing wave ratio* or *VSWR*; it is a figure of merit for microwave components. To define VSWR, consider a waveguide operating in fundamental mode, with voltage

$$\tilde{V}(z) = V_F e^{-j\beta z} + V_R e^{j\beta z},$$

and imagine a small probe sampling but not perturbing the electric field in the waveguide. Let us suppose the output signal is proportional to the time-averaged squared voltage V_{rms}^2, and compute this. The real voltage as a function of time is

$$V(z,t) = \Re\left\{\tilde{V}(z)e^{j\omega t}\right\} = \Re\left\{V_F e^{j\omega t - j\beta z} + V_R e^{j\omega t - j\beta z}\right\},$$

and we wish to compute the mean squared voltage,

$$V_{rms}^2(z) = \frac{\omega}{2\pi}\int_0^{2\pi/\omega} dt\, V(z,t)^2,$$

and after some algebra the result is

$$V_{rms}^2 = \frac{1}{2}\left\{|V_F|^2 + |V_R|^2 + 2\Re\left(V_F V_R^* e^{-2j\beta z}\right)\right\}.$$

This is an oscillatory function of z, with period equal to one-half the guide

wavelength of the mode. Maxima and minima of this curve are

$$\max V_{rms} = |V_F| + |V_R|, \qquad \min V_{rms} = |V_F| - |V_R|.$$

Therefore if the output of the detector is plotted versus position on the slotted line, we should get a curve looking something like that of Fig. 2.7. From such a curve one can determine the guide wavelength (and thus the frequency), and one can determine the ratio between the maxima and mimima of the standing-wave pattern, the VSWR

$$\text{VSWR} = \frac{\max V_{rms}}{\min V_{rms}} = \frac{|V_F| + |V_R|}{|V_F| - |V_R|}. \tag{2.47}$$

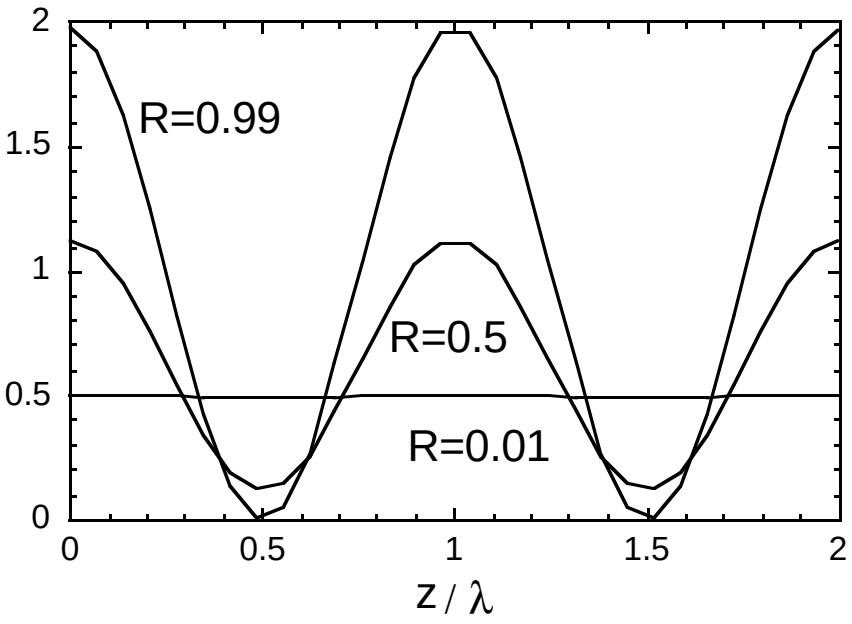

FIGURE 2.7. Illustration of squared voltage versus probe position normalized to the guide wavelength, for various values of the reflection coefficient *R*.

In terms of the reflection coefficient, this may be expressed simply as

$$\text{VSWR} = \frac{1 + |R|}{1 - |R|}. \tag{2.48}$$

Evidently, VSWR≥1, with VSWR=1 only in the case of no reflection---a "perfect match." In the case of total reflection, VSWR→∞. Observe that VSWR is a function of frequency, since *R* is. In fact, microwave components come with specifications for maximum VSWR over a range of frequency. *Low* VSWR over a

broad band costs extra.

Exercise 2.9 Consider fundamental mode lossless guide with an iris and a short as illustrated in the sketch. In terms of angular frequency ω, wavenumber b, and shunt admittance Y of the iris, determine the reflection coefficient as a function of z, the distance to the left of the iris. If the admittance is a pure susceptance, what is the VSWR on the line?

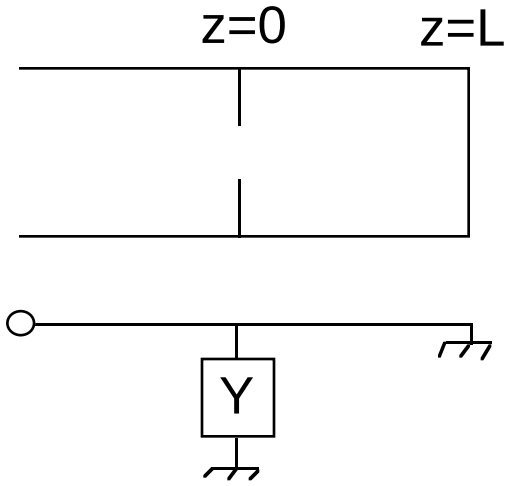

2.10 An Elementary Cavity

In the discussion at the end of Sec. 1, we found that, for electromagnetic acceleration, we required either (1) a terminated interaction or (2) a synchronous mode, one with phase-velocity equal to c, for an extended interaction. We then embarked on the treatment of waveguide to appreciate how power could be coupled into such an interaction region, so as to accelerate a beam. We will consider (1) in detail in Sec. 3, and (2) in Sec. 4. However, with the help of the previous analyses, we are at a point where we can consider case (1), in its most elementary form, without beam: the filling of a cavity with microwave energy. In Sec. 2.11 we will provide a similar elementary treatment of case (2).

For illustration we will make a cavity from a length of waveguide terminated in an iris followed by a shorting plane, as seen in Fig. 2.8. The turn-on of the rf drive corresponds to the launching of a wave down the waveguide, toward the cavity formed by the iris and the short. For a small iris one expects that most of the incident wave will be promptly reflected. Some of the wave will scatter through the obstacle. The forward wave in the cavity travels to the short, is reflected, returns to the iris, radiates a little bit through it, but for the most part is reflected. Over time, the cavity *fills*, and in steady-state the prompt reflection of the incident wave at the iris *interferes* with the radiation from the cavity. Thus during the transient filling of the cavity a left-going signal or "reverse voltage" appears; in steady-state the reverse voltage may look different.

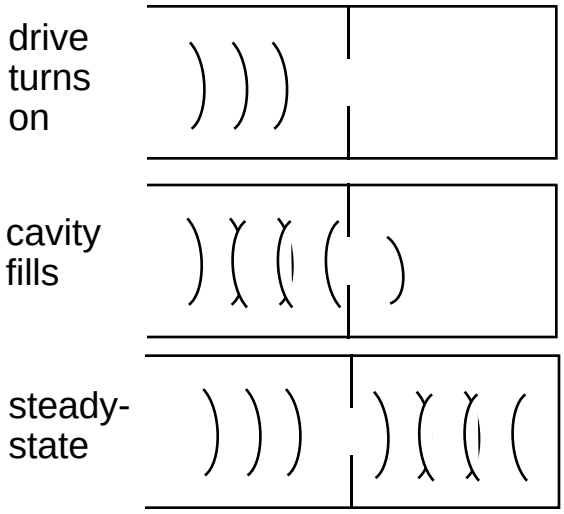

FIGURE 2.8. Illustration of the transient filling of a cavity. For simplicity we consider a length of waveguide terminated in a shorting plane. In front of the plane is an obstacle, for example, a thin iris.

To characterize this system we must perform a calculation and this will be aided by the circuit-equivalent picture of Fig. 2.9. An incident wave represented by phasor $\tilde{V}_+$ results in a prompt reflected wave $R\tilde{V}_+$, where R is the (complex) reflection coefficient of the iris. This coefficient is just the steady-state reflection coefficient of the iris when placed on smooth waveguide. Meanwhile, a wave $T\tilde{V}_+$ is transmitted through the iris. This wave will travel to the short, be reflected, and return to the iris in a time $\tau=2L/V_g$ where V_g is the group velocity in the unloaded guide. Let us refer to the right-going wave phasor, just to the right of the iris, and evaluated at time $n\tau$, as $\tilde{A}(n)$. Evidently $\tilde{A}(0) = T\tilde{V}_+$. To determine the cavity voltage on subsequent bounces we simply follow this wave through the cavity and back to the iris. Propagation to the shorting plane corresponds to the map $\tilde{A}(n) \to e^{-\gamma L}\tilde{A}(n)$, where $\gamma = j\beta + \alpha$ is the propagation coefficient for the smooth guide, and is determined from the guide wavenumber β, and the attenuation parameter α. Reflection at the shorting plane corresponds to $e^{-\gamma L}\tilde{A}(n) \to -e^{-\gamma L}\tilde{A}(n)$, and we neglect losses on the endwall for simplicity. Propagation back to the iris corresponds to $-e^{-\gamma L}\tilde{A}(n) \to -e^{-2\gamma L}\tilde{A}(n)$, and reflection there results in $-e^{-2\gamma L}\tilde{A}(n) \to -Re^{-2\gamma L}\tilde{A}(n)$. Evidently the right-going amplitude in the cavity on the next bounce is

$$\tilde{A}(n+1) = T\tilde{V}_+ - Re^{-2\gamma L}\tilde{A}(n).$$

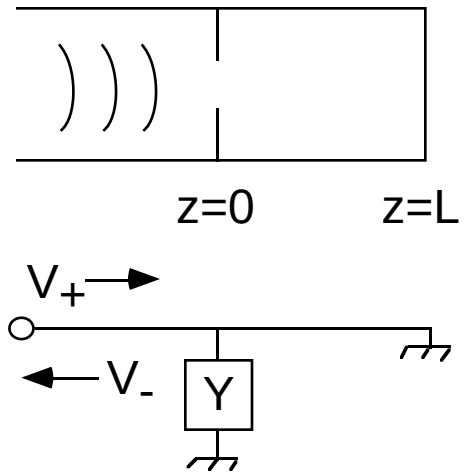

FIGURE 2.9. Transmission line picture for the cavity filling problem. The cavity has length L, and the iris corresponds to a normalized shunt admittance Y. The forward voltage V_+ is specified, and we wish to solve for the reflected signal, and the wave amplitudes in the cavity.

Similar reasoning shows that the left-going wave to the left of the iris, $\tilde{V}_-(n)$, satisfies

$$\tilde{V}_-(n+1) = R\tilde{V}_+(n+1) - Te^{-2\gamma L}\tilde{A}(n).$$

Due to the finite losses on a single-bounce, the system reaches a steady-state, where $\tilde{A}(n+1) = \tilde{A}(n)$. In this limit, we have

$$\frac{\tilde{A}}{\tilde{V}_+} = \frac{T}{1+Re^{-2\gamma L}}. \tag{2.49}$$

The reflected signal will asymptote to

$$\frac{\tilde{V}_-}{\tilde{V}_+} = \frac{R+\left(R^2-T^2\right)e^{-2\gamma L}}{1+Re^{-2\gamma L}}. \tag{2.50}$$

We can simplify these results by taking account of our previous work on the problem of a thin obstacle in a guide. We found that continuity of tangential electric field at the thin iris implies $T=1+R$. In addition, the reflection coefficient is related to the normalized shunt admittance, and for a lossless obstacle we may express R in terms of the normalized shunt susceptance, $\hat{B}$,

$$\frac{1}{R} = -1 + j\frac{2}{\hat{B}}.$$

Thus in this problem there are only two free geometric parameters, one is $\hat{B}$ and the other is the cavity length L.

Exercise 2.10 Show that the condition for zero reverse wave in steady-state (*critical coupling*) corresponds to

$$\frac{R}{1+2R} = \exp(-2\gamma L),$$

and confirm that, for small losses ($\alpha L << 1$) this may be expressed as

$$\cos 2\beta L = \exp(-2\alpha L) \Leftrightarrow \beta L \approx N\pi, \qquad \text{(resonance)}$$

$$\sin 2\beta L = -2/\hat{B} \Leftrightarrow \hat{B} \approx 1/\sqrt{\alpha L}, \qquad \text{(matching)}$$

where N is an integer. Check that the steady-state amplitude is much larger than the incident voltage, $\tilde{A}/\tilde{V}_+ \approx -j/2\sqrt{\alpha L}$.

2.11 An Elementary Periodic Line

Let us consider next how to produce a synchronous wave, with phase-velocity equal to *c*---*i.e.*, how to design a dispersion relation. In Sec. 2.10 we considered the effect of one iris; let us next analyze the effect of many irises forming a periodically loaded waveguide, as depicted in Fig. 2.10. In the smooth portion of the waveguide, a general solution for voltage and current phasors in a single mode is

$$V(z) = V_n^+ e^{-j\beta z} + V_n^- e^{j\beta z} \quad (-L < z < 0),$$
$$Z_{c1} I(z) = V_n^+ e^{-j\beta z} - V_n^- e^{j\beta z} \quad (-L < z < 0),$$

with iris separation L. Recall Z_{c1} is the characteristic impedance of the fundamental waveguide mode,

$$Z_{c1} = Z_0 \frac{\beta_0}{\beta},$$

and β is the propagation constant, or wavenumber, $\beta = \left(\beta_0^2 - \beta_c^2\right)^{1/2}$, with β_c the cutoff wavenumber. Let us compute the wave incident on the next port, and in this way formulate propagation in a periodically-loaded guide. This notation comes with the picture of Fig. 2.11.

Just to the right of the *n*-th iris we have

$$V(z) = V_{n+1}^+ e^{-j\beta(z-L)} + V_{n+1}^- e^{j\beta(z-L)} \quad (0 < z < L),$$
$$Z_{c1} I(z) = V_{n+1}^+ e^{-j\beta(z-L)} - V_{n+1}^- e^{j\beta(z-L)} \quad (0 < z < L).$$

To solve for V_{n+1}^+, V_{n+1}^- we apply two conditions. The voltage at node *n* is continuous (since tangential electric field is continuous at a thin iris), so

$$V(0-) = V(0+) \quad \Leftrightarrow \quad V_n^+ + V_n^- = V_{n+1}^+ e^{j\beta L} + V_{n+1}^- e^{-j\beta L}.$$

Since current is shunted through the iris, there is a discontinuity in tangential magnetic field given by

$$I\,(0+) = I\,(0-) - Y_s V(0),$$

and this may be written

$$V_{n+1}^{+} e^{j\beta L} - V_{n+1}^{-} e^{-j\beta L} = V_n^{+} - V_n^{-} - \hat{Y}_s\left(V_n^{+} + V_n^{-}\right),$$

abbreviating, $\hat{Y}_s = Y_s Z_{c1}$. These are two equations for V_{n+1}^{+}, V_{n+1}^{-} in terms of V_n^{+}, V_n^{-}.

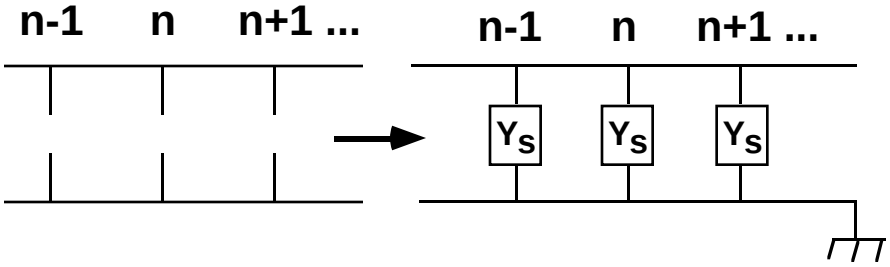

FIGURE 2.10. We examine a waveguide periodically-loaded with thin irises, and develop a transmission line model as indicated on the right.

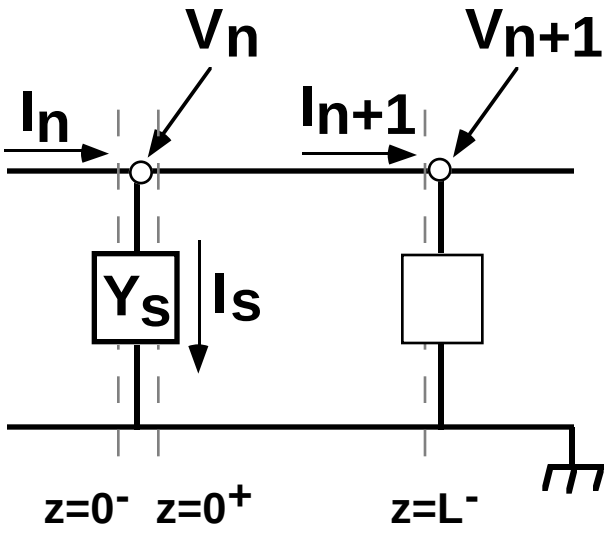

FIGURE 2.11. Notation for voltages and currents in the vicinity of an iris.

Solving them we find,

$$\begin{pmatrix} V^{+} \\ V^{-} \end{pmatrix}_{n+1} = \mathbf{M} \begin{pmatrix} V^{+} \\ V^{-} \end{pmatrix}_{n},$$

where

$$\mathbf{M} = \begin{pmatrix} \left(1 - \frac{\hat{Y}_s}{2}\right) e^{-j\theta_0} & -\frac{\hat{Y}_s}{2} e^{-j\theta_0} \\ \frac{\hat{Y}_s}{2} e^{j\theta_0} & \left(1 + \frac{\hat{Y}_s}{2}\right) e^{j\theta_0} \end{pmatrix}$$

and $\theta_0 = \beta L$ is the phase-advance per cell in the unloaded line. The matrix $\mathbf{M}$ describes propagation on the loaded line. Notice that $\det \mathbf{M} = 1$ and

$$\frac{\mathrm{tr}\mathbf{M}}{2} = \cos\theta_0 + j\frac{\hat{Y}_s}{2}\sin\theta_0 .$$

The eigenvalues of $\mathbf{M}$ are then

$$e^{j\theta_\pm} = \frac{\mathrm{tr}\mathbf{M}}{2} \pm j\sqrt{1 - \left(\frac{\mathrm{tr}\mathbf{M}}{2}\right)^2} .$$

and they convey attenuation and phase-shift in the loaded line. In the simplest case of a *lossless* junction, we have a pure susceptance, $\hat{Y}_s = j\hat{B}_s$, and the dispersion relation for the loaded line takes the form

$$\cos\theta = \cos\theta_0 - \frac{\hat{B}_s}{2}\sin\theta_0 . \qquad (2.51)$$

A sketch of θ and θ_0 versus ω is depicted in Fig. 2.12 for illustration. Note that for some frequencies, in the loaded guide, there is no solution for real θ. The presence of such "stop-bands" corresponds, in the wave picture, to destructive interference over the course of multiple reflections from each obstacle.

Let us define $\theta^{(0)}$ to be the solution for phase-advance per cell in the interval $-\pi < \theta^{(0)} < \pi$. Evidently then $\theta^{(n)} = \theta^{(0)} + 2n\pi$ is also a solution. In terms of phase-advance one may define a wavenumber for the loaded line, $\beta^{(0)} = \theta^{(0)} / L$ and evidently there are infinitely many of these,

$$\beta^{(n)} = \beta^{(0)} + \frac{2n\pi}{L} .$$

The implication of this is that a periodic line will support infinitely many "space-harmonics," all propagating with the same group velocity,

$$V_g^{(n)} = \left(\frac{d\beta^{(n)}}{d\omega}\right)^{-1} = \left(\frac{d\beta^{(0)}}{d\omega}\right)^{-1} = V_g^{(0)},$$

but all with different phase-velocities,

$$V_\varphi^{(n)} = \left(\frac{\beta^{(n)}}{\omega} \right)^{-1} = \left(\frac{\beta^{(0)}}{\omega} + \frac{2n\pi}{\omega L} \right)^{-1} = \left(1 + \frac{2n\pi}{\beta^{(0)} L} \right)^{-1} V_\varphi^{(0)}.$$

In general, in driving such a transmission line, one excites fields that correspond to a superposition of space-harmonics. The field lines include the contribution of the evanescent fields that arise in the vicinity of the irises.

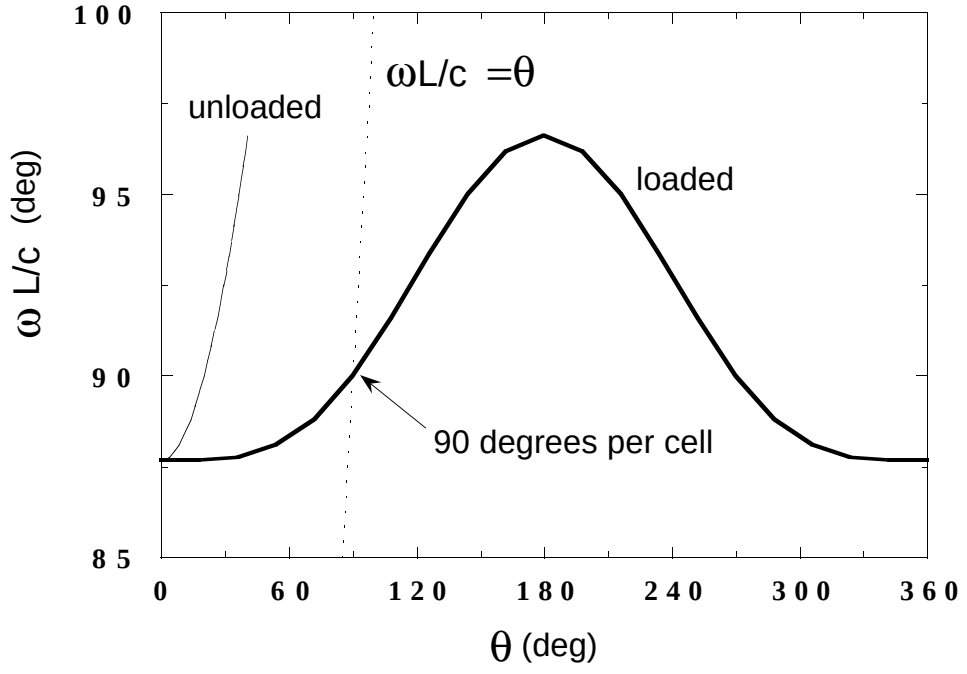

FIGURE 2.12. Dispersion relation for smooth guide and a guide periodically loaded with capactive shunts (Brillouin diagram).

2.12 Common Microwave Elements

Before turning to analyze cavities and periodic lines for acceleration, we should take a moment to note that a practical waveguide network for an accelerator will include more than just straight waveguide and an accelerator cavity. To describe common elements in the most simple fashion, it is helpful first to consider the S-matrix for a network of lines connected to a device (sometimes called the "device under test" or DUT) as illustrated in Fig. 2.13.

To simplify our work, we assume all the transmission line impedances are the same (renormalizing voltages if necessary). Typically the DUT will consist only of copper; we will assume at least, though, that any medium in the DUT may be described by lossless, symmetric ("reciprocal"), linear permittivity and permeability

tensors. We define the S-Matrix for the DUT element-wise as follows. Let voltage V_b^+ be incident on line *b*, and all other lines terminated in their characteristic impedance (matched load on all other ports). Let the voltage transmitted to the load on the *a*-th port be V_a^-, then $S_{ab} = V_a^- / V_b^+$ is the *a*-*b* element of the scattering matrix for the DUT. Notice that since the voltage coefficients in a transmission line depend on the plane of reference, the S-matrix is not uniquely specified unless the reference planes for the measurement are defined. If there are *N* ports then the scattering matrix is an $N \times N$ matrix of frequency-dependent elements. Lorentz reciprocity implies that for such a source-free device, the S-matrix must be symmetric, $S_{ab} = S_{ba}$, or $\mathbf{S}^t = \mathbf{S}$. Since the device is lossless the complex Poynting theorem implies that the scattering matrix is unitary, $\overline{\mathbf{S}} = \mathbf{S}^{-1}$, where recall that $\left(\overline{\mathbf{S}}\right)_{ab} = (\mathbf{S})^*_{ba}$ is the hermitian conjugate. To prove these statements it is helpful to know how to describe the DUT in terms of admittance or impedance matrices. The admittance matrix $\mathbf{Y}$ relates total current at the reference plane in the port to total voltage at the respective reference planes in each port,

$$I_a = V_a^+ - V_a^- = \sum_b (\mathbf{Y})_{ab} V_b = \sum_b (\mathbf{Y})_{ab} \left(V_b^+ + V_b^-\right),$$

or, in vector form,

$$\vec{I} = \vec{V}^+ - \vec{V}^- = \mathbf{Y}\left(\vec{V}^+ + \vec{V}^-\right) = \mathbf{Y}\vec{V}.$$

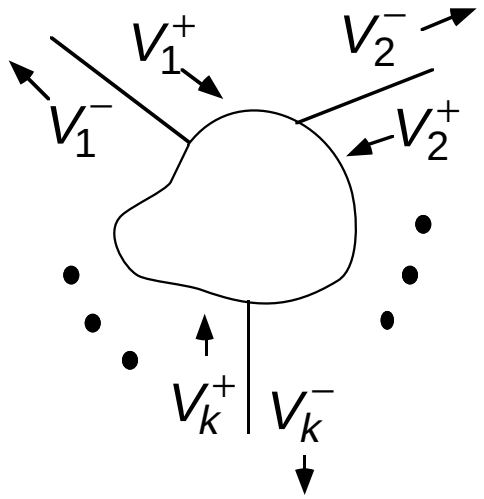

FIGURE 2.13. The general problem of network analysis for a device under test attached by means of ports to a series of transmission lines, labelled *k*=1,...,*N*.

The impedance matrix $\mathbf{Z}$ relates voltage to current, $\vec{V} = \mathbf{Z}\vec{I}$, and is evidently just the inverse of the admittance matrix, $\mathbf{Z} = \mathbf{Y}^{-1}$. On the other hand, using the definition of the scattering matrix, and the principle of superposition, we have $\vec{V}^- = \mathbf{S}\,\vec{V}^+$, and this permits us to determine the scattering matrix in terms of the

admittance or impedance matrices. Specifically,

$$\vec{V}^+ - \vec{V}^- = \mathbf{Y}\left(\vec{V}^+ + \vec{V}^-\right) \Rightarrow (\mathbf{I}-\mathbf{Y})\vec{V}^+ = (\mathbf{I}+\mathbf{Y})\vec{V}^- \Rightarrow \vec{V}^- = (\mathbf{I}+\mathbf{Y})^{-1}(\mathbf{I}-\mathbf{Y})\vec{V}^+,$$

so that $\mathbf{S} = (\mathbf{I}+\mathbf{Y})^{-1}(\mathbf{I}-\mathbf{Y})$.

Exercise 2.11 Show that $\mathbf{S} = (\mathbf{Z}+\mathbf{I})^{-1}(\mathbf{Z}-\mathbf{I})$.

Symmetry of the S-matrix then follows from the symmetry of the admittance matrix, $\mathbf{Y} = \mathbf{Y}^t$. Unitarity of the S-matrix follows for a lossless junction from $\mathbf{Z} = \mathbf{Z}^*$. Modern vector network analyzers permit one to measure *S*-matrices in a very straightforward fashion, provided the DUT operates at frequencies below cut-off for all but fundamental mode in the connecting guide. The unitarity and symmetry theorems are extremely helpful insofar as they permit one to determine the minimum number of essential parameters needed to characterize an element.

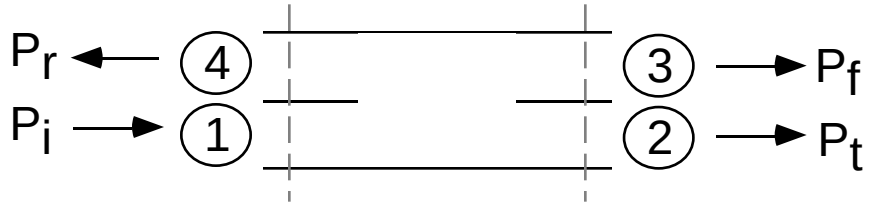

FIGURE 2.14. Illustration of a directional coupler.

For example, the most common microwave element is the *directional coupler*. This is a four-port device as illustrated in Fig. 2.14. An *ideal* directional coupler is symmetric upon reflection in the horizontal or vertical, is lossless and is perfectly matched. These conditions restrict the S-matrix to the form

$$\mathbf{S} = \begin{pmatrix} 0 & \alpha & j\sqrt{1-\alpha^2} & 0 \\ \alpha & 0 & 0 & j\sqrt{1-\alpha^2} \\ j\sqrt{1-\alpha^2} & 0 & 0 & \alpha \\ 0 & j\sqrt{1-\alpha^2} & \alpha & 0 \end{pmatrix},$$

for some parameter $\alpha \leq 1$, and choice of reference planes. A *real* directional coupler is described by coupling *C* and directivity *D*, defined with respect to the quantities indicated in the sketch: power incident on port 1, P_i, transmitted power to port 2, P_t, forward power on port 3, P_f, and reverse power, P_r, on port 4. The coupling and directivity are

$$C = 10\log_{10}\left(\frac{P_i}{P_f}\right), \quad \text{(coupling)} \qquad D = 10\log_{10}\left(\frac{P_f}{P_r}\right). \quad \text{(directivity)}$$

The isolation is defined according to

$$I = 10\log_{10}\left(\frac{P_i}{P_r}\right). \qquad \text{(isolation)}$$

A *hybrid tee* is a four-port device as illustrated in Fig. 2.15. In the ideal case, it is lossless and symmetry precludes coupling of ports 1 and 4. A *magic tee* is a hybrid tee that is matched on all ports; matching requires in practice obstacles (a post and a step) at the junction. A magic tee is formally equivalent to a 3 dB coupler, however, the natural choice of reference planes makes it easy to distinguish. Constraints of symmetry and unitarity reduce the possible forms of the S-matrix to just one, after a choice of reference planes,

$$\mathbf{S} = \frac{1}{\sqrt{2}}\begin{pmatrix} 0 & 1 & 1 & 0 \\ 1 & 0 & 0 & -1 \\ 1 & 0 & 0 & -1 \\ 0 & 1 & -1 & 0 \end{pmatrix}.$$

Exercise 2.12 (a) What is the directivity of an ideal directional coupler? Relate the coupling C to the S-matrix parameter α. **(b)**The SLAC modified Bethe hole coupler has a coupling of 52 dB and 80 dB isolation. What is the directivity? **(c)** An ideal "3 dB" coupler has $C=10\log_{10}2 \approx 3\text{dB}$ and infinite directivity. What is the S-matrix? **(d)**Compute the outgoing signals for the situation depicted in the sketch, and explain how a 3 dB coupler and a phase-shifter can be used to make a switch.

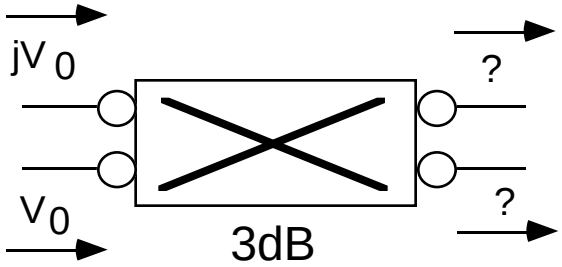

Exercise 2.13 (**Magic Tee**) Show that with voltages incident on arms 2 and 3, arm 4 provides a difference signal, and arm 3 a sum signal. Justify this referring to the field lines sketched in Fig. 2.15.

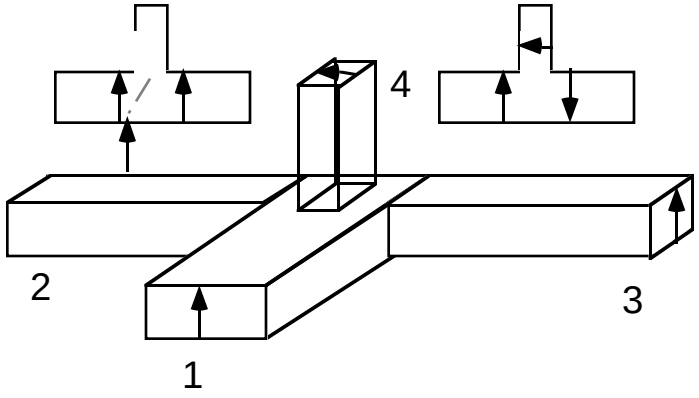

FIGURE 2.15. Illustration of a hybrid tee.

3. Standing-Wave Accelerators

We have reached a point now where we can deliver power by means of a waveguide and appreciate the coupling of a waveguide to a cavity, by means of an iris. We consider in this section the question: What are we looking for in a cavity? What features are important in characterizing its performance as an accelerator? Here we develop the subject of beam-cavity interaction for a relativistic beam, and the logical consequences.

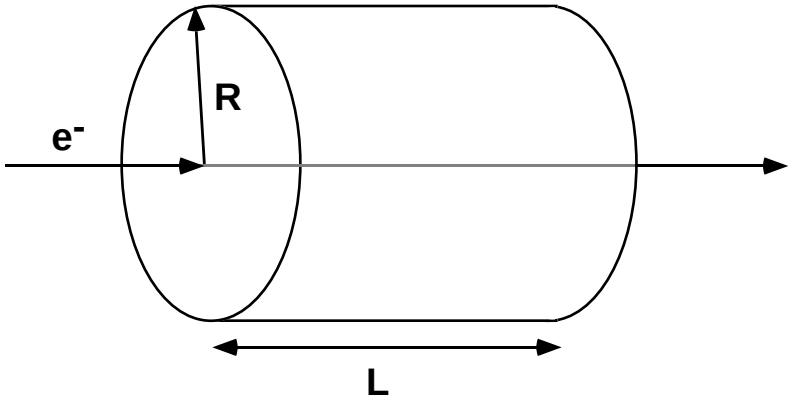

FIGURE 3.1. Acceleration in terminated waveguide.

We require an electric field, $\vec{E}$, to produce any change in particle energy, $\varepsilon = m_e c^2 \gamma$, *i.e.*, $d\varepsilon / dt = q\vec{E} \bullet \vec{V}$, where $\vec{V}$ is the particle velocity and q is the charge. We assume the beam is relativistic so that $V \approx c$ is constant. We suppose for simplicity, as in the previous section, that our cavity is formed by a terminated piece of straight waveguide. The mode employed should have an electric field component along the direction of beam motion. For ballistic motion along a beam axis $\hat{s}$, that coincides with the waveguide axis this requires a TM mode. The axial component of the electric field will take the form

$$E_s = \Re \tilde{E}_0 \exp(j\omega t - j\beta s),$$

where $\tilde{E}_0 = E_0 e^{j\varphi_{rf}}$, E_0 is the axial electric field amplitude, and φ_{rf} is the *rf-phase*. The particle energy will therefore vary according to

$$\frac{d\varepsilon}{ds} = \Re q\tilde{E}_0 \exp(j\omega t - j\beta s),$$

where we have changed the independent variable to *s*, with *ds=Vdt*. Notice that in this description, time *t* is a dependent variable,

$$\frac{dt}{ds} = \frac{1}{V} = \frac{1}{c}\left(1 - \frac{1}{\gamma^2}\right)^{-1/2},$$

and corresponds to the particle arrival time at *s*. For continuous acceleration in this field, one would need the beam-phase to remain stationary, implying that the

particle speed should match the phase velocity of the wave, $V \approx c \approx \omega/\beta$, as though the particle were riding the crest of a wave. This isn't possible, since for TM modes in smooth waveguide $\omega/\beta > c$ and the phase-fronts will always wash over the particle. Nevertheless one notices that the electron does gain energy for one-half of an rf-cycle, and this suggests terminating the interaction before the particle has slipped into the decelerating phase, as depicted in Fig. 3.1.

In this form it is straightforward to calculate the energy gain assuming the interaction is terminated. We situate the cavity entrance at s=0, and denote the particle arrival time at s=0 by t_0, so that,

$$t = t_0 + \frac{s}{V}.$$

The energy gain in travelling through a cavity of length L is then

$$\Delta\varepsilon = \Re q\tilde{E}_0 e^{j\omega t_0}\int_0^L ds \exp js\left(\frac{\omega}{V}-\beta\right) = \Re q\tilde{E}_0 e^{j\omega t_0}\,\frac{\exp jL\left(\frac{\omega}{V}-\beta\right)-1}{j\left(\frac{\omega}{V}-\beta\right)}.$$

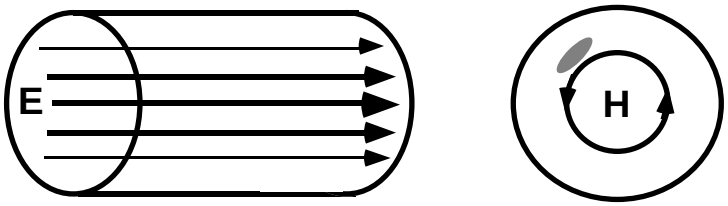

FIGURE 3.2. TM_{010} mode of a right cylindrical pillbox. No ports yet.

3.1 Geometry and [*R/Q*]

To make further quantitative progress with this idea, we need to decide on the actual mode to be employed. Clearly, the "terminated interaction" amounts to using a cavity, since the rf fields cannot make it down the pipe, they must be trapped. In principle we have many choices as to the kind of cavity we pick.[21] Historically, cylindrical cavities have been easier to make, so let us consider those. We will need to plan for ports, at least one port for the input waveguide, and at least two holes for the beam to enter and exit ("beam ports"), but we can treat these later as *perturbations*. Let us consider then just the TM modes in a closed right cylindrical cavity as illustrated in Fig 3.2. In principle we may construct such modes as superpositions of modes of straight guide. In straight guide TM modes are determined by $\tilde{E}_z$ satisfying

$$\left(\frac{1}{r}\frac{\partial}{\partial r}r\frac{\partial}{\partial r}+\frac{1}{r^2}\frac{\partial^2}{\partial\phi^2}+\beta_c^2\right)\tilde{E}_z(r) = 0.$$

In view of cylindrical symmetry, we may decompose any solution into azimuthal

harmonics, varying as $e^{jm\phi}$. For such harmonics one obtains Bessel functions for the radial variation,

$$\tilde{E}_z(r,z) = J_m(\beta_c r)e^{jm\phi}e^{-j\beta s}.$$

The condition $\tilde{E}_z(r=R,s)=0$ dictates that $J_m(\beta_c R)=0$. We may then label these TM modes according to the corresponding zero of the Bessel function, $\beta_c = \beta_{mn} = j_{mn}/R$, where j_{mn} is the n-th root of the m-th Bessel function. To accomodate waveguide shorts at s=0 and s=L, we must consult the transverse fields,

$$Z_0\tilde{H}_\perp = \frac{\beta_0}{j\beta_c^2}\hat{s}\times\nabla_\perp\tilde{E}_z, \qquad \tilde{E}_\perp = \frac{\beta}{j\beta_c^2}\nabla_\perp\tilde{E}_z,$$

and superimpose solutions in such a way as to enforce conducting boundary conditions

$$\tilde{E}_\perp(s=0,r) = \tilde{E}_\perp(s=L,r) = 0, \quad \hat{\phi}\bullet\tilde{E}_\perp(s,r=R)=0, \qquad \hat{r}\bullet\tilde{H}_\perp(s,r=R)=0.$$

Note that the normal component of the magnetic field at the shorting planes is automatically zero for a TM mode. The remaining boundary condition we can meet (1)with $\beta=0$ (infinite phase-velocity wave) or (2) by adding a forward $e^{-j\beta s}$ and reverse $e^{j\beta s}$ wave to form a standing wave. Abbreviating $\psi = E_0 J_m(\beta_c r)e^{jm\phi}$, with normalization constant E_0, the result is

$$\tilde{E}_z(r,s) = \psi\cos\beta s, \qquad \tilde{E}_\perp = \frac{\beta}{\beta_c^2}\sin\beta s\vec{\nabla}_\perp\psi, \quad Z_0\tilde{H}_\perp = \frac{\beta_0}{j\beta_c^2}\cos\beta s\,\hat{s}\times\vec{\nabla}_\perp\psi.$$

The boundary condition at s=L requires $\sin\beta L=0$, or $\beta=\beta_p=\pi p/L$. The resulting mode then has three indices and is referred to as the TM$_{mnp}$ mode. The mode frequencies are

$$\omega_{mnp} = c\left\{\left(\frac{j_{mn}}{R}\right)^2+\left(\frac{p\pi}{L}\right)^2\right\}^{1/2},$$

and we have taken $\mu=\mu_0$ and $\varepsilon=\varepsilon_0$ since we will be passing a beam through this cavity and will probably want a high vacuum.

Next let us discriminate among these modes with an eye to acceleration. Only m=0 modes have a non-zero field on-axis. To decide on the best TM$_{0np}$ mode to use we don't have much to go on yet. Let us consider a particle passing through the cavity on-axis, as in the previous section. It witnesses a field

$$E_z = E_0\cos(\beta s)\cos(\omega t+\varphi_{rf}).$$

Exercise 3.1 Decompose this result into left- and right-going waves. Making use of the transit angles

$$\theta_{\pm} = \left(\frac{\omega}{V} \pm \beta\right)L = \frac{c}{V}\left\{\left(j_{on}\frac{L}{R}\right)^2 + (p\pi)^2\right\}^{1/2} \pm p\pi\,,$$

argue that in the TM_{mnp} mode with $p \neq 0$, the transit angle with respect to the backward wave will be larger than $2\pi p$, corresponding to deceleration, and only the forward wave will contribute to acceleration.

Exercise 3.1 suggests using one of the TM_{0n0} modes, as depicted in Fig. 3.3. For these modes, the transit angle is

$$\theta = \frac{\omega L}{V}, \tag{3.1}$$

or, more explicitly, $\theta = j_{on}L/R$. The energy gain may be expressed in terms of the transit angle factor,

$$T = \frac{\sin\left(\frac{1}{2}\theta\right)}{\left(\frac{1}{2}\theta\right)}, \tag{3.2}$$

as $\Delta\varepsilon = qE_0LT\cos\left(\omega t_0 + \varphi_{rf} + \frac{1}{2}\theta\right)$, and this may be expressed in terms of the *gap voltage* or *cavity voltage* phasor, $\tilde{V}_c = E_0LT\exp\left(j\varphi_{rf} + \frac{1}{2}j\theta\right)$, as

$$\Delta\varepsilon = \Re q\tilde{V}_c e^{j\omega t_0}\ . \tag{3.3}$$

Next let's determine the energy required to establish the accelerating voltage. The fields take the form

$$\vec{E} = \hat{z}E_0J_0(\beta_c r)\cos\left(\omega t + \varphi_{rf}\right), \qquad Z_0\vec{H} = \hat{\phi}E_0J_0'(\beta_c r)\sin\left(\omega t + \varphi_{rf}\right),$$

where $\beta_c = \omega_{0n0}/c$. The energy stored in the cavity is then

$$\begin{aligned}
U &= \frac{1}{2}\int dV\left(\varepsilon_0\vec{E}\bullet\vec{E} + \mu_0\vec{H}\bullet\vec{H}\right) = \left\langle\int dV\varepsilon_0\vec{E}\bullet\vec{E}\right\rangle \\
&= \frac{1}{2}\varepsilon_0E_0^2\int dVJ_0(\beta_c r)^2 = \frac{1}{2}\varepsilon_0E_0^2\int_0^R rdr\int_0^L ds\int_0^{2\pi}d\phi\,J_0(\beta_c r)^2 \\
&= \frac{1}{2}\varepsilon_0E_0^2 2\pi L\int_0^R rdrJ_0(\beta_c r)^2 = \varepsilon_0E_0^2\pi LR^2\int_0^1 uduJ_0(j_{on}u)^2 \\
&= \frac{1}{2}\varepsilon_0E_0^2\pi LR^2J_1(j_{on})^2,
\end{aligned}$$

where the brackets denote a time-average. The next question we might have: is this a lot or a little? We can compare stored energy and accelerating voltage directly by considering the amplitude independent ratio,

$$\left[\frac{R}{Q}\right] = \frac{\left|\tilde{V}_c\right|^2}{\omega U}, \tag{3.4}$$

or, explicitly,

$$\left[\frac{R}{Q}\right] = \frac{\left(E_0 LT\right)^2}{\omega \frac{1}{2}\varepsilon_0 E_0^2 \pi L R^2 J_1\left(j_{on}\right)^2} = \left[\frac{2}{\pi j_{on} J_1\left(j_{on}\right)^2}\right] Z_0 T^2 \frac{L}{R} \approx Z_0 T^2 \frac{L}{R}.$$

This quantity, with units of ohms, is referred to as the "*R* upon *Q*" or "*R* over *Q*"; the name and the notation are somewhat unwieldy, but that is convention. Rather than being two separate entities as the notation would imply, it is in fact *a single geometric quantity*. Notice that it has nothing to do with wall losses. Referring to a table of Bessel function zeroes,[22] the quantity in square brackets is equal to 0.982 for n=1, and within 2% of unity for all values of radial mode index n.

Next we might like to try to optimize our cavity, and obtain the largest acceleration for a given amount of energy. We suppose that the frequency has been chosen, thus fixing the cavity radius. In this case, the question amounts to: What is the best choice of transit angle? In terms of θ we have

$$\left[\frac{R}{Q}\right]_{TMono} = Z_0 \frac{2}{j_{on}} \frac{\sin^2\left(\frac{1}{2}\theta\right)}{\left(\frac{1}{2}\theta\right)},$$

varying from 0 at θ=0 through a maximum at θ=133.56° (T=0.788), to 0 again at θ=360°. In this form it is clear that maximum [*R/Q*] at fixed frequency favors the lowest radial mode, n=1, for in this case the cavity is longest. For the TM_{010} mode at optimal transit angle, $\left[R/Q\right] = 0.6\, Z_0 = 221\,\Omega$.

3.2 Loss Factor

Remarkably, [*R/Q*] determines more than just the stored energy required to establish a gap voltage. It also determines the radiation by a beam into the cavity mode. Let us consider a very short bunch of charged particles passing through a structure, as depicted in Fig. 3.3.

Such a bunch will radiate and lose some energy, if the geometry deviates in some way from a smooth perfectly conducting pipe. This is illustrated in Fig. 3.3. If the bunch is quite short, then particles will radiate coherently, so that the energy loss should be a quadratic function of beam charge, q_b, $\Delta\varepsilon = k_l q_b^2$. The quantity k_l, we will refer to as the *loss-factor* for a short bunch. In fact, given a complete enumeration of orthogonal modes for the geometry, one could represent the loss factor as a sum over the loss factors into each mode,

$$k_l = \sum_{\text{modes},\lambda} \left(k_l\right)_\lambda .$$

One of these modes, λ, is our resonant accelerating mode; let us consider that mode alone. After the beam has passed, the mode rings, just as a harmonic oscillator should after a sharp rap,

$$V_\lambda = V_{b\lambda} \cos \omega_\lambda t \, H(t).$$

The voltage waveform is sketched in Fig. 3.4. (Note that in the act of singling out one such narrow-band mode, we inevitably give up resolution of the full cavity-voltage during transient period of length L/c in the vicinity of the beam arrival time t=0.)

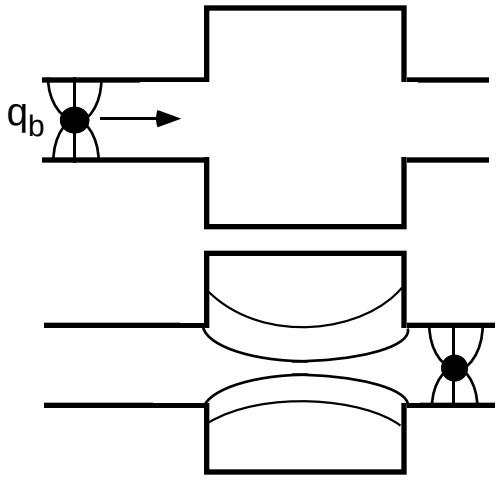

FIGURE 3.3. A charge q_b passing through a cavity deposits energy in the cavity. This energy is lost by the particle, and this energy loss arises from the action of a self-induced voltage V_b acting on the particle. The "shock" excitation of the cavity mode results in ringing at amplitude V_b after the beam has passed.

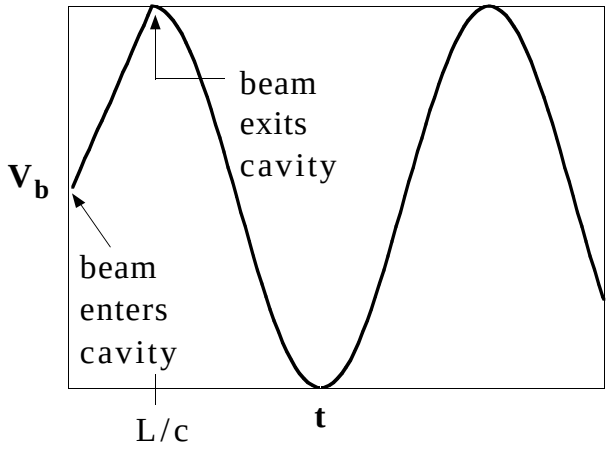

FIGURE 3.4. After a charge q_b has passed through a cavity, the cavity modes ring; here we see the beam-induced voltage in a single mode.

Notice in Fig. 3.4 that, averaged over the transit time, the beam witnesses *one-half* of the final, peak gap voltage. Thus, in order for the beam to lose energy $\Delta\varepsilon_\lambda = k_{l\lambda} q_b^2$ by the action of this self-induced voltage, the peak gap voltage must be $V_{b\lambda} = 2k_{l\lambda} q_b$. Meanwhile, this oscillation corresponds to a stored energy,

$$U = k_{l\lambda} q_b^2 = \frac{V_b^2}{\omega[R/Q]_\lambda} = \frac{\left(2k_{l\lambda} q_b\right)^2}{\omega[R/Q]_\lambda}.$$

We can solve this equation for the loss-factor in terms of the [*R/Q*],

$$k_{l\lambda} = \frac{1}{4}\omega\left[\frac{R}{Q}\right]_\lambda. \tag{3.5}$$

Notice that loss-factor has nothing a priori to do with wall-losses.

Thus [*R/Q*] measures the coupling of the mode to the beam, and the beam to the mode, it determines the energy required for acceleration, and determines how much energy the beam will deposit. Large [*R/Q*] implies that little energy is required to produce a large acceleration. Conversely, this implies a large beam-induced voltage, heavier "beam-loading." Good *accelerators* are good *decelerators.* In this light, it is easy to understand why we were having troubles in Sec. 1, with acceleration in free-space. This result for beam-induced voltage is often referred to as the *fundamental theorem of beam-loading*.

Exercise 3.2 Using the result for beam-induced voltage in mode λ, $dV_{b\lambda}$, from a single short bunch of charge dq_b, arriving at time t=0, $dV_{b\lambda}(t) = 2k_{l\lambda} dq_b \cos(\omega_\lambda t)$, argue that for a continuous current waveform $I(t)$, the net beam-induced voltage must take the form

$$V_{b\lambda}(t) = 2k_{l\lambda} \int_{-\infty}^{t} dt'\, I_b(t') \cos\left(\omega_\lambda [t - t']\right).$$

Go on to show that the beam-induced voltage satisfies the differential equation

$$\left(\frac{d^2}{dt^2} + \omega_\lambda^2\right) V_{b\lambda} = 2k_{l\lambda} \frac{dI_b}{dt}.$$

Justify the form of this equation in a few sentences, from first principles, making reference to Maxwell's equations. In the frequency domain, it is common to characterize beam interaction with a structure in terms of an impedance $Z_{||}$ such that $\tilde{V}_b(\omega) = Z_{||}(\omega)\tilde{I}_b(\omega)$. Show that the beam impedance for a lossless resonant mode λ, in terms of the mode frequency ω_λ, and $[r/Q] = \frac{1}{2}[R/Q]$, takes the form

$$Z_{||_\lambda}(\omega) = \frac{j[r/Q]_\lambda}{\left(\omega_\lambda/\omega - \omega/\omega_\lambda\right)}. \qquad \text{(lossless)}$$

3.3 Wall Losses

Having mentioned stored energy, we are naturally inclined to hook our cavity up to waveguide and fire away. First though let us consider where this energy really will go: it can be reflected, it can go into a beam, or it can be lost in the walls. We know from the work of Sec. 1, that wall-losses arise due to the penetration of the magnetic field into the conductor,

$$P_l = R_s \oint_{walls} dS \left\langle |H|^2 \right\rangle = 2 \times \oint_{endcap} (\ldots) + \oint_{sidewalls} (\ldots),$$

Let's compute the various integrals,

$$\oint_{endcap} (\ldots) = \frac{R_s E_0^2}{Z_0^2} \oint_{endcap} dS \left\langle \left[J_0'(\beta_c r) \sin\left(\omega t + \varphi_{rf}\right) \right]^2 \right\rangle = \frac{R_s E_0^2}{2 Z_0^2} \int_0^R r dr \int_0^{2\pi} d\phi \left[J_0'(\beta_c r) \right]^2$$

$$= \frac{\pi R_s E_0^2 R^2}{Z_0^2} \int_0^1 u du \left[J_0'(j_{on} u) \right]^2 = \frac{\pi R_s E_0^2 R^2}{2 Z_0^2} J_1(j_{on})^2.$$

Next,

$$\oint_{sidewalls} (\ldots) = \frac{R_s E_0^2}{Z_0^2} \oint_{sidewalls} dS \left\langle \left[J_0'(\beta_c r) \sin\left(\omega t + \varphi_{rf}\right) \right]^2 \right\rangle$$

$$= \frac{R_s E_0^2}{2 Z_0^2} \int_0^L ds \int_0^{2\pi} R d\phi \left[J_0'(\beta_c r) \right]^2 = \frac{\pi R_s E_0^2 L R}{Z_0^2} J_1'(j_{on})^2.$$

Thus the total power flowing into the walls is

$$P_l = \frac{\pi R_s E_0^2}{Z_0^2} J_1(j_{on})^2 R(R + L).$$

We may characterize this result in terms of *wall Q* defined according to

$$Q_w = \frac{\omega U}{P_l}. \tag{3.6}$$

In practical units we have

$$Q_w = \frac{j_{on}}{2} \frac{Z_0}{R_s} \frac{L}{L + R} \approx \frac{5.46 \times 10^4}{\sqrt{f(\text{GHz})}} \frac{1}{1 + R/L},$$

where, in the last equality, we selected the TM_{010} mode and used $R_s = 8.3\ \text{m}\Omega \sqrt{f(\text{GHz})}$ as for copper at room temperature. For our [*R/Q*] optimized cavity with θ=133.56° and *L/R*=0.969, this gives $Q_w = 2.69 \times 10^4 / \sqrt{f(\text{GHz})}$. In the time-domain,

$$\frac{dU}{dt} = -P_l = -\frac{\omega U}{Q_w}$$

and energy U_0 initially stored in the cavity will decay exponentially, according to

$$U = U_0 \exp\left(-\frac{\omega t}{Q_w}\right);$$

thus the fields decay with a time-constant

$$T_0 = \frac{2Q_w}{\omega} = \frac{Q_w}{\pi}\frac{1}{f}. \tag{3.7}$$

For an [*R/Q*] optimized cavity this gives $T_0 = 8.56\mu\text{s}/\,f(\text{GHz})^{3/2}$.

Thus far we have considered stored energy as though that were an important quantity to minimize. However, for practical purposes, one may wish to know, given the maximum microwave *power* available, what kind of accelerating voltage could be achieved. For this purpose let us suppose that we have figured out how to couple energy into the cavity (we will examine this shortly). If the beam to be accelerated is of sufficiently low current, then the maximum energy we can put into the cavity will be determined by a steady-state between power P_e flowing into the cavity, and thence into the walls. Let us assume the power source has a natural pulse length long enough to bring the cavity into this steady-state. Then

$$\frac{dU}{dt} = P_e - P_l = 0,$$

so that $P_e = P_l = \omega U / Q_w$. Since in this case our voltage is limited by the peak power available from the source, it is natural to define a quantity

$$R = Q_w\left[\frac{R}{Q}\right] = Q_w \frac{\left|\tilde{V}\right|^2}{\omega U} = \frac{\left|\tilde{V}\right|^2}{P_l}, \tag{3.8}$$

with units of ohms, and referred to as the *shunt impedance*. This quantity determines, at the practical level, what accelerating voltage one can achieve with a single cavity, in terms of the power available, assuming a pulse sufficiently long to reach steady-state. Using our optimum $[R/Q]$ parameters, one finds $R = 5.95\text{M}\Omega/\sqrt{f(\text{GHz})}$. A few illustrative numbers are included in Table 3.2, actual mileage will vary depending on the arrangement of beam ports and particulars of the cavity shape. In practice, introduction of beam ports can reduce [*R/Q*] by a factor of two. These are nevertheless, good "zeroth-order" estimates for single-cavity scalings versus frequency.

Exercise 3.3 If in fact our accelerator were peak-power limited, we might like to optimize our cavity design by maximizing *shunt impedance* as a function of transit angle. Show that the maximum shunt impedance for the first radial mode occurs for θ=158.08° (T=0.712, aspect ratio L/R=1.147) and is 7% larger than the result obtained for maximum [*R/Q*]. Show that the wall Q and decay time are 9% larger. Sample sensitivity to transit angle to determine that R is 67% of optimal for θ=90°, 89% for 120°, and 97% for 180°. Check that for the second radial mode, maximum shunt impedance occurs for θ=166.46° and corresponds to 63% of the maximum for the first radial mode. Confirm the TM_{010} scalings with transit angle illustrated in Fig. 3.5.

Exercise 3.4 For copper at room temperature and the TM_{010} mode of a right cylindrical cavity, make a table of scalings for Q_W, k_l, R_{shunt}, $[R/Q]$, T_0, and the steady-state power dissipation required to provide a 10-MeV/m accelerating gradient. Take note of the exponent by which each quantity varies with wavelength and the value at 2856 MHz. Assume a transit angle of $2\pi/3$.

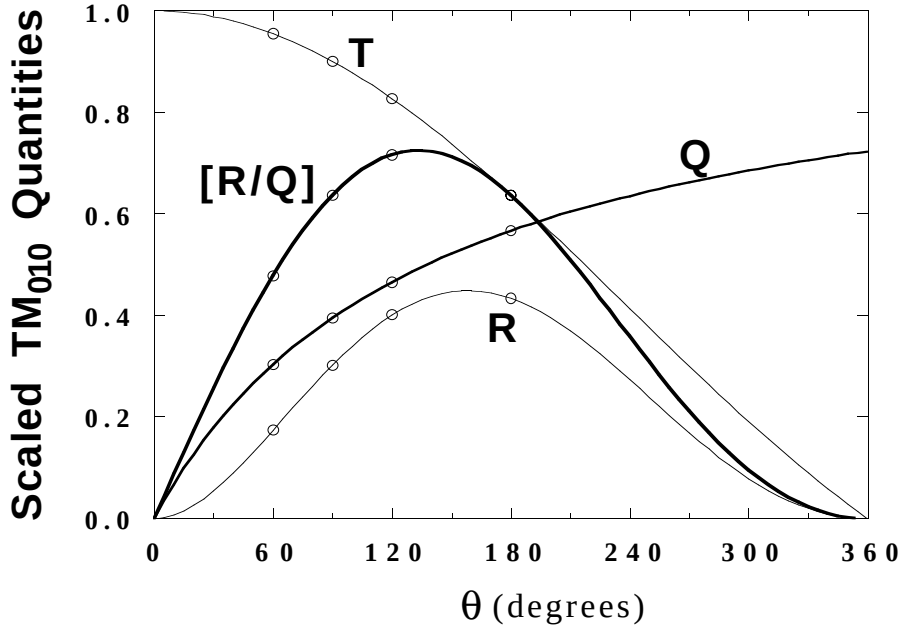

FIGURE 3.5. Scalings with transit angle for the TM_{010} mode of a closed pillbox.

Table 3.2 To illustrate the scaling of cavity parameters. θ=133.56°

band	frequency	Q_W	T_0	$[R/Q]$	R
UHF	714 MHz	3.2×10^4	14 μs	221 Ω	7 MΩ
S	2.856 GHz	1.6×10^4	1.8 μs	221 Ω	3.5 MΩ
X	11.424 GHz	8.0×10^3	0.22 μs	221 Ω	1.8 MΩ
W	91.392 GHz	2.8×10^3	9.8 ns	221 Ω	0.6 MΩ

3.4 Cavity With Beam and Ports

Now that we have a rough idea of what we are looking for in a cavity, let us consider putting a port on the cavity and the details of how to get power into it. Our question is: what do we want out of a port? We consider first a closed cavity with

perfectly conducting walls, and resonant angular frequency Ω_0,

$$\left\{\frac{d^2}{dt^2}+\Omega_0^2\right\}V_c=0. \qquad \text{(no port, beam or losses)}$$

We next cut a port in the cavity and connect it to waveguide. From our analysis of the thin iris in a waveguide, we understand that tangential electric field in the guide is continuous across the iris. This amounts to the statement that cavity voltage V_c must track the tangential electric field on the waveguide side of the iris. From our analysis of waveguide modes, we know that this tangential field amplitude varies as the sum of forward and reverse voltages, V^+ and V^-, in the waveguide, defined as in Sec. 2. At the same time, we recognize that the cavity voltage may be quite a bit larger than the voltages in the connecting guide. Indeed, as we saw in the example of Sec. 2, resonant charging of a cavity can produce large amplitude oscillations even when the driving displacement is small, much as in a swing or a pendulum. Recognizing this, let us employ normalized voltages, $V_F=nV^+,\ \ V_R=nV^-$, such that our continuity condition reads simply

$$V_c=V_F+V_R. \tag{3.9}$$

The factor *n* we will refer to as the *turns ratio*, or *transformer ratio*. Later, we will return and calculate *n*, based on conservation of energy.

Next we account for perturbations to our harmonic oscillator,

$$\left\{\frac{d^2}{dt^2}+\Omega_0^2\right\}V_c=[\text{lossy walls}]+[\text{waveguide}]+[\text{beam}].$$

Notice that each of the perturbatons may be thought of as a current. Wall current has been dealt with and for practical purposes its effect is damping. The beam current term also has been treated and its effect may be viewed as excitation of the oscillator. As for the waveguide "current term," this represents the threading of magnetic flux from the waveguide into the cavity, as illustrated in Fig. 3.6, and excitation of the oscillator by induction. We know from our analysis of waveguide modes that the amplitude of the magnetic field may be represented in terms of a current coefficient, itself, the difference in the forward and reverse voltages in the guide. Thus we may express our result as

$$\left\{\frac{d^2}{dt^2}+\omega_0^2\right\}V_c=-\frac{\omega_0}{Q_w}\frac{dV_c}{dt}+\frac{\omega_0}{Q_e}\frac{d}{dt}\left(V_F-V_R\right)+\omega_0\left[\frac{r}{Q}\right]\frac{dI_b}{dt}, \tag{3.10}$$

for some dimensionless coefficient Q_e, the *external Q*. The notation ω_0 we adopt for the resonant frequency *after* perturbations---having added finite wall conductivity and having cut copper to make the beam port and waveguide coupler. Introducing the *loaded Q*,

$$\frac{1}{Q_L}=\frac{1}{Q_e}+\frac{1}{Q_w}, \tag{3.11}$$

and making use of the continuity condition, we may rewrite this in the form

$$\left\{\frac{d^2}{dt^2}+\frac{\omega_0}{Q_L}\frac{d}{dt}+\omega_0^2\right\}V_c = 2\frac{\omega_0}{Q_e}\frac{dV_F}{dt}+\omega_0\left[\frac{r}{Q}\right]\frac{dI_b}{dt}. \tag{3.12}$$

A more formal development of this result can be found in Appendix C.

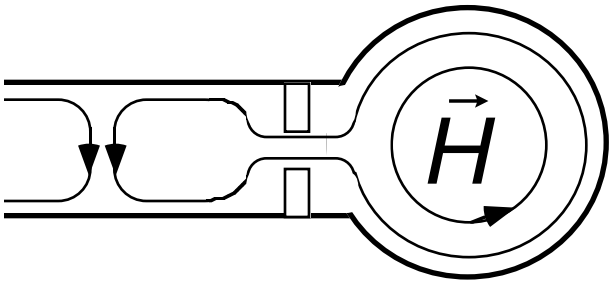

FIGURE 3.6. A waveguide excites a cavity via the threading of magnetic flux through the coupling iris, and Faraday's law. The beam travels into the page.

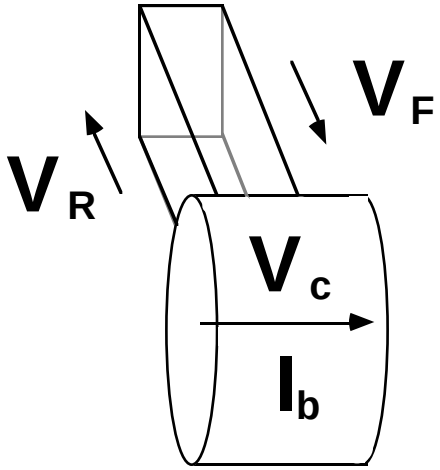

FIGURE 3.7. Sketch of the dynamic variables for a single cavity mode coupled to a waveguide fundamental mode, and a beam.

This simple model affords a complete description of the kinematics of the cavity-beam-waveguide system. The dynamic variables are summarized in Fig. 3.7. We will show later that it can be employed for multi-cavity systems. We turn next to explore the ramifications of the two coupling parameters we have introduced, external Q, and transformer ratio, n, and other features of this system.

3.5 Cavity on the Bench

Absent beam the system we have analyzed is the simplest of all microwave elements: it is a one-port element, the S-matrix is a single element S_{11}, that is a function of frequency, simply referred to as the reflection coefficient. If the cavity is lossless, then unitarity implies that $|S_{11}|=1$, and all power is reflected from the cavity. In the more interesting case of a cavity with wall losses, we may compute the reflection coefficient, using our waveguide-cavity equation, Eq. (3.12). Our model takes the form

$$\left\{\frac{d^2}{dt^2}+\frac{\omega_0}{Q_L}\frac{d}{dt}+\omega_0^2\right\}V_c = 2\frac{\omega_0}{Q_e}\frac{dV_F}{dt}.$$

We consider steady-state excitation at angular frequency ω,

$$V_F = \Re\left(\tilde{V}_F e^{j\omega t}\right), \qquad V_R = \Re\left(\tilde{V}_R e^{j\omega t}\right), \qquad V_C = \Re\left(\tilde{V}_C e^{j\omega t}\right).$$

Our equation takes the form

$$\left\{j\frac{\omega_0\omega}{Q_L}+\omega_0^2-\omega^2\right\}\tilde{V}_c = 2j\frac{\omega_0\omega}{Q_e}\tilde{V}_F.$$

It is conventional to characterize the difference in drive frequency from the resonant frequency of the cavity by the *tuning angle* ψ,

$$\tan\psi = Q_L\left(\frac{\omega_0}{\omega}-\frac{\omega}{\omega_0}\right). \tag{3.13}$$

In terms of tuning angle,

$$\tilde{V}_c = \frac{2\beta}{1+\beta}\cos\psi e^{j\psi}\tilde{V}_F, \tag{3.14}$$

and we have introduced the parameter β,

$$\beta = \frac{Q_w}{Q_e}. \tag{3.15}$$

Notice that tuning angle is the angle the cavity voltage phasor $\tilde{V}_C$ makes with the forward drive phasor $\tilde{V}_F$. On resonance, the two are in phase,

$$\tilde{V}_C = \frac{2\beta}{1+\beta}\tilde{V}_F, \qquad \left(\psi = 0 \Leftrightarrow \omega = \omega_0 \Leftrightarrow \textit{resonance}\right) \tag{3.16}$$

and a reflected signal is propagating back up the waveguide toward the source,

$$\tilde{V}_R = \tilde{V}_C - \tilde{V}_F = \frac{\beta-1}{\beta+1}\tilde{V}_F. \qquad \left(\psi = 0 \Leftrightarrow \omega = \omega_0 \Leftrightarrow \textit{resonance}\right) \tag{3.17}$$

If β>1 the external Q is lower than the wall Q, and the cavity is said to be *over-*

coupled. In this case the reflected signal is in phase with the forward drive. If β<1 the cavity is said to be *under-coupled* and in this case the reflected signal is 180° out of phase with the drive. If β=1 the cavity is said to be *critically-coupled*, and there is no reflected signal in steady-state.

With this result for cavity voltage, we may compute the reflection coefficient using the continuity condition, $\tilde{V}_R = \tilde{V}_c - \tilde{V}_F$,

$$S_{11} = \frac{\tilde{V}_R}{\tilde{V}_F} = \frac{2\beta}{1+\beta}\cos\psi e^{j\psi} - 1. \tag{3.18}$$

Notice that measurement of the (complex) S-matrix can permit one to determine the resonant frequency ω_0, the coupling factor β, and the loaded Q. Thus one can extract as well the external Q.

Exercise 3.5 Show that for small detuning from resonance, δ<<1, with $\delta = (\omega - \omega_0)/\omega_0$ that $\tan\psi \approx -2Q_L\delta$. Show that $Q_L = Q_W/(1+\beta)$. Sketch qualitatively a plot of tuning angle versus frequency.

Exercise 3.6 Show that the minimum in $|S_{11}|$ occurs on resonance, $\min|S_{11}| = |\beta - 1|/|\beta + 1|$ at $\omega = \omega_0$ and is zero for critical coupling. Considering the three cases of under-coupling, critical coupling and over-coupling, compute VSWR on resonance. Make qualitative sketches of $|S_{11}|$ and $|V_c|$ versus frequency. Evidently regardless of the frequency, not all energy is reflected by the cavity; where does this energy go?

3.6 Cavity on the Beamline

Having examined the properties of our cavity on the bench, let us next consider it, with beam. Typically one is interested either in a very short bunch of charge, much shorter than an rf period (*single-bunch*), or one is interested in a train of such bunches, spaced at or near the rf period (*bunch-train*). In this sections we will consider each of these in turn. We will assume that the beam is a high-energy beam and therefore does not slow down or speed up appreciably in the structure. This assumption does not hold, for example, in an injector or a klystron cavity.

Let us take the drive terms to be varying at roughly the frequency ω, but allow for some slow variation in the envelopes,

$$V_F = \Re\left(\tilde{V}_F(t)e^{j\omega t}\right), \qquad I_b = \Re\left(\tilde{I}_b(t)e^{j\omega t}\right), \qquad V_C = \Re\left(\tilde{V}_C(t)e^{j\omega t}\right).$$

In this case, in the slowly-varying envelope approximation, $\left|d\tilde{V}_C/dt\right| << \left|\omega\tilde{V}_C\right|$, the cavity responds to the waveguide and beam excitation according to

$$\frac{d\tilde{V}_C}{dt} + \frac{\omega_0}{2Q_L}(1 - j\tan\psi)\tilde{V}_C = \frac{\omega_0}{Q_e}\tilde{V}_F + k_l\tilde{I}_b. \tag{3.19}$$

where k_l is the loss-factor, and ψ is the tuning angle. It is often convenient to express this as

$$\frac{d\tilde{V}_C}{d\tau} + (1 - j\tan\psi)\tilde{V}_C = \frac{2\beta}{1+\beta}\tilde{V}_F + r_l\tilde{I}_b, \tag{3.20}$$

where

$$\tau = \frac{t}{T_f} = \frac{\omega_0 t}{2Q_L}$$

is time measured in units of the fill-time, and the "circuit-equivalent loaded resistance" may be expressed in various forms as

$$r_l = Q_L\left[\frac{r}{Q}\right] = \frac{1}{2}Q_L\left[\frac{R}{Q}\right] = \frac{1}{2}\frac{Q_L}{Q_w}R_{shunt} = \frac{R_{shunt}}{2(1+\beta)}. \tag{3.21}$$

In steady-state $d\tilde{V}_C / d\tau = 0$ and the cavity and reflected voltages take the forms

$$\tilde{V}_C = \cos\psi e^{j\psi}\left(\frac{2\beta}{1+\beta}\tilde{V}_F + r_l\tilde{I}_b\right), \tag{3.22}$$

$$\tilde{V}_R = \tilde{V}_C - \tilde{V}_F = \cos\psi e^{j\psi}\left(\frac{2\beta}{1+\beta}\cos\psi e^{j\psi} - 1\right)\tilde{V}_F + r_l\tilde{I}_b\cos\psi e^{j\psi}. \tag{3.23}$$

These steady-state relations are often depicted in the form of a phasor diagram, as shown in Fig. 3.8.

It will be important, in treating this system, to account for the flow of power, and we can accomplish this with the "transformer ratio" alluded to previously. Recall that the power flowing in a waveguide may be expressed in terms of the incoming and outgoing voltage phasors, $\tilde{V}^+$, $\tilde{V}^-$, combining Eqs. (2.20) and (2.29),

$$P_w = \frac{\left|\tilde{V}^+\right|^2 - \left|\tilde{V}^-\right|^2}{2Z_c},$$

with Z_c the characteristic mode impedance, just

$$Z_c = Z_0\frac{\omega}{c\beta_z} = Z_0\left(1 - \frac{\lambda_c^2}{\lambda^2}\right)^{-1/2},$$

for the TE_{10} mode in the waveguide, with λ the free-space wavelength, and λ_c the cut-off wavelength in the guide. The forward and reverse voltages V_F and V_R are proportional to these normalized amplitudes, $V_F = nV^+$, $V_R = nV^-$. Thus the net

power flowing in the waveguide may be expressed as

$$P_w = \frac{\left|\tilde{V}_F\right|^2 - \left|\tilde{V}_R\right|^2}{2Z_c n^2}.$$

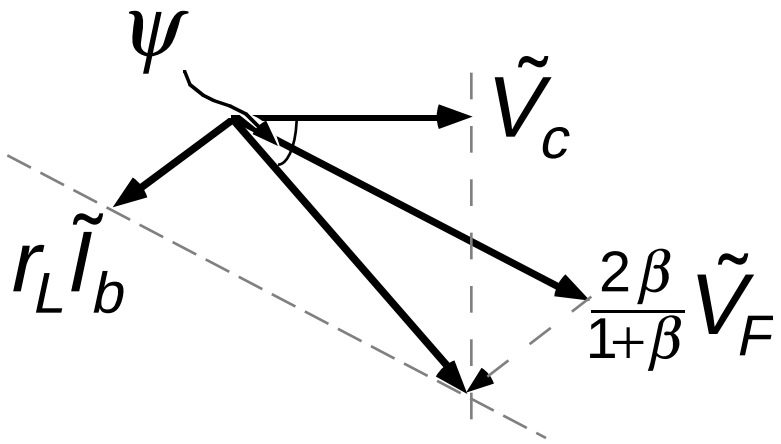

FIGURE 3.8. Phasor diagram for a beam-cavity waveguide system in steady-state.

In steady-state, with no beam, conservation of energy dictates that this equal the rate at which power is being dissipated in the cavity walls, and this is

$$P_d = \frac{\omega U}{Q_w} = \frac{\left|\tilde{V}_c\right|^2}{Q_w\left[\frac{R}{Q}\right]} = \frac{\left|\tilde{V}_c\right|^2}{R_{shunt}}.$$

Equating these two, we may determine the transformer ratio, *n*. We make use of the following identities:

$$\left|\tilde{V}_c\right|^2 = \left(\frac{2\beta}{1+\beta}\right)^2 \cos^2\psi \left|\tilde{V}_F\right|^2, \qquad \text{(beam off)}$$

$$\left|\tilde{V}_R\right|^2 = \left\{\left(\frac{1-\beta}{1+\beta}\right)^2 \cos^2\psi + \sin^2\psi\right\}\left|\tilde{V}_F\right|^2, \qquad \text{(beam off)}$$

$$\left|\tilde{V}_F\right|^2 - \left|\tilde{V}_R\right|^2 = \frac{4\beta}{(1+\beta)^2}\cos^2\psi \left|\tilde{V}_F\right|^2. \qquad \text{(beam off)}$$

Exercise 3.7 Derive these identities starting from the steady-state relation, Eq, (3.22), with beam-off, and making use of $\tilde{V}_R = \tilde{V}_c - \tilde{V}_F$.

Using these identities we find

$$P_d = \left(\frac{2\beta}{1+\beta}\right)^2 \cos^2\psi \frac{\left|\tilde{V}_F\right|^2}{R_{shunt}}, \qquad \text{(beam off)}$$

$$P_w = \frac{4\beta}{(1+\beta)^2}\cos^2\psi\,\frac{\left|\tilde{V}_F\right|^2}{2Z_c n^2}, \qquad \text{(beam off)}$$

and equating these two results gives us the *turns ratio* or *transformer ratio*,

$$n = \left(\frac{R_{shunt}}{2Z_c\beta}\right)^{1/2} = \left(\frac{Q_e\left[\frac{r}{Q}\right]}{Z_c}\right)^{1/2}. \tag{3.24}$$

Note that while we have derived this under beam-off conditions, *n* is a function of geometry alone, independent of source terms.

Turning the beam back on, we can derive some generally useful results. The forward-going power in the waveguide is

$$P_F = \frac{\left|\tilde{V}_F\right|^2}{2Z_c n^2} = \beta\frac{\left|\tilde{V}_F\right|^2}{R_{shunt}},$$

and, if the rf source is isolated from the cavity-beam system, this is just the power supplied by the source. Typically such isolation is achieved with an arrangement involving a magic tee (and another cavity), or a high-power isolator, or both.

For illustration, let us consider the problem of optimizing the coupling parameter β to maximize power delivered to the beam; we suppose that forward power and beam current are fixed and that the beam-phase relative to the cavity voltage has been prescribed.The power delivered to the beam is just

$$P_b = \frac{1}{2}\Re\left(\tilde{V}_c\tilde{I}_b^*\right) = \frac{1}{2}\left|\tilde{V}_c\right|\left|\tilde{I}_b\right|\cos\phi_s,$$

with ϕ_s the prescribed angle between the beam-phasor and the cavity voltage phasor. Evidently maximum power corresponds to maximum cavity amplitude. This on the other hand corresponds to maximum power dissipated in the walls. Energy conservation, $P_F = P_R + P_d + P_b$, or

$$\beta\frac{\left|\tilde{V}_F\right|^2}{R_{shunt}} = \beta\frac{\left|\tilde{V}_R\right|^2}{R_{shunt}} + \frac{\left|\tilde{V}_c\right|^2}{R_{shunt}} + \frac{1}{2}\left|\tilde{V}_c\right|\left|\tilde{I}_b\right|\cos\phi_s,$$

tells us then that we are attempting to maximize the sum of the two terms on the right, and this corresponds uniquely to a minimization of the first term, reflected power, given that the sum of all three is fixed. Minimum reflected power corresponds to zero reflected signal, or $\tilde{V}_c = \tilde{V}_F$, and this condition permits us to solve for β,

$$\beta\frac{\left|\tilde{V}_F\right|^2}{R_{shunt}} = \underbrace{\beta\frac{\left|\tilde{V}_R\right|^2}{R_{shunt}}}_{0} + \frac{\left|\tilde{V}_c\right|^2}{R_{shunt}} + \frac{1}{2}\left|\tilde{V}_c\right|\left|\tilde{I}_b\right|\cos\phi_s,$$

or

$$\frac{(\beta-1)}{\beta}P_F=(\beta-1)\frac{\left|\tilde{V}_c\right|^2}{R_{shunt}}=\frac{1}{2}\left|\tilde{V}_c\right|\left|\tilde{I}_b\right|\cos\phi_s=P_b.$$

Thus,

$$\frac{1}{\beta}=1-\frac{P_b}{P_F}.$$

Using,

$$P_d=\frac{\left|\tilde{V}_c\right|^2}{R_{shunt}}=\frac{1}{\beta}P_F, \qquad \text{(no reflection)}$$

we may also express this as

$$\beta=1+\frac{P_b}{P_d}. \qquad \text{(no reflection)} \qquad (3.25)$$

This summarizes the basic features of steady-state beam-loading. Our beam-cavity-waveguide model is also adequate to analyze the effect of transient beam-loading, and this is illustrated with the help of a few exercises.

Exercise 3.8 Consider filling a cavity with a step turn-on of the drive V_F,

$$\tilde{V}_F(t)=\begin{cases}0 & ;\ t<0\\ 1 & ;\ t>0\end{cases}$$

under beam-off conditions. With the drive tuned on-resonance, $\omega=\omega_0$, compute the cavity and reverse voltages as a function of time. Confirm the steady-state results,

$$\lim_{t\to\infty}\frac{\tilde{V}_C}{\tilde{V}_F}=\frac{2\beta}{\beta+1}, \qquad \lim_{t\to\infty}\frac{\tilde{V}_R}{\tilde{V}_F}=\frac{\beta-1}{\beta+1},$$

where $\beta=Q_W/Q_e$. Evaluate and sketch the results, $\tilde{V}_R$ and $\tilde{V}_C$ versus time for β=1/2,1,2. Sketch also the oscilloscope waveform that would be observed from a crystal detector looking at the reflected waveform. What is the clear difference appearing on these scope waveforms, between an over-coupled and under-coupled cavity?

Exercise 3.9 Express the beam-cavity waveguide equation in the form

$$\left\{\frac{d^2}{dt^2}+\frac{\omega_0}{Q_L}\frac{d}{dt}+\omega_0^2\right\}V_c=\omega_0\left[\frac{r}{Q}\right]\frac{dI_c}{dt},$$

identifying the waveguide (or "generator") contribution to the "cavity current" I_c. Show that

$$V_c(t)=\int_{-\infty}^{t}dt'\,G(t-t')\frac{dI_c}{dt}(t')$$

is a solution of this system, with Green's function,

$$G(\tau) = 2k_l \frac{\sin(\Omega\tau)}{\Omega} \exp\left(-\tfrac{1}{2}\nu\tau\right) H(\tau),$$

H the step-function, $\Omega = \sqrt{\omega_0^2 - \tfrac{1}{4}\nu^2}$, and $\nu = \omega_0 / Q_L$. Integrating by parts, express this as

$$V_c(t) = \int_{-\infty}^{t} dt' \, G'(t-t') I_c(t').$$

Exercise 3.10 Using the exact Green's function, compute the response of the cavity to a train of point bunches, each of charge q_b, spaced at time intervals *T*. You will want to make use of the identity

$$\sum_{m=0}^{M-1} x^m = \frac{\left(1 - x^M\right)}{(1-x)}.$$

Evaluate the result after the *M*-th bunch has passed, in the limit *MT*>>fill-time, and assuming the bunches arrive at the fundamental mode frequency, or a sub-harmonic of it, $\omega T = 2\pi k$, with *k* an integer. Compare this result to the steady-state result

$$\frac{\omega_0}{2Q_L}(1 - j\tan\psi)\tilde{V}_C = k_l \tilde{I}_b \quad \Leftrightarrow \quad \tilde{V}_C = Q_L \left[\frac{r}{Q}\right] \tilde{I}_b e^{j\psi} \cos\psi .$$

In developing the expression for $\tilde{I}_b$, you may wish to use the identity

$$T \sum_{m=-\infty}^{+\infty} \delta(t - mT) = 1 + 2 \sum_{n=0}^{\infty} \cos\left(2\pi n \frac{t}{T}\right),$$

as a consequence of which, $\tilde{I}_b = 2q_b / T$ for a train of zero-length charges q_b spaced at interval *T*. Argue that the steady-state voltage induced by a beam of average current $\bar{I}_b$, bunched on resonance, is equal to the voltage induced by a single bunch of charge $\bar{I}_b T_f$, with T_f the fill time for the mode. Given a cavity with a fill-time of 100 ns, which one excites a larger cavity voltage, a single bunch with 5 nC charge, or a 1 μs pulse of total charge 50 nC?

Exercise 3.11 Show that the impedance presented by a single cavity mode to the beam is

$$Z_{||}(\omega) = \frac{j\,\omega\,\omega_0 [r/Q]}{\omega_0^2 - \omega^2 + j\,\omega\,\omega_0 / Q_L},$$

and express this in the equivalent forms

$$Z_{||}(\omega) = \frac{Q_L [r/Q]}{1 - j\,Q_L \left(\omega_0/\omega - \omega/\omega_0\right)} = Q_L [r/Q] \cos\psi \, e^{j\psi}.$$

Exercise 3.12 One often-used equivalent circuit for the beam-cavity-waveguide system takes the form show here.

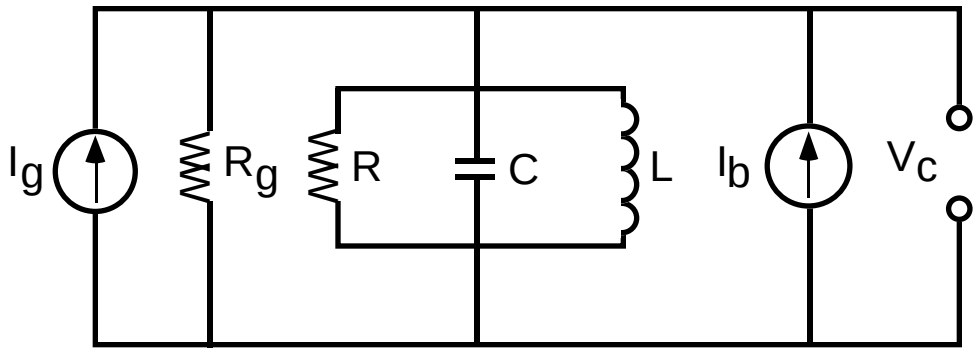

Analyze this circuit in the frequency domain, and identify parameters and dynamic variables with those used in Eq. (3.12).

Exercise 3.13 A standing-wave accelerator is powered with a klystron putting out a square pulse. **(a)** How long, in units of the fill-time, must the power source pulse-length be to achieve 90% of the steady-state gap voltage? **(b)** After the gap voltage has reached steady-state, the klystron turns off. Sketch cavity voltage, and forward and reverse voltage waveforms versus time. What is the maximum in the reflected power waveform relative to the klystron output?

Exercise 3.14 Our transient cavity-beam-guide formulation may be expressed as

$$\frac{d\tilde{V}_c}{d\tau} + (1 - j\tan\psi)\tilde{V}_c = \hat{V}_F + \hat{V}_b,$$

where $\tau = t/T_f$,

$$\hat{V}_F = \frac{2\beta}{1+\beta}\tilde{V}_F, \qquad \hat{V}_b = \frac{1}{2}Q_L\left[\frac{R}{Q}\right]\tilde{I}_b.$$

(a) Driving the cavity on resonance (ψ=0), with rf drive turn-on at t=0, determine the beam turn-on time τ_b>0, such that gap voltage V_c is constant when the beam is present. **(b)** Sketch forward, reverse, beam-induced and gap voltage waveforms versus time.

Exercise 3.15 Consider a single cavity coupled to a waveguide. It is to be operated at 2856 MHz, with a transit angle of 90° for a speed-of-light particle. **(a)** Select the connecting guide from the following: WR510, WR284, WR187. Calculate the guide wavelength λ_g. Calculate the characteristic impedance Z_c of the TE_{10} mode at this frequency. **(b)** Calculate the dimensions, wall Q, [R/Q], R_{shunt}, and fill-time for the cavity based on closed pillbox TM_{010} scalings. What external Q is required for critical coupling? **(c)**Assuming critical coupling and a long klystron pulse length, determine the power requirement for V_c=2.5 MV, neglecting beam-loading. Calculate the transformer ratio, n. **(d)**The klystron available puts out a peak power of 5 MW, how much current can be accelerated while meeting the gap voltage requirement? **(e)**Assuming a current requirement of 100 mA and using steady-state scalings, determine the optimal β for transfer of power to the beam, the requirement on beam-injection time, for constant loaded gap voltage during the beam-pulse, and the overall rf to beam efficiency for this system.

Exercise 3.16 For a cavity connected to a guide, relate the rate of change of cavity-phase with frequency, relative to that of the forward voltage in the guide, to the ratio of stored energy and input power.

Exercise 3.17 The designers of a 2856-MHz accelerating structure quote an estimate of sensitivity of resonant frequency, to cavity diameter $2b$, $\delta f / \delta(2b) \approx 0.9$ Mc/mil, where Mc=megacycle, *i.e.*, MHz. Explain this referring to TM_{010} mode scalings. Based on analysis of a single cavity, what tolerance, in mils, should be enforced to ensure a gap voltage within 95% of design, assuming the drive frequency is fixed? What temperature regulation is required in °C? (The coefficient of thermal expansion for copper is $\alpha \approx 1.7 \times 10^{-5} / {}^{\circ}\mathrm{K}$.)

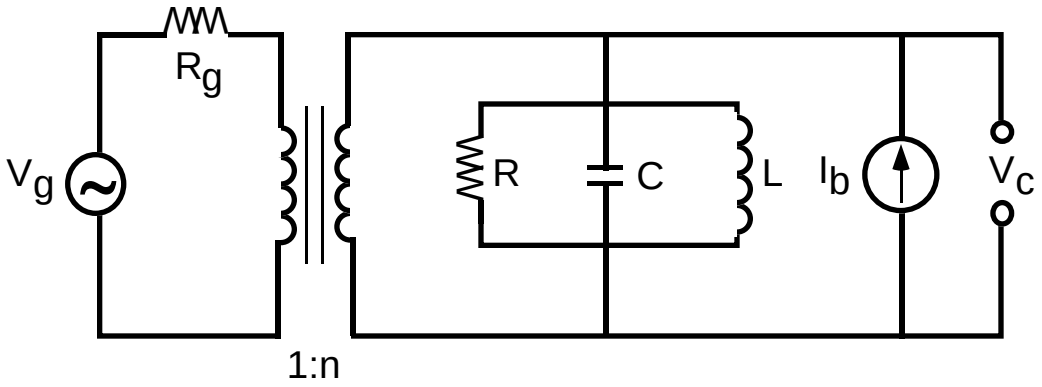

Exercise 3.18 Consider the circuit in the adjacent sketch, in the frequency domain, and compute the voltage V_c, assuming all elements are ideal. For zero current I_b, what is the equivalent impedance seen from the primary? Identify parameters and dynamic variables with those used in Eq. (3.12).

Exercise 3.19 Consider a cavity connected to a waveguide. Taking a forward voltage of the form

$$V_F(t) = \begin{cases} 0 & ; t < 0 \\ V_0 & ; 0 < t < T_1 \\ -V_0 & ; T_1 < t < T_2 \\ 0 & ; T_2 < t \end{cases}$$

with $T_1 = 2T_{fill}$ and $T_2 = 2.5T_{fill}$. Assuming β=5, sketch cavity, forward and reflected voltages versus time. What is the maximum reverse voltage amplitude? What is the maximum ratio of reflected voltage to input amplitude attainable in this geometry for any T_1, T_2 and β?

Exercise 3.20 At 77°K the resistivity of pure copper is $0.2 \times 10^{-8} \Omega - m$. If a mode of this cavity has a wall Q of 15,000 at 294°K, what is the wall Q when the copper is cooled to 77°K?

Exercise 3.21 A cylindrical cavity, with radius equal to its length, has sidewalls of

copper and endwalls made of brass. The same design made of all copper has a wall Q of 15,000. What is the wall Q with brass endcaps?

3.7 Two Coupled Cavities

Occasionally one cavity is adequate for the job at hand; more typically, we have a single source of power, and would like to achieve 5-20 MeV of acceleration with it. Our analysis of single cavities indicates this isn't possible at microwave frequencies with a single cavity and typical power sources. We could split the power and drive multiple cavities with multiple feeds, however this takes up space and adds complexity to the system. In this case not only must each cavity be properly tuned, but each waveguide arm and each power splitter must be tuned to the correct "electrical length," measured in degrees of rf phase. Happily, it is possible to couple cavities together and power them with a *single feed*. Let us start with the simplest coupled cavity system, consisting of two cavities, as depicted in Fig. 3.9.

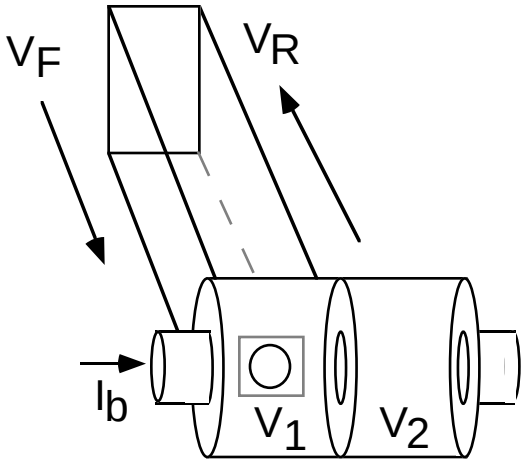

FIGURE 3.9. The simplest coupled-cavity accelerator consists of two cavities.

From the field-line point of view, this problem can take several distinct forms, as illustrated in Fig. 3.10. We will consider the TM_{01} mode with coupling by a centered circular iris as depicted on the left in the figure.

We can determine the behavior of this system starting from Maxwell's equations, as illustrated in Appendix C. Here let us decide on intuitive grounds what to expect. Let V_1 be the voltage in cell #1, with V_2 the voltage in cell #2. We expect the usual simple harmonic oscillator behavior of V_1 to be modified,

$$\frac{d^2V_1}{dt^2} + \omega_0^2 V_1 = [\text{perturbation}],$$

and we would like to know what form this perturbation should take. Inspecting the electric field lines and magnetic field lines for one unperturbed cell, we see that it

has the character of an *LC* circuit, with an electric field between two conducting planes, and an azimuthal magnetic field filling the outer volume. Cutting a hole in the center---where electric field is large, and the magnetic field is small---should have the effect of lowering the capacitance. Lowering the capacitance in an *LC* circuit raises the resonant frequency of the circuit, thus

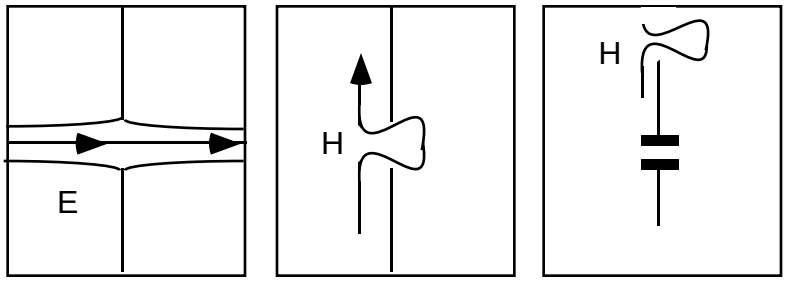

FIGURE 3.10. Cavity modes may be center or side-coupled, magnetically or electrically coupled. On the left one sees center-coupled TM_{01} mode, in the center, TM_{11} coupling, and on the right, off-center coupled TM_{01}.

$$\frac{d^2V_1}{dt^2}+\omega_0^2V_1=-\frac{1}{2}\kappa\omega_0^2V_1\ldots,$$

where the dimensionless constant κ >0 should depend on the size of the hole. However, this description must be incomplete, for we expect too that electric field lines from cell #2 might find their way into cell #1; the cell amplitudes should be coupled. In fact, the form of this coupling is determined from symmetry---from the observation that if the voltage in cell #2, V_2, is equal to that in cell #1, then every field line in cell #1 continues through to cell #2, and none terminates on the iris edge. In this case, there is no deformation of the field lines; as far as they are concerned one might as well replace the hole with copper. Thus when the cavities are in phase, they should oscillate as they would if there were no iris. This implies the coupling

$$\frac{d^2V_1}{dt^2}+\omega_0^2V_1=-\frac{1}{2}\kappa\omega_0^2\left(V_1-V_2\right), \tag{3.26}$$

and, from symmetry,

$$\frac{d^2V_2}{dt^2}+\omega_0^2V_2=-\frac{1}{2}\kappa\omega_0^2\left(V_2-V_1\right). \tag{3.27}$$

Exercise 3.22 Considering cavity voltages varying as $\propto\exp(j\omega t)$ show that there are two possible angular frequencies ω. Go on to show that one of these modes of oscillation corresponds to the two cavities in-phase (0-mode), and oscillating at the original resonant frequency of the unperturbed cavity. Show that in the second mode, the two cavities oscillate 180° out of phase (π-mode) with resonant frequency, $\omega=\omega_0(1+\kappa)^{1/2}$. Show that the no-load accelerating voltage for this two-cavity system takes the form

$$\tilde{V}_{NL} = \tilde{V}_1 2e^{j\theta/2} \times \begin{cases} \cos\left(\frac{1}{2}\theta\right) ; 0-\text{mode} \\ j\sin\left(\frac{1}{2}\theta\right) ; \pi-\text{mode} \end{cases},$$

where θ is the transit angle for a single cavity, and $\tilde{V}_1$ is the no-load voltage phasor for a single cavity. Which mode would be best for acceleration? Justify the answer by computing the [*R/Q*] for the two-cavity system, defined, as previously, according to

$$\left[\frac{R}{Q}\right] = \frac{\left|\tilde{V}_{NL}\right|^2}{\omega U},$$

with *U* the stored energy. For each mode, determine the maximum [*R/Q*] as a function of transit angle. Show that the optimal transit angle in π-mode is 159.6°, for which the [*R/Q*] is 1.9 times that of the optimal [*R/Q*] for a single cavity. In this connection it will be helpful to recall that the [*R/Q*] for a closed pillbox operated in TM_{010} mode takes the form

$$\left[\frac{R}{Q}\right]_1 = 313\Omega \frac{\sin^2\left(\frac{1}{2}\theta\right)}{\left(\frac{1}{2}\theta\right)}.$$

3.8 Multicell Structures

From the analysis of two coupled cavities, we have seen that one does not need to power each cavity separately, one can couple them together, and form what amounts to one long cavity consisting of two cells. This motivates the analysis of multi-cell structures, as illustrated in Fig. 3.11. We neglect wall-losses, ports, and the beam, as they can be added later as perturbations.

We consider *N* cavities that have been modified by coupling holes. We denote $\omega_0^2(\kappa) = \omega_0^2(\kappa = 0)(1+\kappa)$, in terms of which our problem takes the form

$$\frac{\partial^2 V_n}{\partial t^2} + \omega_0^2 V_n = \frac{1}{2}\omega_0^2 \kappa\left(V_{n-1} + V_{n+1}\right), \qquad \text{(interior cells)} \qquad (3.28)$$

for interior cells n=2,3,...,$N-1$. The end-cells, n=1,N, find themselves in circumstances different from the interior cells, since each has had only one coupling iris cut in it. In general, it is desirable to modify the end-cells in such a way as to insure the existence of an accelerating mode with good [*R/Q*].

To determine the eigenfrequencies of the structure, we consider the problem in the frequency domain, looking for solutions $V_n = \Re\tilde{V}_n e^{j\omega t}$, so that

$$-\left(\tfrac{1}{2}\omega_0^2\kappa\right)\tilde{V}_{n-1} + \left(\omega_0^2 - \omega^2\right)\tilde{V}_n - \left(\tfrac{1}{2}\omega_0^2\kappa\right)\tilde{V}_{n+1} = 0. \qquad \text{(interior cells)} \qquad (3.29)$$

A general solution should consist of a left- and a right- going wave, $\tilde{V}_n = Ae^{jn\phi} + Be^{-jn\phi}$, and substituting this in the difference equation, it can be shown that the phase-advance per cell must satisfy

$$\cos\phi = \frac{\omega_0^2 - \omega^2}{\omega_0^2 \kappa}. \tag{3.30}$$

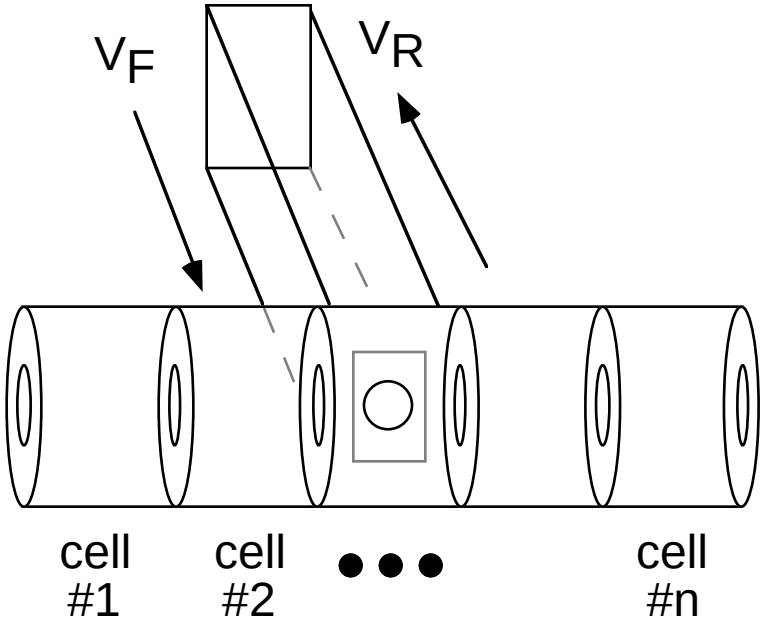

FIGURE 3.11. Concept for a multi-cell standing-wave structure.

It is at this point that the conditions on the end-cells enter. This is illustrated with an exercise.

Exercise 3.23 Suppose that the end-cells are designed so as to satisfy

$$\frac{\partial^2 V_1}{\partial t^2} + \omega_0^2 V_1 = \omega_0^2 \kappa_e V_2, \quad \frac{\partial^2 V_N}{\partial t^2} + \omega_0^2 V_N = \omega_0^2 \kappa_e V_{N-1}.$$

Show that these conditions on the end-cells are satisfied only for certain discrete values of phase-advance per cell, corresponding to α=1,2,...*N* discrete *modes* of oscillation, indexed by α, with frequencies, $\omega_\alpha = \omega_0 \sqrt{1 - \kappa \cos\phi_\alpha}$. Make a sketch of the ω vs ϕ relation, and remark on the density of modes. Where are modes most dense? Least dense? Determine the mode excitation patterns corresponding to $\kappa_e = \kappa/2$, and those corresponding to $\kappa_e = \kappa$.

Realistic standing-wave structures will have diverse features, including boundary conditions corresponding to half-cells at each end, and perhaps a biperiodic character.[23,24] Those features of multicell structures that are qualitatively different from the single-cell case can already be seen in the two-cell example. For example, if a mode α satisfies the synchronism condition $\theta = \phi_\alpha$, then one can show that $[R/Q] = [R/Q]_1 \times N/2$. At the same time, this choice of phase-advance per cell is

not optimal. Instead, optimal [*R/Q*] corresponds to that mode with phase-advance per cell closest to π. Indeed, standing-wave structures typically operate in π-mode, and do not satisfy the synchronous phase-advance condition. To emphasize, π-mode does not imply a transit angle of π. This is a rather subtle difference between the standing-wave and travelling-wave linacs. Synchronous interaction in the travelling-wave linac requires a geometric phase-advance per cell θ matching the kinematic phase-shift witnessed by a speed-of-light particle, $\omega L/c$, with L the cell-length. On the other hand, for the terminated interaction in the standing-wave linac, optimal [*R/Q*] occurs near π phase-advance.

Starting from the perturbed cavity equations,

$$\frac{\partial^2 V_n}{\partial t^2} + \omega_0^2 V_n = \frac{1}{2}\omega_0^2 \kappa\left(V_{n-1} + V_{n+1}\right) - \frac{\omega_0}{Q_w}\frac{\partial V_n}{\partial t} - \frac{\omega_0}{Q_{eM}}\frac{\partial V_n}{\partial t}\delta_{n,M} + \frac{2\omega_0}{Q_{eM}}\frac{\partial V_F}{\partial t}\delta_{n,M},$$

one can show that introduction of losses corresponds to a shift in mode resonance frequency,

$$\Omega_\alpha^2 \approx \omega_\alpha^2\left(1 - \frac{1}{Q_w}\right) + j\frac{\omega_\alpha^2}{Q_w}.$$

One can also show that introduction of a port in one cell contributes a correction in the form of an external Q for each mode, inversely proportional to the squared mode amplitude in that cell. The external features of the cavity, as determined from measurement of S_{11}, must take the form,

$$S_{11}(\omega) = \frac{\tilde{V}_R}{\tilde{V}_F} = \sum_{\alpha=1}^{N} \frac{2j\omega\omega_0 / Q_{e\alpha}}{\left(\omega_\alpha^2 + j\omega\omega_\alpha / Q_{L\alpha} - \omega^2\right)} - 1,$$

and are determined by those modes with finite external Q (*i.e.*, the modes that are non-zero in the coupling cavity). In the end, the description of a perfectly tuned multi-cell structure, operated in a particular mode, can be reduced to the form Eq. (3.12).

4. Travelling-Wave Accelerators

We began by considering how to accelerate particles and realized that material boundaries were needed, either to terminate the interaction, or to provide for a synchronous wave. In the last section, we considered the terminated interaction in detail, the standing-wave linac. In this section, we consider how to form a synchronous wave, a travelling-wave linac.

In light of our work on coupled cavities, the description of a travelling-wave linac can be made quite simple: it is a multi-cavity accelerator, with critically coupled input to the first cell, and a critically coupled output waveguide attached to the last cell, with the output waveguide terminated in a high-power matched load. These facts are enough to permit us to work out the basic design features of the coupled cavity system, viewed as a *transmission line*. The picture is that of Fig 4.1.

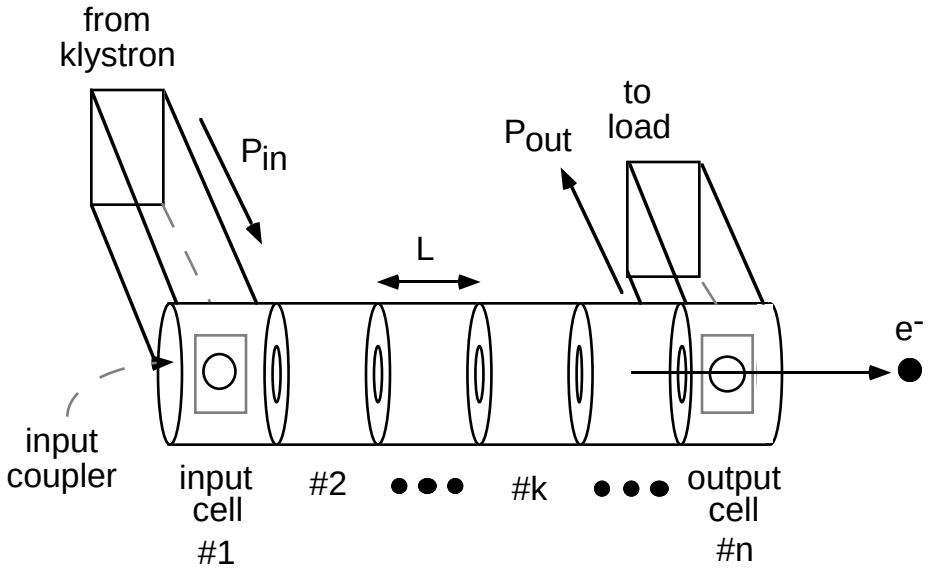

FIGURE 4.1. Schematic of a travelling-wave accelerating structure.

4.1 Transmission Line Model

We assume that the transmission lines is operated at a frequency where the input and output couplers are matched, and we analyze the steady-state established with an input power P_{in}. If the energy stored in cell *#k* is U_k, then we may speak of an energy per unit length at $z=z_k=(k-1)L$ given by $u(z_k)=U_k/L$, with L the cell length. The power flowing past the point z is

$$P(z) = V_g u(z),$$

with V_g the local group velocity. In steady-state the energy density stored in one cell

is constant in time, and thus

$$0 = dU = \text{change in stored energy in time } dt = \left(P_- - P_+\right)dt - \frac{\omega_0 U}{Q_w}dt,$$

where Q_w is the wall Q of a single cell. The power flowing into the cell from the left is P_-, and the power flowing out is P_+. Thus,

$$P_- - P_+ \approx L\frac{dP}{dz} = -\frac{\omega_0 U}{Q_w} = -\frac{\omega_0 uL}{Q_w},$$

or

$$\frac{dP}{dz} = -\frac{\omega_0 u}{Q_w} = \frac{d}{dz}\left(V_g u\right). \tag{4.1}$$

In the simplest case, the geometry of the line is strictly periodic, and it forms a *constant impedance* structure. In general, however, we may find it helpful to vary the cell dimensions adiabatically along the structure, as in the *constant gradient* structure.

Given the group velocity variation along the structure, if any, one may solve the first-order differential equation for u, Eq. (4.1), to determine the energy stored per unit length. In solving this, one requires the energy stored in the first cell and this may be determined from the input power P_{in},

$$u(0) = P_{in} / V_g(0).$$

In passing we note that this also provides a simple way to estimate the external Q required for the input coupler geometry in the first cell,

$$P_{in} = \frac{\omega_0}{Q_e}u(0)L = V_g(0)u(0) \Rightarrow Q_e \approx \frac{\omega_0 L}{V_g(0)},$$

and this external Q roughly characterizes the transmission bandwidth of the structure, although not the useful bandwidth for acceleration, as we will see.

We will be interested in acceleration with this device so let us suppose the shunt impedance for a single cell is R, and define the *shunt impedance per unit length*,

$$r = \frac{R}{L} = \frac{Q_w[R/Q]}{L} = \frac{Q_w}{L}\frac{|V|^2}{\omega_0 U},$$

where V is the voltage gain in one cell. This may be expressed in terms of the accelerating *gradient* G, according to $V=GL$, so that,

$$r = \frac{Q_w}{L}\frac{(GL)^2}{\omega_0 U} = \frac{Q_w}{\omega_0 u}G^2 = \frac{G^2}{-dP/dz}. \tag{4.2}$$

Let us consider, first, a perfectly periodic (*constant impedance*) structure. In this case V_g is a constant, and

$$\frac{d}{dz}\left(V_g u\right) = V_g \frac{du}{dz} = -\frac{\omega_0 u}{Q_w},$$

so that

$$u(z) = u(0)\exp(-2\alpha z),$$

where

$$\alpha = \frac{\omega_0}{2Q_w V_g}.$$

Thus the gradient at a distance z along the structure is

$$G(z) = \left(\frac{\omega_0 u}{Q_w} r\right)^{1/2} = G(0)\exp\left(-\alpha z\right).$$

The net accelerating voltage is just the integral of this,

$$V_{NL} = \int_0^{L_s} G(z)dz = G(0)\frac{1-e^{-\alpha L_s}}{\alpha},$$

where $L_s=NL$ is the structure length. Let us define an *attenuation parameter*, τ,

$$\tau = \alpha L_s = \frac{\omega_0 L_s}{2 Q_w V_g}.$$

Note that the attenuation parameter determines the power to the load,

$$P\left(L_s\right) = P(0)e^{-2\tau}, \tag{4.3}$$

and the *fill time*,

$$T_f = \int_0^{L_s} \frac{dz}{V_g} = \frac{L_s}{V_g} = \frac{2Q_w}{\omega_0}\tau. \tag{4.4}$$

We may express the accelerating voltage directly in terms of the input power, using

$$G(0) = \left(\frac{\omega_0}{Q_w} u(0) r\right)^{1/2} = \left(\frac{\omega_0}{Q_w}\frac{P_{in}}{V_g} r\right)^{1/2} = \left(2\alpha P_{in} r\right)^{1/2} = \frac{1}{L_s}\left(2\tau P_{in} R_s\right)^{1/2},$$

where we have introduced the shunt impedance of the structure as a whole, $R_s=rL_s$, with L_S the structure length, just NL, with N the number of cells. The voltage with no beam present (*no-load voltage*) is then

$$V_{NL} = \left(2\tau P_{in} R_s\right)^{1/2}\frac{1-e^{-\tau}}{\tau} = \left(P_{in} R_s\right)^{1/2}\left(1-e^{-\tau}\right)\left(\frac{2}{\tau}\right)^{1/2} \text{ (constant impedance).} \tag{4.5}$$

Exercise 4.1 Show that the maximum no-load voltage for fixed input power and shunt impedance in a constant impedance structure occurs for $\tau \approx 1.26$, and is $V_{NL} \approx 0.9\left(P_{in} R_S\right)^{1/2}$. Compute the ratio of maximum to average gradient in this case, and the ratio of maximum to minimum power dissipation per unit length.

Exercise 4.2 Using the TM_{01} pillbox scalings to estimate [*R/Q*] and wall *Q*, roughly what no-load voltage could you expect from a 10' long $\pi/2$-mode constant impedance structure operating at 2856 MHz, with group velocity of 0.01 *c* and 20 MW of input power. What is the fill time? Power to the load? Compare your figures to those for the Mark III structure, with $r \approx 47$ MΩ/m, and other parameters the same.

Such a constant impedance structure is conceptually the simplest travelling-wave linac, but it has a few undesirable features. These include peak gradient higher than the average gradient, nonuniform power dissipation, and some subtle features related to higher frequency modes in the structure. We are free of course to consider more elaborate designs. If we wish to obtain a more uniform field profile, we could taper the group velocity $V_g(z)$ in such a way that stored energy per unit length is constant (*constant gradient* structure). This implies a narrowing of the iris radius as one proceeds down the structure. Let us solve for the required group velocity taper. We have

$$\frac{d}{dz}\left(V_g u\right) = u\frac{dV_g}{dz} = -\frac{\omega_0 u}{Q_w},$$

so that

$$V_g(z) = V_g(0) - \frac{\omega_0}{Q_w} z.$$

The power flowing through the structure takes the form

$$P(z) = V_g u = P(0) + \left\{P(L) - P(0)\right\}\frac{z}{L_s},$$

and in terms of the attenuation parameter, defined with respect to the power to the load,

$$e^{-2\tau} = \frac{P(L)}{P(0)},$$

we may write,

$$P(z) = P(0)\left\{1 - \left(1 - e^{-2\tau}\right)\frac{z}{L_s}\right\}. \tag{4.6}$$

We may also express the initial group velocity in terms of τ, using

$$\frac{dP}{dz} = -P(0)\left(1 - e^{-2\tau}\right)\frac{1}{L_s} = -\frac{\omega_0 u}{Q_w} = -\frac{\omega_0}{Q_w V_g(0)} P(0),$$

so that

$$V_g(0) = \frac{\omega_0 L_s}{Q_w}\left(1 - e^{-2\tau}\right)^{-1}.$$

With this in hand we note the fill time,

$$T_f = \int_0^{L_s} \frac{dz}{V_g} = -\frac{Q_w}{\omega_0}\ln\left(1 - \frac{\omega_0 L_s}{Q_w V_g(0)}\right) = \frac{2Q_w}{\omega_0}\tau.$$

Finally we compute the no-load voltage,

$$V_{NL} = GL_s = \left(\frac{\omega_0 u}{Q_w} r\right)^{1/2} L_s = \left(\frac{\omega_0}{Q_w V_g(0)} P(0) r\right)^{1/2} L_s \qquad \text{(constant gradient)} \quad (4.7)$$

$$= \left(R_s P_{in}\right)^{1/2}\left(1 - e^{-2\tau}\right)^{1/2},$$

making the approximation that r is constant.

Exercise 4.3 Using the TM_{01} pillbox scalings to describe [R/Q] and wall Q, roughly what no-load voltage could one expect from a 10' long $2\pi/3$-mode constant gradient structure operating at 2856 MHz, with initial group velocity of $0.02c$, fill-time of 0.8 μs, and 20 MW of input power. What is the power to the load? Compare to the SLAC 10' structure with $r \approx$ 53 MΩ/m.

Exercise 4.4 The SLAC 10' structure is a constant gradient 86-cell $2\pi/3$ mode travelling-wave structure with nominal 2856 MHz operating frequency. Fill-time is 0.83 μs and attenuation parameter is $\tau \approx 0.57$. Shunt impedance per unit length is $r \approx 53$MΩ/m and initial group velocity is $V_g/c \approx 0.0204$. You have N=245 20-MW klystrons with 3-μs pulse length, and an unlimited number of SLAC 10' structures. Assuming that you couple one klystron to one structure, fill in the following numbers: **a)** V_{NL} for one structure and $V_{net}=NV_{NL}$, **b)** total accelerator length, **c)** average site power. In calculating the accelerator length, assume that 5% of the length is taken up by quads and instrumentation. In calculating the site power, assume a klystron wall-plug efficiency of 10% and a repetition rate of 120 Hz. Suppose next that the power from each klystron is divided in half m times, to feed 2^m structures. Calculate the net unloaded voltage and total accelerator length and evaluate these results for m=1 and m=2.

4.2 Steady-State Beam-Loading

Having considered the no-load accelerating voltage provided by an external power source, let us *turn off* the external power, and consider the beam-induced voltage in a travelling-wave structure. The beam-induced gradient $G_b(z)$ at point z in the structure corresponds to a power $P_b(z)$ flowing through the structure, with

$$P_b = \frac{G_b^2}{2\alpha r},$$

and G_b the peak or on-crest gradient . Conservation of energy takes the form

$$\frac{dP_b}{dz} = I_b G_b - 2\alpha P_b,$$

with I_b the beam current (charge per bucket times frequency). In terms of the beam-induced gradient, this is

$$\frac{d}{dz}\frac{G_b^2}{2\alpha r} = I_b G_b - \frac{G_b^2}{r},$$

or

$$\frac{dG_b}{dz} + \left(\alpha - \frac{1}{2\alpha}\frac{d\alpha}{dz}\right)G_b = \alpha r I_b.$$

Defining

$$\mu = \int_0^z dz' \left\{\alpha - \frac{1}{2\alpha}\frac{d\alpha}{dz}\right\} = \tau(z) - \frac{1}{2}\ln\left(\frac{\alpha(z)}{\alpha(0)}\right),$$

this may be expressed as

$$\frac{d}{dz} G_b e^{\mu} = \alpha r I_b e^{\mu}$$

or

$$G_b(z) = e^{-\mu(z)} G_b(0) + e^{-\mu(z)} \int_0^z dz' \alpha r I_b e^{\mu(z')}.$$

On the other hand, $G_b(0)=0$ since the beam must travel a finite length before losing energy. Thus,

$$G_b(z) = I_b e^{-\mu(z)} \int_0^z dz' \alpha r e^{\mu(z')}, \tag{4.8}$$

and we take current to be constant for a relativistic beam. We may then express the beam-induced voltage as an integral,

$$V_b(z) = -\int_0^{L_s} dz' G_b(z') = -mI_b, \tag{4.9}$$

where the minus sign reminds us that the beam-induced voltage is decelerating. The beam-loading coefficient for the structure is

$$m = \int_0^{L_s} dz' e^{-\mu(z')} \int_0^{z'} dz'' \alpha r e^{\mu(z'')}. \tag{4.10}$$

The net voltage when the structure is powered may then be expressed as

$$V_{net} = V_{NL}\cos\psi - mI_b, \tag{4.11}$$

where ψ is the phase of the applied rf. For a constant impedance structure, α and r are constants, so that

$$G_b(z) = rI_b\left(1 - e^{-\alpha z}\right), \qquad \text{(constant impedance)} \qquad (4.12)$$

$$m = R_s\left(1 - \frac{1 - e^{-\tau}}{\tau}\right), \qquad \text{(constant impedance)} \qquad (4.13)$$

with $R_s = rL_s$.

For a constant gradient structure, one can show that

$$\alpha = -\frac{1}{2V_g}\frac{dV_g}{dz} = \frac{1}{2}\frac{1}{\xi - z},$$

with

$$\xi = \frac{L_s}{1 - e^{-2\tau}}.$$

In this case μ=0, and one has

$$G_b(z) = \frac{1}{2}rI_b \ln\frac{\xi}{\xi - z}. \qquad \text{(constant gradient)} \qquad (4.14)$$

After an integration one finds

$$m = R_s\left(\frac{1}{2} - \frac{\tau}{e^{2\tau} - 1}\right). \qquad \text{(constant gradient)} \qquad (4.15)$$

Exercise 4.5 A travelling-wave linac is designed to produce a net no-load voltage V_{NL}. If the linac current I_b is chosen to optimize power transfer to the beam in steady-state, what is the net loaded voltage?

Exercise 4.6 Considering a structure excited only by a beam, show that power to the load takes the form

$$P_b(L_s) = R_s I_b^2 \begin{cases} \dfrac{\left(1 - e^{-\tau}\right)^2}{2\tau}; & \text{constant impedance} \\ \dfrac{\tau^2}{\left(e^{2\tau} - 1\right)}; & \text{constant gradient} \end{cases},$$

What is the result for a 100-mA beam in the SLAC 10' structure (53 MΩ/m, $\tau \approx 0.57$, constant gradient)?

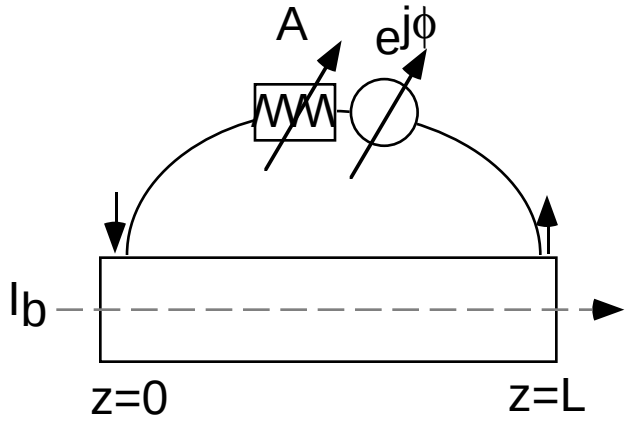

Exercise 4.7 A constant impedance structure has the output coupled through a phase shifter and attenuator, and fed back into the input, as illustrated in the adjacent sketch. Assuming the structure is excited only by the beam, compute the steady-state voltage in the structure, and determine what input power would be required to produce the equivalent no-load voltage. Evaluate this for a 50-cell, $2\pi/3$, 91.39 GHz constant impedance structure, with group velocity $0.09c$, driven by a 0.5-A beam bunched at the 11.4 GHz subharmonic. Neglect the finite bunch length.

4.3 Coupled-Cavity Model

The transmission line model is quite adequate for understanding the scalings for ideal travelling-wave structures. In general however we may be interested in the effect of tuning errors, transient input waveforms and other more realistic features of accelerator operation. These problems are simplified by analysis of the structure as a series of coupled cavities. The picture is that of Fig 4.2.

Let us consider the accelerating voltage in the first cell. The first cell is a cavity coupled to a waveguide, another cavity, and the beam. The model for such a system follows from Eqs. (3.10) and (3.28),

$$\left(\frac{\partial^2}{\partial t^2}+\frac{\omega_1}{Q_{L1}}\frac{\partial}{\partial t}+\omega_1^2\right)V_1=\frac{1}{2}\omega_1^2\kappa_{3/2}V_2+2\frac{\omega_1}{Q_{e1}}\frac{\partial V_F}{\partial t}+\omega_1\left[\frac{r}{Q}\right]_1\left[\frac{\partial I_b}{\partial t}\right]_1.$$

The first cavity reflects a voltage $V_R=V_1-V_F$ back up the connecting guide toward the source. The loaded Q includes the wall Q of the unperturbed (no ports) first cavity

$$\frac{1}{Q_{L1}}=\frac{1}{Q_{w1}}+\frac{1}{Q_{e1}},$$

and the external Q due to the connecting guide.

For interior cells $k=2,3,\ldots N-1$, the cell voltage evolves according to

$$\left(\frac{\partial^2}{\partial t^2}+\frac{\omega_k}{Q_{wk}}\frac{\partial}{\partial t}+\omega_k^2\right)V_k=\frac{1}{2}\omega_k^2\left(\kappa_{k-1/2}V_{k-1}+\kappa_{k+1/2}V_{k+1}\right)++\omega_k\left[\frac{r}{Q}\right]_k\left[\frac{\partial I_b}{\partial t}\right]_k,$$

and the output coupler cell, $k=N$, evolves according to

$$\left(\frac{\partial^2}{\partial t^2}+\frac{\omega_N}{Q_{LN}}\frac{\partial}{\partial t}+\omega_N^2\right)V_N=\frac{1}{2}\omega_N^2\kappa_{N-1/2}V_{N-1}+2\frac{\omega_N}{Q_{eN}}\frac{\partial V_{FN}}{\partial t}+\omega_N\left[\frac{r}{Q}\right]_N\left[\frac{\partial I_b}{\partial t}\right]_N.$$

The subscript on the beam-current term reminds us that there is a finite transit time to cell #*k*.

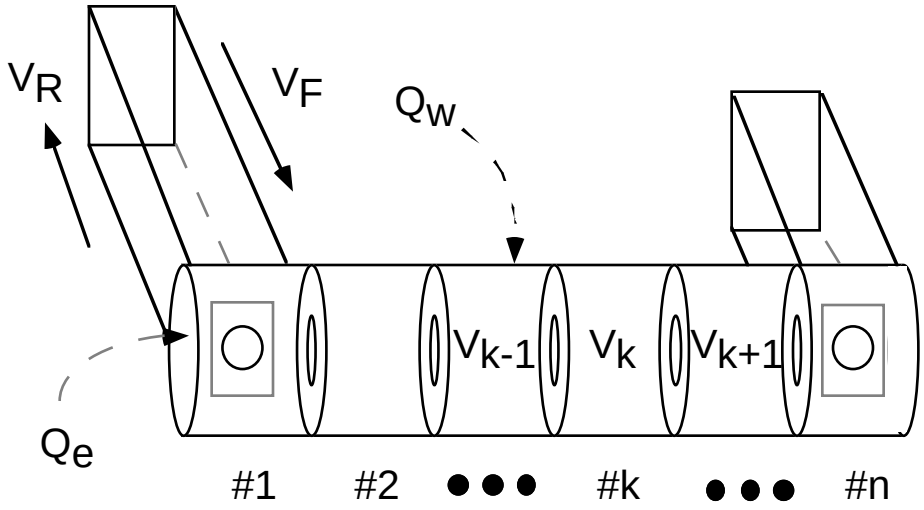

FIGURE 4.2. Model of a travelling-wave structure as a series of coupled cavities.

Having stated the most general model we will ever need to call on, let us now consider some simplifying approximations. It is typically the case that shunt impedance varies slowly with cell dimension, and so, for our purposes here may be thought of as a constant. If the output load is well-matched, the term V_{FN} vanishes, as there is no power reflected back into the output cell. Wall Q varies slowly with cell dimension and may be taken as a constant. To avoid a profusion of subscripts we will simply drop the cavity subscript on the beam current term. Interior cells are then described as a chain of coupled oscillators, driven by the beam, and ultimately the input cell,

$$\left(\frac{\partial^2}{\partial t^2}+\frac{\omega_k}{Q_w}\frac{\partial}{\partial t}+\omega_k^2\right)V_k=\frac{1}{2}\omega_k^2\left(\kappa_{k-1/2}V_{k-1}+\kappa_{k+1/2}V_{k+1}\right)+2k_l\frac{\partial I_b}{\partial t},$$

where we refer to the loss-factor for the fundamental mode, k_l. Our procedure for analyzing the structure will be to analyze propagation in the interior cells. We then return to the first cell and examine the requirements imposed on cell resonance frequency ω_1, and external Q_{e1} to insure a good match to the structure. Finally we

visit the last cell and examine the requirements imposed on ω_N and external Q_{eN} to insure a good match out of the structure.

4.4 Coupled Cavity Model, Constant Impedance, No Beam

First consider the perfectly periodic structure. Our model for interior cells is simply

$$\left(\frac{\partial^2}{\partial t^2}+\frac{\omega_0}{Q_w}\frac{\partial}{\partial t}+\omega_0^2\right)V_k=\frac{1}{2}\omega_0^2\kappa\left(V_{k-1}+V_{k+1}\right).$$

In steady state at angular frequency ω, we may express this as a simple difference equation,

$$\tilde{V}_{k-1}+2\alpha V_k+\tilde{V}_{k+1}=0,$$

just as for a standing-wave structure, with

$$\alpha=\frac{\omega^2-\omega_0^2-j\omega\omega_0/Q_w}{\omega_0^2\kappa}.$$

We wish to insure a travelling-wave, not a standing-wave solution, so we seek a right-propagating solution of this difference equation. We leave some of the work to the next exercises.

Exercise 4.8 Show that the dispersion relation for structure voltages $V_k \propto \exp\left(j\omega t-k\gamma\right)$, takes the form $\gamma=j\theta_0+\Gamma$, with

$$\cos\theta_0=\frac{\omega_0^2-\omega^2}{\omega_0^2\kappa}, \tag{4.16}$$

and an attenuation in nepers per cell of

$$\Gamma\approx\frac{\omega/\omega_0}{\kappa Q_W\sin\theta_0},$$

assuming that $\Gamma<<\theta_0$. What is the relation between drive frequency and the cell resonant frequency for **(a)** a π/2-mode structure, **(b)** a 2π/3-mode structure?

Exercise 4.9 Show that group velocity in this constant-impedance structure is given by

$$\beta_g=\frac{L}{c}\frac{d\omega}{d\theta}=\frac{1}{2}\frac{\kappa\theta_0\sin\theta_0}{\left(1-\kappa\cos\theta_0\right)},\ \text{or}\ \kappa=\frac{\beta_g}{\frac{1}{2}\theta\sin\theta+\beta_g\cos\theta}\approx\frac{2\beta_g}{\theta\sin\theta} \tag{4.17}$$

and show that the attenuation parameter,

$$\tau=N\Gamma\approx\frac{N}{\kappa Q_W\sin\theta_0}\approx\frac{N\theta_0}{Q_W\beta_g}\approx\frac{N}{Q_e}.$$

Given the macroscopic parameters characterizing the structure (group velocity, phase-advance per cell, attenuation parameter) one would like to determine the circuit parameters required for the coupled-cavity model. The last exercises developed the relations between these macroscopic parameters, and the circuit parameters for interior cells. Let us consider conditions on the end cells. The voltage in the input cell satisfies

$$\left(\frac{\partial^2}{\partial t^2}+\frac{\omega_1}{Q_1}\frac{\partial}{\partial t}+\omega_1^2\right)V_1=\frac{1}{2}\omega_1^2\kappa_1 V_2+2\frac{\omega_1}{Q_{e1}}\frac{\partial V_F}{\partial t},$$

where the forward-going voltage in the connecting guide has been transformed to V_F, and reverse waveform V_R, satisfying $V_1=V_F+V_R$. The loaded Q of the first cell is

$$\frac{1}{Q_1}=\frac{1}{Q_{e1}}+\frac{1}{Q_{w1}}.$$

The input cell resonance frequency, and external Q, Q_{e1} are adjusted to insure no reflected signal in steady-state ($V_1=V_F$), corresponding to a match on the transmission line to a forward-wave with phase-advance per cell θ_0. Thus

$$\left(-\omega^2+\frac{\omega_1}{Q_1}j\omega+\omega_1^2\right)=\frac{1}{2}\omega_1^2\kappa_1 e^{-j\theta_0}\left(1-\Gamma\right)+2\frac{\omega_1}{Q_{e1}}j\omega,$$

with ω the drive angular frequency for synchronism. Equality permits us to solve for the input coupler cell parameters,

$$\omega_1=\frac{\omega}{\sqrt{1-\frac{1}{2}\kappa_1\left(1-\Gamma\right)\cos\theta_0}},\quad \frac{1}{Q_{e1}}=\frac{1}{Q_w}+\frac{1}{2}\frac{\kappa_1\left(1-\Gamma\right)\sin\theta_0}{\sqrt{1-\frac{1}{2}\kappa_1\left(1-\Gamma\right)\cos\theta_0}}. \tag{4.18}$$

Similarly, the output cell should be matched, and this requires

$$\left(-\omega^2+\frac{\omega_N}{Q_N}j\omega+\omega_N^2\right)=\frac{1}{2}\omega_N^2\kappa_N e^{j\theta_0}(1+\Gamma),$$

This implies,

$$\omega_N=\frac{\omega}{\sqrt{1-\frac{1}{2}\kappa_N(1+\Gamma)\cos\theta_0}},\quad \frac{1}{Q_{eN}}=-\frac{1}{Q_w}+\frac{1}{2}\frac{\kappa_N\left(1+\Gamma\right)\sin\theta_0}{\sqrt{1-\frac{1}{2}\kappa_N(1+\Gamma)\cos\theta_0}}. \tag{4.19}$$

Based on this analysis, one may expect to find that input and output cells are detuned from those in the interior of the structure.

Equations (4.16)-(4.19) determine the circuit parameters from the macroscopic quantities: wall Q, phase-advance per cell, group velocity, angular frequency. With them one is freed from dependence on the transmission line picture, and can engage in realistic modelling of the structure behavior, in particular, observables, such as transient waveforms viewed from couplers at the input and output, no-load voltage under transient conditions, effects of cell-tuning

errors, and the like.

Perhaps the first application one might make of the circuit model is the calculation of the S-matrix for the structure. We will consider a perfectly tuned structure for illustration, where the problem is solvable analytically. Given that one is most often interested in assessing *errors* in tuning, the primary value of such a result will be as a check of the numerical circuit solution that we will shortly be discussing.

Let us drive a perfectly tuned structure from the input, at angular frequency Ω, the S-matrix elements are

$$S_{11}(\Omega) = \frac{\tilde{V}_1(\Omega)}{\tilde{V}_F(\Omega)} - 1, \qquad S_{21}(\Omega) = \frac{\tilde{V}_N(\Omega)}{\tilde{V}_F(\Omega)}. \tag{4.20}$$

In this notation, we have transformed the impedance of the connecting guide to that of the structure. We may compute the terms explicitly as follows. The cell excitations in general consist of forward and backward waves,

$$\tilde{V}_k = Ae^{-(k-1)\gamma} + Be^{(k-1)\gamma},$$

where A, B and γ are functions of Ω. We wish to determine A and B, the propagation constant we know is $\gamma = j\theta + \Gamma$, with

$$\cos\theta(\Omega) = \frac{\omega_0^2 - \Omega^2}{\omega_0^2 \kappa}, \qquad \Gamma(\Omega) = \frac{\Omega/\omega_0}{\kappa Q_w \sin\theta(\Omega)}.$$

The forward and backward wave amplitudes, A and B, may be computed from the conditions on the end cells,

$$\left(j\frac{\omega_1\Omega}{Q_1} + \omega_1^2 - \Omega^2\right)(A+B) = \frac{1}{2}\omega_1^2\kappa_1\left(Ae^{-\gamma} + Be^{\gamma}\right) + 2j\frac{\omega_1\Omega}{Q_{e1}}\tilde{V}_F,$$

$$\left(j\frac{\omega_N\Omega}{Q_N} + \omega_N^2 - \Omega^2\right)\left(Ae^{-(N-1)\gamma} + Be^{(N-1)\gamma}\right) = \frac{1}{2}\omega_N^2\kappa_N\left(Ae^{-(N-2)\gamma} + Be^{(N-2)\gamma}\right).$$

Abbreviating

$$\Delta_k = j\frac{\omega_k\Omega}{Q_k} + \omega_k^2 - \Omega^2,$$

we may express this as an equation for the two unknowns, A and B,

$$\begin{pmatrix} \Delta_1 - \frac{1}{2}\omega_1^2\kappa_1 e^{-\gamma} & \Delta_1 - \frac{1}{2}\omega_1^2\kappa_1 e^{\gamma} \\ \left[\Delta_N - \frac{1}{2}\omega_N^2\kappa_N e^{\gamma}\right]e^{-(N-1)\gamma} & \left[\Delta_N - \frac{1}{2}\omega_N^2\kappa_N e^{-\gamma}\right]e^{(N-1)\gamma} \end{pmatrix}\begin{pmatrix} A \\ B \end{pmatrix} = 2j\frac{\omega_1\Omega}{Q_{e1}}\tilde{V}_F\begin{pmatrix} 1 \\ 0 \end{pmatrix}.$$

with the solution,

$$\begin{pmatrix} A \\ B \end{pmatrix} = \frac{1}{\Xi}\begin{pmatrix} \left[\Delta_N - \frac{1}{2}\omega_N^2\kappa_N e^{-\gamma}\right]e^{(N-1)\gamma} & -\left[\Delta_1 - \frac{1}{2}\omega_1^2\kappa_1 e^{\gamma}\right] \\ -\left[\Delta_N - \frac{1}{2}\omega_N^2\kappa_N e^{\gamma}\right]e^{-(N-1)\gamma} & \Delta_1 - \frac{1}{2}\omega_1^2\kappa_1 e^{-\gamma} \end{pmatrix}\begin{pmatrix} 1 \\ 0 \end{pmatrix} 2j\frac{\omega_1\Omega}{Q_{e1}}\tilde{V}_F,$$

where

$$\Xi = \left(\Delta_1 - \tfrac{1}{2}\omega_1^2\kappa_1 e^{-\gamma}\right)\left[\Delta_N - \tfrac{1}{2}\omega_N^2\kappa_N e^{-\gamma}\right]e^{(N-1)\gamma}$$
$$-\left(\Delta_1 - \tfrac{1}{2}\omega_1^2\kappa_1 e^{\gamma}\right)\left[\Delta_N - \tfrac{1}{2}\omega_N^2\kappa_N e^{\gamma}\right]e^{-(N-1)\gamma}.$$

The S-matrix elements are then

$$S_{11}(\Omega)+1 = \frac{A+B}{\tilde{V}_F(\Omega)} = 2j\frac{\omega_1\Omega}{Q_{e1}}\frac{1}{\Xi}\left(\left[\Delta_N - \tfrac{1}{2}\omega_N^2\kappa_N e^{-\gamma}\right]e^{(N-1)\gamma} - \left[\Delta_N - \tfrac{1}{2}\omega_N^2\kappa_N e^{\gamma}\right]e^{-(N-1)\gamma}\right),$$

$$S_{12}(\Omega) = \frac{Ae^{-(N-1)\gamma} + Be^{(N-1)\gamma}}{\tilde{V}_F(\Omega)} = 2j\frac{\omega_1\Omega}{Q_{e1}}\frac{1}{\Xi}\omega_N^2\kappa_N\cosh\gamma.$$

These results are most easily visualized by numerical calculation for particular examples.

Exercise 4.10 Calculate and plot the modulus of the S-matrix elements for a constant impedance, 7-cell structure, with group velocity $0.09c$ and $2\pi/3$ phase-advance per cell. Assume the structure is perfectly tuned to operate at a frequency of 91.39 GHz, with a wall Q of 2500. Make a similar plot for the cases **(a)** first cell detuned by +0.1%, **(b)** cells perfectly tuned but Q_w=500.

4.5 Numerical Solution of the Circuit Equations

For simulation of bench measurements and calculation of the effect of fabrication errors, we can solve these coupled oscillator equations in the frequency domain. For calculation of transient waveforms we will solve them in the time-domain. We set down the numerical formalisms employed in either case. The coupled circuit model consists of N 2nd-order differential equations,

$$\left(\frac{\partial^2}{\partial t^2} + \frac{\omega_n}{Q_n}\frac{\partial}{\partial t} + \omega_n^2\right)V_n = \frac{1}{2}\omega_n^2\left(\kappa_{n-1/2}V_{n-1} + \kappa_{n+1/2}V_{n+1}\right) + \frac{2\omega_n}{Q_{en}}\frac{\partial V_F}{\partial t}\delta_{n,1},$$

with $\delta_{n,1}$ the Kronecker delta function, $\delta_{n,1}$=0 unless n=1, in which case $\delta_{n,1}$=1. In the frequency domain at drive frequency Ω, we have

$$-\frac{1}{2}\omega_n^2\kappa_{n-1/2}\tilde{V}_{n-1} + \left(j\Omega\frac{\omega_n}{Q_n} + \omega_n^2 - \Omega^2\right)\tilde{V}_n - \frac{1}{2}\omega_n^2\kappa_{n+1/2}\tilde{V}_{n+1} = 2j\Omega\frac{\omega_n}{Q_{en}}\tilde{V}_F\delta_{n,1}.$$

This is a tri-diagonal matrix equation and may be inverted quickly, using, for example, the subroutine `tridag` from Numerical Recipes.[25] In this way one can quickly evaluate Eq. (4.20) for the S-matrix components. In a similar fashion, adding a drive to the output cell, one can compute S_{12} and S_{22}.

In the time-domain one may solve the second-order equations directly, or make an eikonal approximation, preferred for speed of calculation. In the first case one writes the equations as

$$W_n = \frac{\partial V_n}{\partial t},$$
$$\frac{\partial W_n}{\partial t} = -\frac{\omega_n}{Q_n} W_n - \omega_n^2 V_n + \frac{1}{2}\omega_n^2\left(\kappa_{n-1/2} V_{n-1} + \kappa_{n+1/2} V_{n+1}\right) + \frac{2\omega_n}{Q_{en}} \frac{\partial V_F}{\partial t}\delta_{n,1},$$

and proceeds to a discrete time step, using a leap-frog approach, where W is computed at midpoints $t_{l+1/2}$, and V is computed at the time-centered points t_l. Thus

$$W_n^{l+1/2} = \frac{V_n^{l+1} - V_n^l}{\Delta t},$$
$$\frac{W_n^{l+1/2} - W_n^{l-1/2}}{\Delta t} = -\frac{\omega_n}{Q_n}\frac{W_n^{l+1/2} + W_n^{l-1/2}}{2}$$
$$-\omega_n^2\left(V_n^l - \frac{1}{2}\kappa_{n-1/2} V_{n-1}^l - \frac{1}{2}\kappa_{n+1/2} V_{n+1}^l\right) + \frac{2\omega_n}{Q_{en}}\frac{\partial V_F}{\partial t}(t_l)\delta_{n,1}.$$

More explicitly, starting at time t_l, with $W_n^{l-1/2}$, V_n^l known, one proceeds to the next time step using,

$$W_n^{l+1/2} = \left(\frac{1 - \frac{\omega_n \Delta t}{2Q_n}}{1 + \frac{\omega_n \Delta t}{2Q_n}}\right) W_n^{l-1/2} - \frac{D_n^l \Delta t}{\left(1 + \frac{\omega_n \Delta t}{2Q_n}\right)}, \qquad V_n^{l+1} = V_n^l + W_n^{l+1/2}\Delta t, \tag{4.21}$$

where we abbreviate

$$D_n^l = \omega_n^2\left(V_n^l - \frac{1}{2}\kappa_{n-1/2} V_{n-1}^l - \frac{1}{2}\kappa_{n+1/2} V_{n+1}^l\right) + \frac{2\omega_n}{Q_{en}}\frac{\partial V_F}{\partial t}(t_l)\delta_{n,1}. \tag{4.22}$$

This approach requires 60 steps per rf period and is unnecessarily time-consuming for a narrow-band drive. This approach is useful, however, as a check of the following eikonal (slowly-varying envelope) technique in the case of a short pulse excitation.

In the eikonal approach we assume a narrow band rf drive taking the form

$$V_F(t) = \Re\left\{\tilde{V}_F(t) e^{j\Omega t}\right\},$$

where "narrow-band" means,

$$\left|\frac{\partial \tilde{V}_F}{\partial t}\right| << \Omega\left|\tilde{V}_F\right|.$$

We look for a solution for cell voltages also taking the form of slowly varying phasor amplitudes modulating the signal at the carrier frequency Ω,

$$2j\Omega\frac{\partial \tilde{V}_n}{\partial t} + \left(j\Omega\frac{\omega_n}{Q_n} + \omega_n^2 - \Omega^2\right)\tilde{V}_n = \frac{1}{2}\omega_n^2\left(\kappa_{n-1/2}\tilde{V}_{n-1} + \kappa_{n+1/2}\tilde{V}_{n+1}\right) + \frac{2j\Omega\omega_n}{Q_{en}}\tilde{V}_F\delta_{n,1}.$$

Letting

$$\Delta_n = j\Omega\frac{\omega_n}{Q_n} + \omega_n^2 - \Omega^2, \tag{4.23}$$

the time-centered discrete form of the equations for *n*-th cell voltage at time step *a*, $\tilde{V}_n^a$, is

$$2j\Omega\frac{\tilde{V}_n^{a+1} - \tilde{V}_n^a}{\Delta t} + \Delta_n\frac{\tilde{V}_n^{a+1} + \tilde{V}_n^a}{2}$$
$$= \frac{1}{2}\omega_n^2\left(\kappa_{n-1/2}\frac{\tilde{V}_{n-1}^{a+1} + \tilde{V}_{n-1}^a}{2} + \kappa_{n+1/2}\frac{\tilde{V}_{n+1}^{a+1} + \tilde{V}_{n+1}^a}{2}\right) + \frac{2j\Omega\omega_n}{Q_{en}}\tilde{V}_F^a\delta_{n,1},$$

and this may be rewritten as

$$\begin{aligned} &-\frac{1}{4}\omega_n^2\kappa_{n-1/2}\tilde{V}_{n-1}^{a+1} + \left(\frac{2j\Omega}{\Delta t} + \frac{\Delta_n}{2}\right)\tilde{V}_n^{a+1} - \frac{1}{4}\omega_n^2\kappa_{n+1/2}\tilde{V}_{n+1}^{a+1} \\ &= \frac{1}{4}\omega_n^2\kappa_{n-1/2}\tilde{V}_{n-1}^{a+1} + \left(\frac{2j\Omega}{\Delta t} - \frac{\Delta_n}{2}\right)\tilde{V}_n^{a+1} + \frac{1}{4}\omega_n^2\kappa_{n+1/2}\tilde{V}_{n+1}^{a+1} + \frac{2j\Omega\omega_n}{Q_{en}}\tilde{V}_F^a\delta_{n,1} \end{aligned} \tag{4.24}$$

Thus the eikonal form of the equations can be solved by a time-centered difference and one tri-diagonal matrix inversion at each time-step. Since the number of time-steps is governed only by the structure and drive bandwidths, this approach can be much faster than solution of the full 2nd-order system.

4.6 Cell Tuning Errors

Having rested our hopes on resonant energy storage for acceleration, let us consider the effect of deviation from resonance, on accelerating voltage. The net voltage experienced by a particle entering the first cell at time t_0 may be expressed as

$$V_{NL}(t_0) = \sum_{k=1}^{N} V_k(t_0 + t_k),$$

where $t_k=(k-1)L$ is the beam arrival time at cell #*k* (we take $V=c$). Expressed in eikonal form this is

$$V_{NL}(t_0) = \Re\left(\tilde{V}_{NL}e^{j\omega t_0}\right) = \Re\sum_{k=1}^{N}\tilde{V}_k e^{j\omega t_0 + j\omega t_k},$$

or

$$\tilde{V}_{NL} = \sum_{k=1}^{N}\tilde{V}_k e^{j(k-1)\varphi},$$

where $\varphi = \omega L/c$ is the synchronous phase-advance per cell, and we assume no

errors in cell length. In this form $\tilde{V}_k$, the phasor in the rotating frame, may yet have some time-dependence. For simplicity, we specialize to the steady-state case. We consider a uniform complex phase-advance per cell $\gamma = j\theta + \Gamma$ at the drive frequency ω. Then,

$$\tilde{V}_{NL} = \tilde{V}_1 \sum_{k=1}^{N} \exp\{(k-1)(j\delta - \Gamma)\} = \tilde{V}_1 \frac{1 - e^{N(j\delta - \Gamma)}}{1 - e^{(j\delta - \Gamma)}}, \tag{4.25}$$

where $\delta = \varphi - \theta$.

Considering a constant impedance structure, evaluating this for $\delta = 0$ (corresponding to synchronous phase-advance), and identifying the attenuation parameter $\tau = N\Gamma$, we recover Eq. (4.5). Evidently the quantity δ provides a figure of merit for the useful accelerating bandwidth of the structure,

$$\delta = \varphi(\omega) - \theta(\omega) = \varphi(\omega) - \theta(\omega_s) - \frac{d\theta}{d\omega}(\omega - \omega_s) + \ldots = \left(\frac{L}{c} - \frac{L}{V_g}\right)\delta\omega + \ldots,$$

or

$$\delta \approx -2\pi \frac{L_s}{\lambda} \frac{\delta\omega}{\omega} \frac{1}{\beta_g} \approx -T_f \delta\omega, \tag{4.26}$$

where ω_s is the drive frequency for synchronism, and L is the cell length. Thus the useful bandwidth varies inversely with the fill time and is much narrower than the transmission bandwidth.

Exercise 4.11 Plot the loss in no-load voltage as a function of a uniform deviation from synchronism, δ, for $\tau \approx 1.26$.

Exercise 4.12 The Mark III accelerator at Stanford was a 2856 MHz linac consisting of twenty-one 20 MW klystrons each powering one 3.05 m constant-impedance $\lambda/4$ structure. Fill time was $T_f = 1$ μsec, and wall Q ~10,000. Shunt impedance per unit length was $r \approx 47.3$ MΩ/m. Calculate the loss in no-load voltage for the Mark III for a drive frequency error of 100 kHz. What are the implications for temperature regulation? (Recall that the temperature coefficient of expansion of copper is $\alpha \approx 1.7 \times 10^{-5}$ /°K).

For a constant-gradient structure, the analysis is similar to that for a constant-impedance structure, except that the term $\Gamma = 0$,

$$\tilde{V}_{NL} = \tilde{V}_1 \frac{1 - e^{j\delta N}}{1 - e^{j\delta}} = \tilde{V}_1 e^{j\frac{1}{2}(N-1)\delta} \frac{\sin\left(\frac{1}{2}N\delta\right)}{\sin\left(\frac{1}{2}\delta\right)}.$$

Thus, for a small deviation from synchronism, one has

$$\frac{\left|\tilde{V}_{NL}(\delta)\right|}{\left|\tilde{V}_{NL}(0)\right|} \approx 1-\frac{1}{6}\left(N^2-1\right)\delta^2 \approx 1-\frac{1}{6}\left(T_f\delta\omega\right)^2 \approx 1-\frac{1}{6}\left(2\pi\frac{L_s}{\lambda}\frac{\delta\omega}{\omega}\frac{1}{\beta_g}\right)^2. \tag{4.27}$$

Next we consider the more general problem of cell-to-cell detuning. We will consider a transmission line consisting of coupled cavities, with all but the *m*-th cavity perfectly tuned, as illustrated in Fig. 4.3.

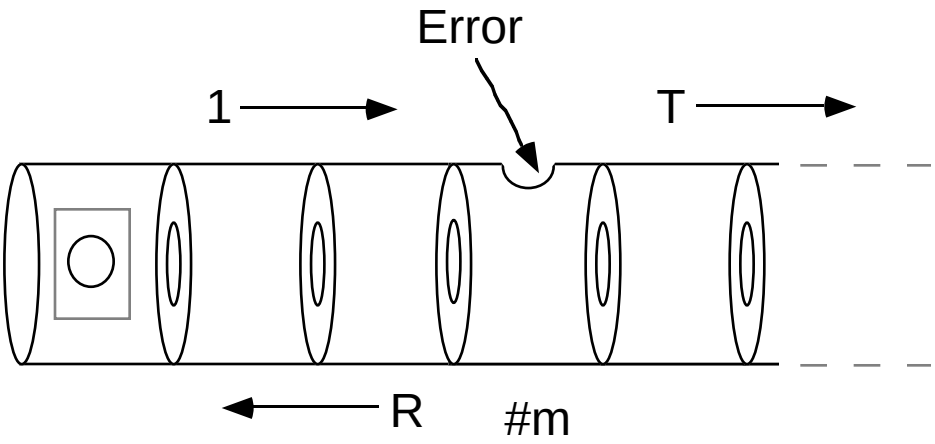

FIGURE 4.3. We consider first the case of a travelling-wave structure with a single tuning error. The tuning error results in a reflected signal *R*, and a transmitted signal *T*.

In steady-state, with a wave launched into the structure from the input cell, a reflection will occur at the *m*-th cell, and the voltage in the *k*-th cell will take the form

$$V_k = \begin{cases} e^{-k(j\theta+\Gamma)} + \left[e^{-2m(j\theta+\Gamma)}R\right]e^{k(j\theta+\Gamma)} & ;\ k \le m \\ Te^{-k(j\theta+\Gamma)} & ;\ m \le k \end{cases},$$

where continuity requires $T=1+R$, and perfect tuning would correspond to $R=0$. We can compute the reflection coefficient, R, in terms of the cell-detuning by applying the coupled-cavity model,

$$\left(\delta\omega_m^2+\omega_m^2-\omega^2+j\frac{\omega\omega_m}{Q_w}+\delta\omega_m^2\right)V_m = \frac{1}{2}\omega_m^2\left(\kappa_{m-1/2}V_{m-1}+\kappa_{m+1/2}V_{m+1}\right).$$

Explicitly this is

$$\left(\delta\omega_m^2+\omega_m^2-\omega^2+j\frac{\omega\omega_m}{Q_w}\right)\left(Te^{-m(j\theta+\Gamma)}\right)$$
$$= \frac{1}{2}\omega_m^2\kappa_{m-1/2}\left(e^{-(m-1)(j\theta+\Gamma)}+\left[e^{-2m(j\theta+\Gamma)}R\right]e^{(m-1)(j\theta+\Gamma)}\right)+\frac{1}{2}\omega_m^2\kappa_{m+1/2}Te^{-(m+1)(j\theta+\Gamma)},$$

and after rearranging terms, and making use of the tuning condition,

$$\omega_m^2 - \omega^2 + j\frac{\omega\omega_m}{Q_w} = \frac{1}{2}\omega_m^2\left(\kappa_{m-1/2}e^{-(m-1)(j\theta+\Gamma)} + \kappa_{m+1/2}e^{-(m+1)(j\theta+\Gamma)}\right),$$

one can show that

$$R = -\frac{\delta\omega_m^2}{\delta\omega_m^2 + \omega_m^2\kappa_{m-1/2}(\Gamma\cos\theta + j\sin\theta)}.$$

Thus we find that transmission through cell #*m* with detuning corresponds to a transmission coefficient $T_m = \exp(j\delta_m)$, where the term δ_m is in general complex, but to a good approximation is just

$$\delta_m \approx \frac{1}{2}\frac{\delta\omega_m^2}{\omega_m^2}\frac{\theta}{\beta_g}. \tag{4.28}$$

With this result, we proceed to calculate the loss in no-load voltage due to cell detuning. To simplify the problem, we will assume that all detunings are quite small, and neglect multiple reflections, making the approximation

$$\tilde{V}_k = e^{-(k-1)\gamma}T_kT_{k-1}\cdots T_1\tilde{V}_1,$$

where $\gamma = j\theta + \Gamma$ is the propagation constant for the tuned structure. This is expressed more simply as

$$\tilde{V}_k = e^{j\varepsilon_k}e^{-(k-1)\gamma}\tilde{V}_1,$$

where ε_k is the cumulative error in phase-advance at cell *k*,

$$\varepsilon_k = \sum_{m=1}^{k}\delta_m .$$

The no-load voltage is then

$$\tilde{V}_{NL} = \sum_{k=1}^{N}\tilde{V}_k e^{j(k-1)\varphi} = \tilde{V}_1\sum_{k=1}^{N}e^{(k-1)(j\varphi-\gamma)}e^{j\varepsilon_k}.$$

In this form it is straightforward to compute the no-load voltage, given small errors in cell tuning.

To appreciate the tolerances implied for fabrication and assembly, it is helpful to have something still more explicit, so let us consider the case of a large number of structures, fabricated with a particular distribution in cell detuning errors. For simplicity, we assume the distribution in δ_m, for any *m*, is a Gaussian, with rms σ_δ. The average (over a large-number of structures) no-load voltage is given by

$$\left\langle\tilde{V}_{NL}\right\rangle = \tilde{V}_1\sum_{k=1}^{N}e^{(k-1)(j\varphi-\gamma)}\left\langle e^{j\varepsilon_k}\right\rangle,$$

and to compute the average, $\left\langle e^{j\varepsilon_k}\right\rangle$, we note that the cumulative error ε_k is

distributed according to a Gaussian, with rms $\sigma_{\varepsilon_k}^2 = k\sigma_\delta^2$. This implies that

$$\left\langle e^{j\varepsilon_k} \right\rangle = \int_{-\infty}^{\infty} d\varepsilon_k \frac{1}{\sqrt{2\pi}\sigma_{\varepsilon_k}} \exp\left(j\varepsilon_k - \frac{\varepsilon_k^2}{\sigma_{\varepsilon_k}^2} \right) = \exp\left(-\frac{1}{2}\sigma_{\varepsilon_k}^2 \right).$$

The average no-load voltage is then

$$\left\langle \tilde{V}_{NL} \right\rangle = \tilde{V}_1 \sum_{k=1}^{N} \exp\left\{ (k-1)(j\varphi - \gamma) \right\} \exp\left(-\frac{1}{2} k\sigma_\delta^2 \right).$$

This is just a geometric series and easily summed. For illustration, consider the case of a constant gradient structure, with no error in drive frequency,

$$\left| \frac{\left\langle \tilde{V}_{NL}(\sigma_\delta) \right\rangle}{\tilde{V}_{NL}(0)} \right| = \exp\left(-\tfrac{1}{2}(N+1)\sigma_\delta^2 \right) \frac{\sinh\left(\tfrac{1}{4} N\sigma_\delta^2 \right)}{N \sinh\left(\tfrac{1}{4}\sigma_\delta^2 \right)}.$$

For $N\sigma_\delta^2 / 4 << 1$, this is simply

$$\left| \frac{\left\langle \tilde{V}_{NL}(\sigma_\delta) \right\rangle}{\tilde{V}_{NL}(0)} \right| \approx 1 - \frac{1}{2}(N+1)\sigma_\delta^2. \tag{4.29}$$

Comparing this with the result for a uniform frequency error, we can see that the structure is more tolerant of random errors by a factor of $\approx \sqrt{N/3}$.

Exercise 4.13 Consider a 91.39 GHz, 60-cell, 2π/3-mode constant-gradient structure, with initial group velocity 0.09*c*. Calculate the rms fractional cell frequency error tolerance for an average loss of 1% in no-load voltage. Estimate the absolute tolerance in microns, assuming $\delta L / L = -\delta\omega / \omega$.

Exercise 4.14 For the structure of the previous exercise, write a short program to check the analytic estimate. For each of 10 values of σ_δ, generate a sample of 100 structures with Gaussian-distributed detuning errors, compute the no-load voltage reduction for each, and make a scatter plot of no-load phasor amplitude versus σ_ω, with the theoretical mean overlayed.

Epilogue

These notes are intended as an introduction to electrodynamics as applied to microwave linacs. However, let us not leave without mentioning the challenges at the forefront of research in electromagnetic accelerators. The ultimate goal of accelerator research for high energy physics is *high energy*, and to reach high energy in a reasonable length, one requires a *high gradient*. For example, a 5-TeV collider fitting on any existing laboratory site would require a gradient of 1 GeV/m or more.

To place such a gradient in context, let us take note of the phenomena known to limit gradient, and gradients achieved to date. A glimpse of these may be seen in Fig. E.1. This plot includes results for a laser wakefield accelerator (LWFA), a plasma beat-wave accelerator (PBWA), and several 0.5-TeV collider concepts.[9] The block marked "SLC" extends from 20 MV/m as for a typical structure, to 40 MV/m as for certain higher gradient structures on the linac. The phenomena of concern are *field-emission*, *breakdown*, *trapping*, and *pulsed heating*.

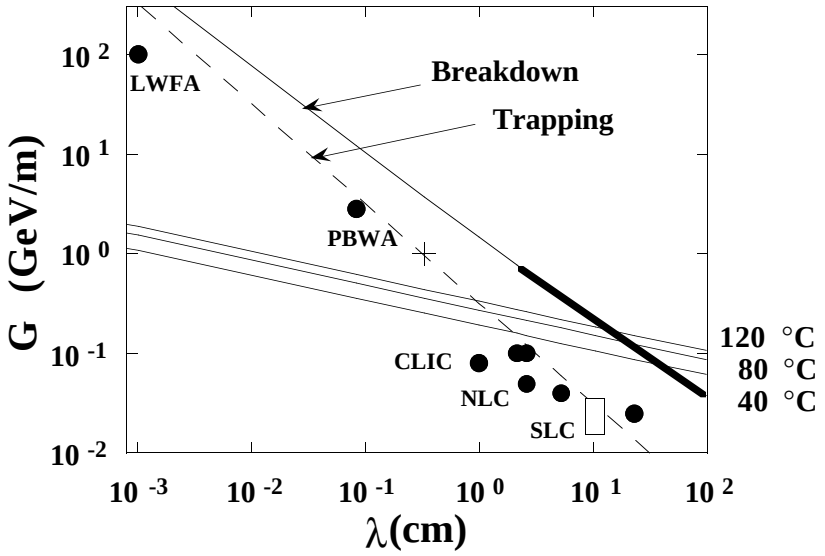

Figure E.1. Current state of the art in high-gradient accelerator research.

Field-emission refers to the extraction of electrons from a surface in the presence of a large electric field. The picture associated with this process consists of a potential well binding electrons to the bulk of the solid, modified by the presence of the applied electric field. Electrons tunnel through the modified potential barrier at the surface and escape. For such a quantum-mechanical tunneling process, one can show that emitted current density J varies roughly as $\ln J \approx -D/E$ with D a constant depending on the work function, and E the electric field. In practice, in high-power rf work, the exponent inferred from collected current is 50-200 times as

large as one would expect based on the expected surface electric field. To operate at a gradient of 1 GeV/m one would require a much lower field-enhancement, on the order of 5, to control loading and structure damage.

Known mechanisms for enhancement of field emission are (1) a roughened surface, causing geometrical enhancement of the local electric field, and (2) surface impurities, tending to lower the work function. Control of field emission is an ongoing research activity at present, concerning itself with surface finish, coatings and cleanliness.[26] At the same time, there is experimental evidence that field emission is inhibited on short, nanosecond time-scales,[27] and this suggests that to reach high gradient, one could consider structures with natural fill times on the nanosecond scale. This implies a short rf wavelength, on the order of millimeters.

Field emission is sometimes associated with *breakdown*.[28] For high-power pulsed rf systems operated at high vacuum (10^{-9}-10^{-7} torr) as employed on rf linacs, *breakdown* refers to a collection of three coincident symptoms: (1) a sudden change in the rf waveform, e.g., a sudden increase in the reflected voltage from a resonant device, (2) an increase in x-ray emission, (3) a degrading of the vacuum. The field level at which breakdown occurs for a given structure is known to depend on the history of the structure (fabrication, assembly, cleaning, handling), in particular, its previous exposure to rf (conditioning cycle). In general one may say that breakdown occurs at a higher field level for a shorter pulse and this too suggests that for high gradient, structures operating on shorter time-scales would be desirable.

Trapping refers to the acceleration from rest of field-emitted or injected electrons in the structure. Trapping fraction is a function of the product $G\lambda$ of the gradient G and the rf wavelength λ. This is easy to see. We express the accelerating electric field in a travelling-wave structure as $-eE_z = eE_0 \cos\psi$, where the phase $\psi = \beta s - \omega t$, with β the wavenumber for the rf signal. The angular frequency of the microwave system is ω. Given an initial value for an electron's phase and energy, we may track its longitudinal motion according to

$$\frac{d\psi}{ds} = \beta - \frac{\omega}{V_z}, \qquad \frac{d}{ds}\left(mc^2\gamma\right) = eE_0 \cos\psi .$$

One can show for for an electron injected into a speed-of-light structure $(\omega / \beta = c)$, with initial speed over c, β_0 and phase ψ_0, that at any later time, its phase ψ, and speed over c, β are related according to the "binding-field" expression,

$$\sin\psi = \sin\psi_0 + \frac{1}{\alpha}\left\{\sqrt{\frac{1-\beta}{1+\beta}} - \sqrt{\frac{1-\beta_0}{1+\beta_0}}\right\},$$

with $\alpha = eE_0 / mc^2\beta$, just the normalized product of gradient and rf wavelength. Analyzing this result one can show that the minimum value of α required for trapping of particles from rest is $\alpha = 1/2$. More generally, one can show that the fraction of a monoenergetic beam trapped in a speed-of-light structure is given by

$$f_{trap} = \frac{1}{2} + \frac{1}{\pi}\sin^{-1}\left(1 - \frac{1}{\alpha}\sqrt{\frac{1-\beta_0}{1+\beta_0}}\right).$$

To control the trapping of parasitic electrons at high gradient, one requires either (1) control of field emission or (2) a short rf wavelength, or both. The curve in Fig. E.1 corresponds to α=1 and a trapping fraction of 50%.

Pulsed heating refers to the deposition of heat, by Ohmic loss, in the conducting structure, in a single pulse. Heat flow within the conducting surface is governed by the diffusion equation,

$$C\frac{\partial T}{\partial t} = \sigma E^2 - \kappa\frac{\partial^2 T}{\partial \xi^2},$$

with σE^2 the local volume rate of Ohmic energy deposition, κ the thermal conductivity, and C the heat capacity. For room-temperature copper $\kappa = 401\ W/°K-m$ and $C = 3.45\times10^6\ J/°K-m^3$. The depth to which heat diffuses in a time t varies as $t^{1/2}$, and accordingly, the temperature rise within the conductor varies as $\Delta T \propto E^2 t^{1/2}$ Curves of constant pulsed temperature rise are shown in Fig. E.1, for pulse length equal to the natural fill-time of a constant-gradient travelling wave structure with attenuation parameter $\tau \approx 1$.

Taking all these considerations together, the phenomena limiting gradient all imply that *high gradient* requires *short wavelength*. For a 1-GeV/m linac, interest begins in the *W-Band*, 75-110 GHz. A cross-mark has been added in Fig. E.1 as a helpful landmark, corresponding to 1 GeV/m. The minimum frequency is close to 91.4 GHz (3.3 mm), the 32nd harmonic of the SLC fundamental frequency, 2.856 GHz. However, the curves of pulsed temperature rise, in Fig. E.1, make clear that such a W-Band linac will suffer severe pulsed heating, and the *conventional* travelling-wave structure, the paradigm for fifty years, will fail. To be sure, it is yet an open question exactly what cyclic pulsed temperature rise a structure can withstand, and this is the subject of ongoing research on materials under conditions of high-power pulsed rf.[29] Other essential research problems include *structure fabrication*,[30] *wakefields*,[31] and *power sources*.[32]

Ultimately the question for any linac concept is: what is the maximum achievable gradient for a concept and technology scalable to a high energy collider? This question is asked for the conducting geometries, as well as the dielectric, for the tube-powered linacs, as well as laser and beam driven linacs. The answers are largely unknown. For the conducting structures, conceptual innovation is required as well as materials research. For the plasma accelerators, basic parameters such as [*R/Q*] have yet even to be calculated, and the collider concept itself is non-existent. The field today is wide-open, and as Fig. E.1 implies, opportunities for research abound.

Appendix A: Numbers and Math

A.1 Constants

A few constants are hard to live without, and are listed for convenience in Table A.1. It is natural to ask: why these constants and not some others? Questions like this are why we have high energy physics programs at many of the national labs!

TABLE A.1. Constants for electrodynamics in this universe.

$mc^2 = 0.5110\,\mathrm{MeV}$	*electron rest energy*
$c = \dfrac{1}{\sqrt{\varepsilon_0\mu_0}} = 2.9979\times10^{8}\ \mathrm{m/s}$	*speed of light*
$r_e = \dfrac{e^2}{4\pi\varepsilon_0 mc^2} = 2.8179\times10^{-15}\,\mathrm{m}$	*classical radius of the electron*
$Z_0 = \sqrt{\dfrac{\mu_0}{\varepsilon_0}} = 376.7\Omega$	*wave impedance of free space*
$I_0 = 4\pi\varepsilon_0\dfrac{mc^3}{e} = 17.03\,\mathrm{kA}$	*Alfven's constant*
$\alpha = \dfrac{e^2}{4\pi\varepsilon_0\hbar c} = \dfrac{1}{137.036}$	*fine structure constant*

To reduce quantities to practical units one needs in addition the charge of an electron, -e, with $e = 1.602\times10^{-19}\,\mathrm{C}$, and $mc/e = 1.7\times10^{-3}\,\mathrm{T-m}$. Occasionally it is helpful to know the ratio of proton to electron mass, $m_p/m \approx 1836$, Avogadro's number $N_A = 6.022\times10^{23}$, and Boltzmann's constant, k_B, where $k_BT = 1/38.7\ \mathrm{eV}$ for T=300°K. It is never necessary to remember $\varepsilon_0 = 8.85\times10^{-12}\,\mathrm{Fm^{-1}}$, $\mu_0 = 4\pi\times10^{-7}\,\mathrm{NA^{-2}}$, nor the mass of the electron $m = 9.109\times10^{-31}\,\mathrm{kG}$.

Exercise A.1 A photon of angular frequency ω carries energy $\hbar\omega$. Using the constants from Table 1.1, and the electronic charge in coulombs, show that a photon of 1 μm wavelength carries energy of about 1 eV. (Evidently one does not need to remember that Planck's constant divided by 2π is $\hbar = 1.05\times10^{-34}\,\mathrm{Js}$.)

Exercise A.2 The binding energy of an electron in the ground state of a hydrogen atom is $m_e c^2\alpha^2/2$. Compute this in units of electron-volts.

In addition, there are a few combinations of numbers that come up so frequently they also should be second nature. In speaking of couplers, attenuation

and the like, decibels come in handy, $10\log_{10}(2) \approx 3$ dB, $10\log_{10}(3) \approx 5$ dB. One someday may wonder whether an error of ± 0.1 dB is important. Since $20\log_{10}(0.99) \approx -0.1$dB, the answer is yes if one is working at the 1% level in voltage, otherwise no. If the error is ± 1 dB then since -1 dB $\approx 10\log_{10}(0.8)$, the uncertainty is of order 20% in power. Mention of units for amplitude reminds us too of units for phase, $\pi \approx 3.14159$ and 1 radian $= 57.3°$. Next, one may need to communicate results in some strange yet conventional set of units, so let us contemplate our choices.

A.2 Units For All Occasions

The conventional set of units is the International System of Units, colloquially, MKS. That said, in some places, to get something machined one needs 1 inch $= 2.54$ cm and 1 mil $= 0.001$ inch $= 25.4$ μm. If surface finish is a concern, for a machined part, *Class XX* means XX μinches *roughness average* or R_a. Roughness average is the average peak-to-valley depth over the surface. A rough surface exhibits greater losses than a smooth surface, for then the wall currents must traverse a greater path length. In addition, rough surfaces are rumored to have lower breakdown thresholds at high power. So a good finish is a good thing. A Class 1 finish has a roughness average of 1 μinch ≈ 250 A. Other units that may come up: 1 m $= 3.3$ ft , 1 mile $= 5280$ f*t* $= 1609$ m. Electrons in linacs often come in bunches a few mm in length, where 1 mm ≈ 3.3 ps.

Area too is a broad subject. Accelerators are often built based on the expected cross-section for some event. Cross-sections are usually measured in picobarns (10^{-12} barn) or, worse yet, femtobarns (10^{-15} barn) nowadays and so one may need $1\,\text{barn} = 10^{-28}\,\text{m}^2$. Oftentimes one hears experimenters speaking of *inverse picobarns*; what they are referring to is a number (*integrated luminosity*) they can multiply by their expected cross-section to determine the number of events they could produce. Most likely they couldn't produce that many. Area is also significant in the physical layout of an accelerator, with units such as 1 hectare =100 m $\times$ 100 m, 1 acre=43,560 sq. ft $\approx$ 0.4 hectare.

Meanwhile, time is of the essence, so we mention, 1 week=168 hour, $1\,\text{year} = 8760\,\text{hour} = 3.15\times 10^7\,\text{sec}$. Speed we appreciate; electrons in linacs typically travel at about $c \approx 1$ *ft*/*ns*. Signals in coaxial cable (RG-214 or RG-58A, say) often travel at $0.66c \approx 1$ m/5 ns. Let us also take a moment to enjoy the many units for pressure,

$$1.01\times 10^5\,\text{Pa} \approx 1.01\,\text{bar} \approx 760\,\text{mm Hg}(0°\,\text{C}) \approx 760\,\text{torr} \approx 14.7\,\text{psi}.$$

Exercise A.3 A 10-GeV electron beam travels through 8 girders, each girder consisting of 40 feet of accelerating structure. At the end of each girder the beam induces a signal on RG-214 cable. All cables must be run 50 feet up to exit the accelerator housing, and then must be run to one location, directly above the end of one of the girders, to permit acquisition of the signal by a single gated analog-to-digital converter (GADC). Cable lengths must be such that all signals arrive simultaneously. At which of the eight locations should the GADC be located to minimize the length of the longest cable?

Accelerators consume a a lot of joules, and this may show up on the power bill in British thermal units, $1\,\mathrm{BTU} = 1.05\,\mathrm{kJ}$. If horsepower is needed, $1\ \mathrm{hp} = 0.746\ \mathrm{kW}$; at the other extreme, $1\ \mathrm{mW} \equiv 0\ \mathrm{dBm}$, i.e., dBm means decibels relative to milliwatt. Speaking of energy and power, it is amusing to note that a typical industrial 5 hp motor will run at 70-80% efficiency, as can a home furnace, or a fluorescent light bulb. Makes one wonder what an accelerator can do.

Exercise A.4 The Stanford Linear Collider (SLC) collides two 46-GeV, 1-mm long bunches, each with about 6 nC of charge, at a rate of 120 Hz during normal operation. What is the average power in one beam? The peak power? If the power drawn by the site during 120 Hz running is 50 MW, what is the practical efficiency of the SLC?

A.3 Vector Identities

A vector recall is a thing with magnitude and direction. For example, wind "velocity" is a vector since it consists of a speed (*e.g.*, 100 miles per hour) and a direction (*e.g.*, from the East). The *dot-product* (or *scalar product*), $\vec{A} \bullet \vec{B}$, of two vectors, $\vec{A}$, $\vec{B}$ is just a number, $|\vec{A}||\vec{B}|\cos\theta$, where $|\vec{A}|$ is the length (or magnitude) of $\vec{A}$, and θ is the angle between $\vec{A}$ and $\vec{B}$. The *cross-product* of two vectors is yet another vector, at right angles to $\vec{A}$ and $\vec{B}$. To picture the cross-product $\vec{A} \times \vec{B}$, one places one's *right* thumb on $\vec{A}$, and index finger on $\vec{B}$; the palm then points in the direction of the cross-product. At some point, use of hands becomes tedious and we resort to an algebraic approach,

$$\vec{A} \times \vec{B} = \begin{vmatrix} \hat{x}_1 & \hat{x}_2 & \hat{x}_3 \\ A_1 & A_2 & A_3 \\ B_1 & B_2 & B_3 \end{vmatrix} = \hat{x}_1\left(A_2B_3 - B_2A_3\right) + \hat{x}_2\left(A_3B_1 - B_3A_1\right) + \hat{x}_3\left(A_1B_2 - B_1A_2\right),$$

referred to an orthogonal right-handed coordinate system with basis vectors $\hat{x}_1, \hat{x}_2, \hat{x}_3$, for example $\left(x_1, x_2, x_3\right) = \left(x, y, z\right)$, corresponding to directions forward, left and up.

It is when a cross-product is involved that the more outrageous of the Vector Identities arise. However, the secrets of these Vector Identities can be unlocked with the anti-symmetric 3-tensor, ε_{ijk}. If *(ijk)* is a cyclic permutation of (123), then $\varepsilon_{ijk} = 1$. Thus $\varepsilon_{123} = \varepsilon_{312} = \varepsilon_{231} = 1$. Moreover if *(ijk)* differs from (123) by an even number of *transpositions*, then $\varepsilon_{ijk} = 1$. A transposition is an interchange of indices, such as $(ijk) \to (jik), (ikj), (kji)$. If *(ijk)* differs from (123) by an odd number of transpositions, then $\varepsilon_{ijk} = -1$. If any of the indices *(ijk)* are identical, then $\varepsilon_{ijk} = 0$. Using these rules, one may check, component-wise, that the cross-product of two vectors may be expressed as

$$\left(\vec{A}\times\vec{B}\right)^i = \sum_{j=1}^{3}\sum_{k=1}^{3}\varepsilon^{ijk}A^jB^k = "\ \varepsilon^{ijk}A^jB^k\ ",$$

where we adopt the abbreviation that repeated indices are summed over the values 1,2,3. This *summation convention* saves one a lot of time and paper. One can also check, component-wise, the *secret to all curl identities*

$$\varepsilon^{ijk}\varepsilon^{ilm} = \delta^{jl}\delta^{km} - \delta^{jm}\delta^{kl},$$

where δ^{kl} is the *Kronecker delta*, $\delta^{kl} = 1$ if $k=l$, and $\delta^{kl} = 0$ otherwise. One can go on to demonstrate infinitely many identities; Exercise A.5 includes three of the more popular ones.

Exercise A.5 Confirm that

$$\vec{A}\bullet\left(\vec{B}\times\vec{C}\right) = \vec{C}\bullet\left(\vec{A}\times\vec{B}\right) = \vec{B}\bullet\left(\vec{C}\times\vec{A}\right),$$
$$\vec{A}\times\left(\vec{B}\times\vec{C}\right) = \left(\vec{A}\bullet\vec{C}\right)\vec{B} - \left(\vec{A}\bullet\vec{B}\right)\vec{C},$$
$$\left(\vec{A}\times\vec{B}\right)\bullet\left(\vec{C}\times\vec{D}\right) = \left(\vec{A}\bullet\vec{B}\right)\left(\vec{C}\bullet\vec{D}\right) - \left(\vec{A}\bullet\vec{D}\right)\left(\vec{B}\bullet\vec{C}\right).$$

We can also use ε_{ijk} to derive some relations for *gradient, divergence* and *curl.* First though, let us define these items.

A.4 Vector Calculus

Given a real-valued (scalar) function $f(\vec{r})$, one may sketch the surfaces of constant f (*equipotentials*); the gradient of f, denoted $\vec{\nabla}f(\vec{r})$, is a vector normal to the surface passing through $\vec{r}$, given in Cartesian coordinates by

$$\vec{\nabla}f = \hat{x}\frac{\partial f}{\partial x} + \hat{y}\frac{\partial f}{\partial y} + \hat{z}\frac{\partial f}{\partial z}.$$

Recall that the partial derivative, $\partial f / \partial x$, is just an ordinary derivative with respect to x, when the other independent variables, y and z are looked on as constants. This ordinary derivative is just the instantaneous slope of the curve f vs x.

As for divergence, first consider a vector field $\vec{A}(\vec{r})$, *i.e.*, an assignment of a vector $\vec{A}$ to each point in space $\vec{r}$. For example, we may consider particles of hail in a thunderstorm---specifically, the *flux* of hail particles, defined as the local number density of hail multiplied by its local velocity. (Units would then be number of hail particles per square meter per second, or $m^{-2}s^{-1}$.) The divergence $\vec{\nabla}\bullet\vec{A}$ at a point $\vec{r}$ is just the rate at which particles are leaving a small volume enclosing $\vec{r}$, divided by the volume. Symbolically, we say

$$\vec{\nabla}\bullet\vec{A} = \lim_{V\to 0}\frac{1}{V}\int_{\partial V}\vec{A}\bullet d\vec{S}.$$

The limit symbol means the value when V becomes small. The surface of the volume V is denoted by ∂V and this surface has been divided up into small squares of area dS. The vector $d\vec{S}$ has magnitude dS and points outward, normal to the surface. The dot product $\vec{A} \bullet d\vec{S}$ simply counts particles flowing through the square. The integral sign indicates a sum over each little square. In words, the rate of accumulation in a volume V is the rate at which flux enters.

Given this definition it isn't surprising that for a *finite* volume V, one has an identity,

$$\int_V \vec{\nabla} \bullet \vec{A}\, d^3\vec{r} = \int_{\partial V} \vec{A} \bullet d\vec{S},$$

also referred to as the *divergence theorem*, or sometimes Green's theorem (although George Green developed several, as we will see). On the left-side, the volume V has been divided into little cubes each of volume $d^3\vec{r}$; one can picture a cube of dimensions $dx \times dy \times dz$, in which case $d^3\vec{r} = dx\, dy\, dz$. In Cartesian coordinates, divergence takes the form

$$\vec{\nabla} \bullet \vec{A} = \frac{\partial A_x}{\partial x} + \frac{\partial A_y}{\partial y} + \frac{\partial A_z}{\partial z}.$$

Finally there is the matter of curl. The curl of a vector field $\vec{A}$ is another vector, denoted $\vec{\nabla} \times \vec{A}$, and is most easily defined component-wise. To compute the component of curl along a direction $\hat{n}$, at a point $\vec{r}$, let us draw a small closed contour (a circle, if you like) around the point $\vec{r}$, with normal $\hat{n}$. The curl is defined as

$$\left(\vec{\nabla} \times \vec{A}\right)_{\hat{n}} = \lim_{S \to 0} \frac{1}{S} \int_{\partial S} \vec{A} \bullet d\vec{l}\,.$$

where the area enclosed by the path (the area of the circle) is S, and the contour (the perimeter of S) is denoted ∂S. This contour has been divided into small lengths dl and the vector $d\vec{l}$ is oriented tangent to the contour, with magnitude dl. The integral sign indicates a sum over each length element. Such an integral is referred to as a circulation integral, since it provides the local magnitude and direction of the circulating component of the flux. For a *finite* surface S, one has Stoke's Theorem,

$$\int_S \left(\vec{\nabla} \times \vec{A}\right) \bullet d\vec{S} = \int_{\partial S} \vec{A} \bullet d\vec{l}\,.$$

In Cartesian coordinates, the curl of a vector may be expressed as

$$\left(\vec{\nabla} \times \vec{A}\right)^i = \varepsilon^{ijk} \partial^j A^k,$$

where we adopt the abbreviation $\partial^j = \partial / \partial x^j$.

Exercise A.6 Confirm that $\vec{\nabla} \times \vec{r} = 0$ and $\vec{\nabla} \bullet \left(\vec{r} \times \vec{a}\right) = 0$, where $\vec{a}$ is a constant vector.

Exercise A.7 Verify that

$$\vec{\nabla}\times\left(\vec{\nabla}\times\vec{A}\right)=\vec{\nabla}\left(\vec{\nabla}\bullet\vec{A}\right)-\nabla^2\vec{A}, \qquad \vec{\nabla}\bullet\left(\vec{A}\times\vec{B}\right)=\vec{B}\bullet\left(\vec{\nabla}\times\vec{A}\right)-\vec{A}\bullet\left(\vec{\nabla}\times\vec{B}\right),$$

$$\left\{\vec{A}\times\left(\vec{\nabla}\times\vec{B}\right)\right\}^a=A^b\partial^a B^b-A^b\partial^b B^a, \quad \left(\vec{\nabla}\times\vec{A}\right)\bullet\left(\vec{\nabla}\times\vec{B}\right)=\left(\partial^a A^b\right)\left(\partial^a B^b\right)-\left(\partial^a A^b\right)\left(\partial^b B^a\right).$$

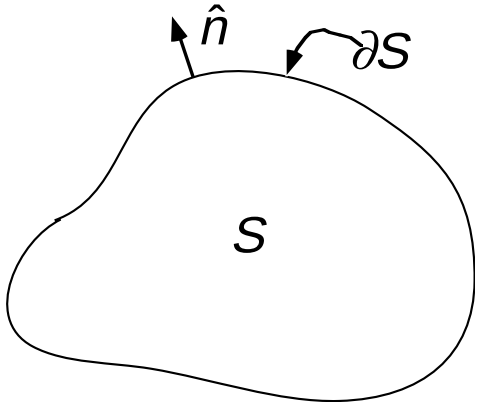

FIGURE A.1 Geometry for application of Green's theorem to a surface *S* and boundary ∂S.

In analyzing waveguide, we will make use of Green's second identity, also called Green's theorem,

$$\int_S\left(\psi_1\nabla_\perp^2\psi_2+\vec{\nabla}_\perp\psi_1\bullet\vec{\nabla}_\perp\psi_2\right)d^2r_\perp=\oint_{\partial S}\psi_1\frac{\partial\psi_2}{\partial n}dl,$$

where ψ_1 and ψ_2 are functions of $\vec{r}_\perp$, the area integral is over the waveguide cross-section *S*, and the line integral is around the waveguide circumference ∂S, as indicated in Fig. A.1. $\partial\psi_2/\partial n$ is the derivative of ψ_2 along the outward oriented normal.

A.5 Cylindrical Coordinates

Cylindrical coordinates are frequently used in accelerator problems, as very often the material geometry (the *beamline*) possesses cylindrical symmetry about some axis, usually denoted $\hat{z}$ or $\hat{s}$. Notations we will use for position are

$$\vec{R}=\vec{r}_\perp+z\hat{z}=\vec{r}_\perp+s\hat{s}=(x,y,z)=\hat{r}r+z\hat{z},$$

where the radial coordinate *r*, and the angle ϕ are determined from $x=r\cos\phi$, $y=r\sin\phi$, so that $r^2=x^2+y^2$. Unit vectors are

$$\hat{r}=\frac{1}{r}(x\hat{x}+y\hat{y}),\ \hat{\phi}=\frac{1}{r}(-y\hat{x}+x\hat{y}).$$

The gradient operator is

$$\vec{\nabla} = \hat{x}\frac{\partial}{\partial x} + \hat{y}\frac{\partial}{\partial y} + \hat{z}\frac{\partial}{\partial z} = \hat{r}\frac{\partial}{\partial r} + \hat{\phi}\frac{1}{r}\frac{\partial}{\partial \phi} + \hat{z}\frac{\partial}{\partial z}.$$

and a few other operators are handy to have,

$$\vec{\nabla} \bullet \vec{A} = \frac{1}{r}\frac{\partial}{\partial r} rA_r + \frac{1}{r}\frac{\partial A_\phi}{\partial \phi} + \frac{\partial A_z}{\partial z},$$

$$\vec{\nabla} \times \vec{A} = \hat{r}\left(\frac{1}{r}\frac{\partial A_z}{\partial \phi} - \frac{\partial A_\phi}{\partial z}\right) + \hat{\phi}\left(\frac{\partial A_r}{\partial z} - \frac{\partial A_z}{\partial r}\right) + \hat{z}\left(\frac{1}{r}\frac{\partial}{\partial r} rA_\phi - \frac{1}{r}\frac{\partial A_r}{\partial \phi}\right),$$

$$\nabla^2 f = \frac{1}{r}\frac{\partial}{\partial r} r\frac{\partial f}{\partial r} + \frac{1}{r^2}\frac{\partial^2 f}{\partial \phi^2} + \frac{\partial^2 f}{\partial z^2}.$$

The volume element in cylindrical coordinates is $d^3\vec{r} = dV = r\,dr\,d\phi\,dz$.

Exercise A.8 Check that, for any constant coefficients f_m,

$$f = \sum_{m=-\infty}^{+\infty} f_m r^m e^{jm\phi}$$

is a solution to $\nabla^2 f = 0$. In the *x*-*y* plane, sketch the curves of constant $r\cos\phi = \Re re^{j\phi}$, and $r^2\cos 2\phi = \Re r^2 e^{2j\phi}$.

A.6 Integrals and Special Functions

The bottom line on integrals is Gradshteyn and Ryzhik.[33] At the top of the list is

$$\int_0^\infty dx\, e^{-x^2} = \tfrac{1}{2}\pi^{1/2}.$$

This can be checked as follows:

$$\left(\int_0^\infty dx\, e^{-x^2}\right)^2 = \frac{1}{4}\left(\int_{-\infty}^\infty dx\, e^{-x^2}\right)\left(\int_{-\infty}^\infty dx\, e^{-y^2}\right) = \frac{1}{4}\iint dx\,dy\, e^{-y^2-x^2}$$

$$= \frac{1}{4}\int_0^{2\pi} d\phi \int_0^\infty dr\, r\, e^{-r^2} = \frac{\pi}{4}\int_0^\infty du\, e^{-u} = \frac{\pi}{4}.$$

In the first line we used the fact that the integrand is even, so that the integral is just one-half of that over the entire real axis. In the second line we identified an integral over the entire *x*-*y* plane. In the third line we changed to polar coordinates in the *x*-*y* plane, and changed variables again from r to $u=r^2$. The remaining integral was just an exponential integral. We can also dress this integral up a bit with a change of

variables,

$$\int_{-\infty}^{\infty} dx\, e^{-\mu x^2+2\nu x} = \left(\frac{\pi}{\mu}\right)^{1/2} \exp\left(\frac{\nu^2}{\mu}\right).$$

Next, there are a few special functions that are essential; all can be found in *Numerical Recipes*.[25] The definition of the *regular Bessel function of the first kind, of order n*, is

$$J_n(\xi) = \frac{1}{2\pi}\int_0^{2\pi} d\theta\, e^{jn\theta} e^{-j\xi\sin\theta},$$

and this may be expressed also as a Taylor series expansion,

$$J_n(\xi) = \left(\frac{\xi}{2}\right)^n \sum_{k=0}^{\infty} \frac{\left(-\frac{1}{4}\xi^2\right)^k}{k!(n+k)!}.$$

One can show that

$$\left(\xi^2\frac{d^2}{d\xi^2} + \xi\frac{d}{d\xi} + \left(\xi^2 - n^2\right)\right)J_n = 0,$$

that is to say, the Bessel function can be employed to construct solutions to the *Helmholtz equation* in problems with circular symmetry,

$$0 = e^{jm\phi}\left(\frac{1}{r}\frac{\partial}{\partial r}r\frac{\partial}{\partial r} - \frac{m^2}{r^2} + \beta_c^2\right)J_n(\beta_c r) = \left(\nabla_\perp^2 + \beta_c^2\right)\left[J_n(\beta_c r)e^{jm\phi}\right].$$

This function and a few others are plotted in Fig. A.2.

Exercise A.9 Confirm that $f = J_m(\beta_c r)e^{j(\omega t-\beta_z z)}e^{jm\phi}$ is a solution to the wave equation,

$$\left(\nabla^2 - \frac{1}{c^2}\frac{\partial^2}{\partial t^2}\right)f = 0,$$

provided $\omega^2 = c^2\left(\beta_c^2 + \beta_z^2\right)$.

A number of Bessel function integrals can be found in the references; one is particularly helpful,

$$\int_0^1 d\xi\,\xi J_n(\alpha\xi)J_n(\beta\xi) = \frac{1}{2}\delta_{\alpha,\beta}J_{n+1}^2(\alpha), \quad \text{if} \quad J_n(\alpha) = J_n(\beta) = 0.$$

In solving the wave equation in an enclosed cylindrical geometry, it is helpful to have j_{mn} the n-th zero of J_m, and j'_{mn} be the n-th zero of J'_m. A few of these are listed in Table A.2, and a more exhaustive listing may be found in

Abramowitz and Stegun.[22] It is worth remembering $j_{01} \approx 2.4$ and $j'_{11} \approx 1.8$, the others one can look up.

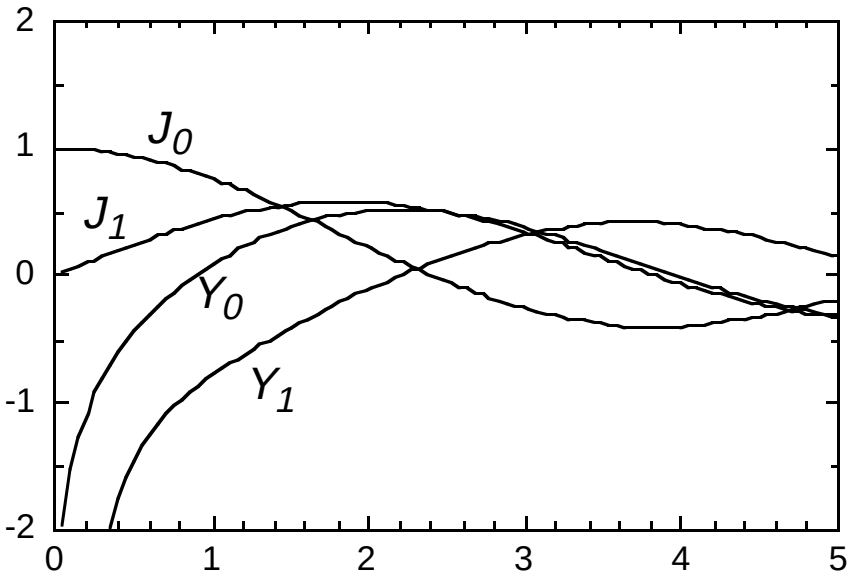

FIGURE A.2. A few Bessel Functions for illustration.

TABLE A.2. A few zeroes of Bessel functions.

j_{0n}	$J_1(j_{0n})$	j_{1n}	$J'_1(j_{1n})$	j'_{0n}	$J_0(j'_{0n})$
2.40483	0.51915	3.83171	-0.40276	3.83171	-0.40276
5.52008	-0.34026	7.01559	0.30012	7.01559	0.30012
8.65378	0.27145	j_{2n}	$J'_2(j_{2n})$	j'_{1n}	$J_1(j'_{1n})$
11.79153	-0.23246	5.13562	-0.33967	1.84118	0.58187
14.93092	+0.20655	8.41724	0.27138	5.33144	-0.34613

A.7 Delta Function

One most helpful tool in the analysis of waveforms is the *delta function*,

$$\delta(x) = \lim_{\sigma \to 0} \delta_\sigma(x),$$

where

$$\delta_\sigma(x) = \frac{1}{\sqrt{2\pi\sigma}} \exp\left(-\frac{x^2}{2\sigma^2} \right).$$

Given the integrals established in the previous section, one can see that

$$\int_{-\infty}^{+\infty} dx \delta_\sigma(x) = 1.$$

In fact, one can see that for a continuous function *f* varying slowly on the scale σ,

$$\int_{a-\varepsilon}^{a+\varepsilon} dx \delta_\sigma(x-a) f(x) \approx \int_{a-\varepsilon}^{a+\varepsilon} dx \delta_\sigma(x-a) f(a) \approx f(a),$$

provided ε is larger than a few σ. Based on these relations one can determine the rules by which δ-functions are employed,

$$\int_a^b dx \delta(x-c) f(x) = \begin{cases} 0 & c < a \\ f(c) & a < c < b \\ 0 & b < c \end{cases}.$$

A related item is the step-function,

$$H(x) = \begin{cases} 0 & x < 0 \\ \frac{1}{2} & x = 0 \\ 1 & 0 < x \end{cases}.$$

One relation is particularly handy, note that

$$\delta_\sigma(x) = \frac{1}{\sqrt{2\pi}\sigma} \exp\left(-\frac{t^2}{2\sigma^2}\right) = \frac{1}{2\pi} \int_{-\infty}^{\infty} d\omega \, \exp\left(-\tfrac{1}{2}\omega^2\sigma^2 + j\omega t\right),$$

so that in the sense of our limit,

$$\delta(t) = \frac{1}{2\pi} \int_{-\infty}^{\infty} d\omega \, e^{j\omega t}.$$

Exercise A.10 The current waveform for a single electron bunch in a linac often takes the approximate form

$$I(t) = \frac{Q}{\sqrt{2\pi}\sigma_t} \exp\left(-\frac{t^2}{2\sigma_t^2}\right),$$

for some *bunch length* $\sigma_z = c\sigma_t$. Confirm that *Q* is the charge in the bunch. Suppose that such a current were passed through a resistor, *R*. Compute the energy dissipated,

$$U = \int_{-\infty}^{+\infty} dt \, I^2 R$$

and the *loss-factor* $k = U / Q^2$.

A.8 Fourier Analysis

The Fourier transformation is the map of an integrable function $f(t)$ to its Fourier transform $\tilde{f}(\omega)$,

$$f(t) \to \tilde{f}(\omega) = \frac{1}{\sqrt{2\pi}} \int_{-\infty}^{+\infty} dt\, e^{-j\omega t} f(t) \ .$$

Since notations differ, it pays to check the normalization when checking another's results. In reading physics papers one often makes the substitution $j \to -i$. Notice that one has an *inverse Fourier transform*

$$\frac{1}{\sqrt{2\pi}} \int_{-\infty}^{+\infty} d\omega\, e^{j\omega t} \tilde{f}(\omega) = \frac{1}{\sqrt{2\pi}} \int_{-\infty}^{+\infty} d\omega\, e^{j\omega t} \frac{1}{\sqrt{2\pi}} \int_{-\infty}^{+\infty} dt'\, e^{-j\omega t'} f(t')$$

$$= \int_{-\infty}^{+\infty} dt'\, f(t') \frac{1}{2\pi} \int_{-\infty}^{+\infty} d\omega\, e^{j\omega t} e^{-j\omega t'} = \int_{-\infty}^{+\infty} dt'\, f(t') \delta(t - t') = f(t)$$

provided the order of integrations may be interchanged, which is to say, if f is sufficiently well-behaved.

Exercise A.11 Show that the Fourier transform of the current waveform for the Gaussian bunch of Exercise A.10 is

$$\tilde{I}(\omega) = \frac{Q}{\sqrt{2\pi}} \exp\left(-\tfrac{1}{2}\omega^2 \sigma_t^2\right).$$

Confirm that the energy loss in Exercise A.10 may be expressed as

$$U = \int_{-\infty}^{+\infty} d\omega \left|\tilde{I}\right|^2 R.$$

Exercise A.12 (Convolution Theorem) Show that if $\tilde{f}(\omega) = \tilde{g}(\omega)\tilde{h}(\omega)$, then

$$f(t) = \int_{-\infty}^{+\infty} dt'\, g(t') h(t - t').$$

For a well-behaved function defined on a finite interval, it is often convenient to use a *Fourier series*. The Fourier series for $F(\phi)$ on the interval $(0,2\pi)$ takes the form

$$F(\phi) = \sum_{n=-\infty}^{+\infty} e^{jn\phi} F_n ,$$

where the coefficients are obtained according to

$$\frac{1}{2\pi}\int_0^{2\pi} d\phi\, e^{-jn\phi} F(\phi) = \frac{1}{2\pi}\int_0^{2\pi} d\phi\, e^{-jn\phi} \sum_{m=-\infty}^{+\infty} e^{jm\phi} F_m$$

$$= \frac{1}{2\pi}\sum_{m=-\infty}^{+\infty} F_m \int_0^{2\pi} d\phi\, e^{-jn\phi} e^{jm\phi} = \frac{1}{2\pi}\sum_{m=-\infty}^{+\infty} F_m 2\pi\delta_{m,n} = F_n.$$

Exercise A.13 Consider the Laplace equation in two dimensions,

$$\nabla_\perp^2 f = \frac{1}{r}\frac{\partial}{\partial r} r \frac{\partial f}{\partial r} + \frac{1}{r^2}\frac{\partial^2 f}{\partial \phi^2} = 0.$$

Argue that at any fixed radial coordinate *r, f(r,ϕ)* should be a periodic function of ϕ. Go on to decompose *f* according to

$$f(r,\phi) = \sum_{n=-\infty}^{+\infty} e^{jn\phi} f_n(r).$$

Determine the equation satisfied by each f_n, and in this way show that the solution given in Exercise A.8 is the most general solution of the problem.

A.9 Numerical Integration

When confronted with a system of ordinary differential equations, it is often easiest to solve the problem numerically. For example, in the simplest case, one might wish to solve

$$\frac{d^2 X}{dt^2} = F(X).$$

We reduce the problem to a first-order system

$$\frac{dX}{dt} = V, \frac{dV}{dt} = F(X),$$

and we employ *time-centering* to insure a stable numerical integration,

$$\frac{X_{n+1} - X_n}{\Delta t} = V_{n+1/2}, \frac{V_{n+1/2} - V_{n-1/2}}{\Delta t} = F(X_n).$$

This method can be applied to more complicated-looking systems, for example, a travelling-wave accelerator, consisting of a chain of coupled oscillators.

Exercise A.14 Consider the leap-frog algorithm applied to the simple-harmonic oscillator problem, $F(X) = -\Omega^2 X$. Show that the angular frequency of oscillation of the numerical system, Ω_n, may be expressed in terms of the time-step Δt as

$$\frac{\Omega_n}{\Omega} = \frac{\sin^{-1}\left(\frac{1}{2}\Omega\Delta t\right)}{\left(\frac{1}{2}\Omega\Delta t\right)},$$

and confirm that for 60 steps per period the frequency is correct to within 0.5 parts per thousand.[34]

A.10 Kinematics

Some features of particle kinematics are assumed in the text, and in any case are helpful in appreciating the demands on accelerators for high-energy physics. We review them here. The *Lorentz factor* for a particle with velocity $\vec{V}$ is

$$\gamma = \left(1 - \frac{\vec{V}^2}{c^2}\right)^{-1/2},$$

and if the particle's mass is m, then its momentum is $\vec{p} = m\gamma\vec{V}$, and its total energy is $\varepsilon = mc^2\gamma = \left(\vec{p}^2c^2 + m^2c^4\right)^{1/2}$. This is different from its kinetic energy which is $mc^2(\gamma - 1)$.

There is one particular kinematic event that has a distinguished place in accelerator physics work, and that is the collision of two-bodies. The algebra behind the great machines of our time, and their gradual evolution over the decades, is the kinematics of the two-body collision. The problem consists of two particles flying together and other particles flying out. Without knowing the details of the interaction, one can make strong statements about the kinematic features of such an event, using simply energy and momentum conservation. To simplify this problem, let us perform a change of reference frame, moving into the "center of momentum frame."

We consider two particles, indexed by i=1,2, of mass m_i, momentum $\vec{p}_i$ and energy ε_i, so that

$$\varepsilon_1 = \sqrt{m_1^2c^4 + \vec{p}_1^2c^2}, \quad \varepsilon_2 = \sqrt{m_2^2c^4 + \vec{p}_2^2c^2}.$$

The total energy in the lab frame is $\varepsilon_{tot} = \varepsilon_1 + \varepsilon_2$, and the total momentum in the lab frame is $\vec{p}_{tot} = \vec{p}_1 + \vec{p}_2$, and if this is non-zero we boost to the center of momentum frame, moving at velocity $\vec{V} = \vec{p}_{tot}\,c^2/\varepsilon_{tot}$. Calling this direction z, the Lorentz-transformed momenta take the form

$$p'_{1z} = \gamma\left(p_{1z} - \frac{V}{c^2}\varepsilon_1\right), \quad p'_{2z} = \gamma\left(p_{2z} - \frac{V}{c^2}\varepsilon_2\right),$$

with transverse momenta unchanged. The Lorentz factor is

$$\gamma = \frac{1}{\sqrt{1 - \vec{V}^2/c^2}} = \frac{\varepsilon_{tot}}{\sqrt{\varepsilon_{tot}^2 - c^2\vec{p}_{tot}^2}}.$$

It is straightforward to check that the sum of the two momenta is zero in this boosted frame. The particle energies in this frame are

$$\varepsilon_1' = \gamma\left(\varepsilon_1 - Vp_{1z}\right), \qquad \varepsilon_2' = \gamma\left(\varepsilon_2 - Vp_{2z}\right),$$

and the total energy in this frame is

$$\varepsilon_{com} = \varepsilon_1' + \varepsilon_2' = \gamma\left(\varepsilon_{tot} - Vp_{tot-z}\right) = \sqrt{\varepsilon_{tot}^2 - c^2 p_{tot-z}^2}$$
$$= \sqrt{m_1^2c^4 + m_2^2c^4 + 2\left(\varepsilon_1\varepsilon_2 - c^2\left|\vec{p}_1\right|\left|\vec{p}_2\right|\cos\theta\right)} \ .$$

with θ the angle between the particle momenta in the lab frame, $\cos\theta = \vec{p}_1 \bullet \vec{p}_2 / \left|\vec{p}_1\right|\left|\vec{p}_2\right|$.

The two common situations where these scalings are employed are the collider and the fixed-target experiment. In a collider, the lab frame and the center-of-momentum frame are roughly the same, and the center-of-momentum frame energy is twice the energy of one beam particle,

$$\varepsilon_{com} = 2\varepsilon_1 . \qquad \text{(collider)}$$

Thus if one wishes to produce a 91.2-GeV particle, one needs two 45.6-GeV particles. At the other extreme, in a fixed-target experiment, one of the participants in the collision is initially at rest. Suppose this is particle #2, then

$$\varepsilon_{com} \approx \sqrt{m_1^2c^4 + m_2^2c^4 + 2\varepsilon_1 m_2 c^2} \ .$$

If $\varepsilon_1 >> m_i c^2$, we have

$$\varepsilon_{com} \approx \sqrt{2\varepsilon_1 m_2 c^2} , \qquad \text{(fixed target)}$$

and the energy in the center of mass frame is scaling as the *square root* of the incident particle energy.

The questions one might ask at this point include: (1) What particles can be produced and collided? (2) What center of momentum energy can be reached? (3) What interaction rate can be achieved? Each of these is a question posed to accelerator physicists. So for example one could ask: what beam energy is required to make $e^-e^- \to \mu^-\mu^-$ energetically possible? This reaction would be new and therefore interesting. Evidently we would need $\varepsilon_{com} \geq 2m_\mu c^2 = 2 \times 106 \ \text{MeV}$. This implies an incident beam energy of

$$\varepsilon_1 = \frac{\varepsilon_{com}^2}{2m_e c^2} = \frac{\left(2 \times 106 \ \text{MeV}\right)^2}{2 \times 0.511 \ \text{MeV}} = 44 \ \text{GeV} .$$

This might be interesting insofar as this energy is achievable with the SLAC beam.

Inspired, or at least not disappointed, by this brush with muons, one may wish to inspect the many other particles available. One can get a glimpse of these from the Review of Particle Physics, published each year in Physical Review D[35]. I list a few in Table A.3 that you will certainly encounter, and a few in Table A.4 that one may hear of in connection with high-energy experiments.

The Higgs (H) has not yet been discovered---the Superconducting Supercollider (SSC) was intended to be the instrument for that. For the future,

folks look toward the Large Hadron Collider (LHC) or the Next Linear Collider (NLC) to be the instrument for discovering the Higgs. The *Z* was discovered at CERN about 15 years ago, together with the *W*. The *Z* is the focus of the SLD studies at the SLC, and determines the energy requirement for the linac. Note that two-body kinematics for $e^+e^- \rightarrow Z \rightarrow$ stuff require the energy of one beam particle to satisfy $\varepsilon > m_Z/2 = 45.6\ \mathrm{GeV}$. SLAC's two-mile accelerator can reach this energy thanks to SLED pulse compression and the 5045 klystron.

Table A.3 Particles with personality.

Name	Mass (MeV)	Type	Lifetime	Decay Mode
γ	0	gauge	∞	
$e^{\pm}$	0.511	lepton	∞	
$\mu^{\pm}$	106	lepton	2.2 μs	$\mu^- \rightarrow e^-\overline{\nu}_e\nu_\mu$
π^0	135	meson	0.1 fs	$\pi^0 \rightarrow \gamma\gamma$
$\pi^{\pm}$	140	meson	26 ns	$\pi^- \rightarrow \mu^-\overline{\nu}_\mu$
p	938	baryon	∞ ?	
n	940	baryon	887 s	$n \rightarrow pe^-\overline{\nu}_e$

Table A.4 A selection of interesting, but shy particles. *l* denotes a lepton (*i.e.* an *e* or a μ or a τ).

Name	Mass (MeV)	Type	Lifetime	Decay Mode
$K^{\pm}$	494	meson	12 ns	$K^+ \rightarrow \mu^+\nu_\mu$
K_S^0	498	meson	89 ps	$K_S^0 \rightarrow \pi^+\pi^-$
K_L^0	498	meson	52 ns	$K_L^0 \rightarrow \pi^+e^-\overline{\nu}_e$
$\tau^{\pm}$	1.78 x 10^3	lepton	0.3 ps	$\tau^- \rightarrow l^-\overline{\nu}_l\nu_\tau$
D^0	1.87 x 10^3	meson	0.4 ps	(mesons etc.)
B^0	5.28 x 10^3	meson	1.6 ps	$B^0 \rightarrow l^-\overline{\nu}_l\, etc$
$W^{\pm}$	80.3 x 10^3	gauge	FW 2.1 GeV	(hadrons)
Z^0	91.2 x 10^3	gauge	FW 2.5 GeV	(hadrons)
H^0	?...			

Appendix B: Low-Frequency Electronics

A number of excellent texts on electronics can be found in the bookstores. At the most elementary level, the short guide by Warring is quite readable.[36] The text by Schwarz and Oldham[37] provides an excellent introduction to electrical engineering, with numerous solved problems. The text by Horowitz and Hill[38] is widely acclaimed. An excellent general reference on construction of apparatus is the text by Moore, Davis and Coplan,[39] and the text by Leo is well worth reading.[40] In the meantime, however, it is good to have a concise review of "ordinary electronics" before ploughing into "microwave electronics."

B.1 Basic Electronics

The basic circuit elements are illustrated in Fig. B.1. An *ideal voltage generator* maintains its voltage at spec (*V* in the figure) regardless of the load. The current through the voltage source is determined by the external circuit to which it is attached. An *ideal current generator* maintains its current at spec (*I* in the figure) regardless of the external circuit. The voltage drop across the the current source is determined by the external circuit.

A *capacitor* is a circuit element which may accumulate charge *Q*, in which case the voltage drop across the capacitor is *Q/C*, where *C* is the capacitance, measured in units of farads. Energy is stored in the electric fields within the volume of the capacitor in the course of charging it up. An *inductor* is an element which develops a voltage drop across its terminals when a current *I*, varying with time *t*, passes through it. The voltage drop is *LdI/dt*, with *L* the inductance, measured in henrys. Energy is stored in the magnetic field within the volume of the inductor, in the course of establishing the current flow through it. A *resistor* is an element that develops a voltage drop across its terminals when current flows through it. The voltage drop is *IR*, with *R* the resistance measured in ohms. A resistor does not store energy; it is, as we see in Chapter 1, simply a collection of collisional conduction band electrons waiting to be pushed around, so they can go and beat up on the ions. A *switch* is an externally controllable element with two states. When the switch is closed, current may flow, when it is open, current may not. The voltage drop is zero across a closed switch, *i.e.*, it is a *short circuit*.

Kirchoff's laws can be employed to figure out how circuits composed of the elements above work; they are (1) the sum of all currents entering a node is zero, and (2) the sum of all voltage drops around a close circuit is zero. The current law derives from the definition of current as time rate of change of charge, together with conservation of charge. Implicit in the voltage law is an assumption about frequency and the elements employed. In this case, as far as terminal voltages are concerned, we are dealing with an electrostatics problem, and voltage may be identified uniquely as work per unit charge. In this case, the voltage law corresponds to conservation of energy.

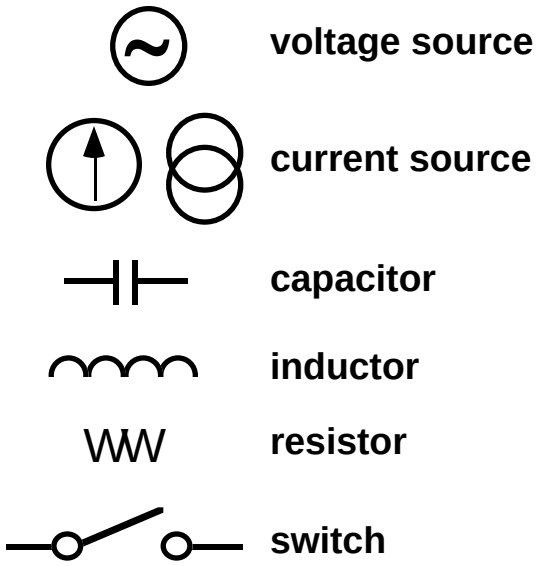

FIGURE B.1. Basic electronic circuit elements include a perfectly regulated voltage generator with no internal *impedance*, a perfectly regulated ideal current source with no internal *admittance*, a capacitor (with no inductance or resistance), an inductor (with no capacitance or resistance), a resistor (with no capacitance or inductance) and a switch.

Very often circuit analysis is aided by the notion of *equivalent circuit*, replacing a complex looking circuit component with a simpler element of the same impedance, as illustrated in Fig B.2. The wavy line inside the symbol for the voltage generator simply indicates that we will be considering an alternating current (AC) signal. That is to say we will consider a voltage varying in

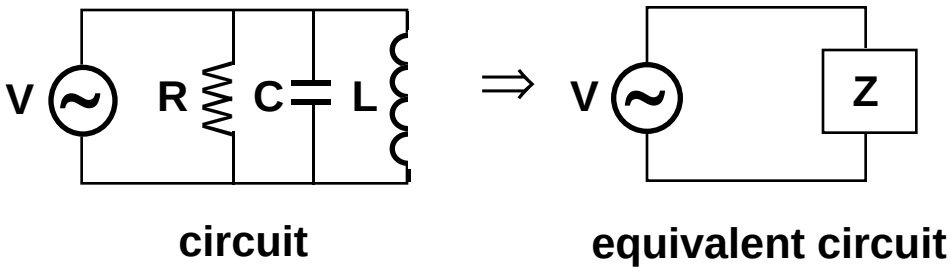

FIGURE B.2. Circuit analysis is aided by the notion of equivalent circuit.

time according to a sinusoidal pattern,

$$V(t) = \Re\left(\tilde{V}e^{j\omega t}\right) = \frac{1}{2}\left(\tilde{V}e^{j\omega t} + \tilde{V}^{*}e^{-j\omega t}\right) = \left|\tilde{V}\right|\cos\left(\omega t + \phi\right),$$

where $\Re$ denotes the real part, and $\tilde{V}$ is the voltage phasor, a complex quantity,

$$\tilde{V} = \left|\tilde{V}\right|e^{j\phi} = \left|\tilde{V}\right|\left(\cos\phi + j\sin\phi\right).$$

Notice that we are always free, in a circuit such as in Fig. B.2, to add a crow's foot to it, to indicate a choice of "ground." This does not mean in reality that this point of the circuit will be at the same potential as the water pipes. Merely that for purposes of circuit analysis, we have chosen a reference point in the circuit, and chosen to analyze voltages with respect to it. For power circuits, and for analysis of pulsed noise ("pick-up" or "ground-loop"), one might be more circumspect about the concept of "ground."

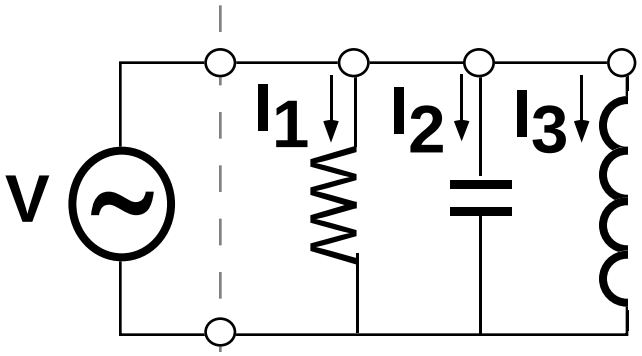

FIGURE B.3. Notation for analysis of the RLC circuit.

B.2 Circuit Analysis

Let us analyze the circuit of Fig. B.2 as it will appear rather frequently, oftentimes disguised under a mass of symbols, that would otherwise mask its simplicity. From Kirchoff's voltage law, the voltage drop across each element is the same, thus, with notation illustrated in Fig B.3,

$$V = L\frac{dI_3}{dt} = \frac{Q_2}{C} = RI_1.$$

The total current drawn through the generator is, by Kirchoff's current law, just the sum of the currents drawn through each element,

$$\tilde{I} = \tilde{I}_1 + \tilde{I}_2 + \tilde{I}_3 = \frac{\tilde{V}}{R} + j\omega C\tilde{V} + \frac{\tilde{V}}{j\omega L},$$

and we switch to phasor notation for simplicity. With this result we may summarize our analysis of the circuit, insofar as the generator is concerned, by a single impedance, "seen" looking into the reference plane marked by the dashed line in Fig. B.3:

$$Z = \frac{\tilde{V}}{\tilde{I}},$$

where

$$\frac{1}{Z(\omega)} = \frac{1}{R} + j\left(\omega C - \frac{1}{\omega L}\right).$$

This result will often appear "dressed up" in the form,

$$Z(\omega) = \frac{R}{1 + jQ\left(\omega/\omega_0 - \omega_0/\omega\right)},$$

where we have made the abbreviations, $\omega_0 = 1/\sqrt{LC}$, $Q = R\sqrt{C/L}$.

In general we may characterize any two-terminal passive circuit by its impedance. That's not to say that impedance determines everything about the circuit element, merely how it behaves in public. (For example, it doesn't convey the peak electric field within the element). We may wish also to distinguish between the real part of the impedance, $\Re Z$, the *resistance*, and the imaginary part, $\Im Z$, the *reactance*. These distinctions become important when we consider energy flow. From the definition of voltage and current we can see that the rate at which the voltage generator is doing work is

$$P(t) = V(t)I(t),$$

or, more explicitly,

$$\begin{aligned} P(t) &= \frac{1}{2}\left(\tilde{V}e^{j\omega t} + \tilde{V}^* e^{-j\omega t}\right)\frac{1}{2}\left(\tilde{I}e^{j\omega t} + \tilde{I}^* e^{-j\omega t}\right) \\ &= \frac{1}{4}\left(\tilde{V}\tilde{I}e^{2j\omega t} + \tilde{V}^*\tilde{I}^* e^{-2j\omega t} + \tilde{V}^*\tilde{I} + \tilde{V}\tilde{I}^*\right) \\ &= \frac{1}{2}\Re\left(\tilde{V}\tilde{I}e^{2j\omega t} + \tilde{V}\tilde{I}^*\right). \end{aligned}$$

Averaging over one cycle we find that average rate of work done by the generator is zero --- unless the load (*Z*) has a resistive component,

$$\overline{P} = \frac{1}{2}\Re\left(\tilde{V}\tilde{I}^*\right) = \frac{1}{2}\Re(Z)\left|\tilde{I}\right|^2 = \frac{1}{2}\Re(Y)\left|\tilde{V}\right|^2.$$

In the last line we introduced the *admittance*,

$$Y = \frac{1}{Z},$$

and we will refer to $\Re Y$ as the *conductance*, and $\Im Y$ as the *susceptance*.

B.3 Simple Filters

With just these basic elements quite a variety of items can be built. Let us consider the three in Fig B.4, for an appreciation of them will come in quite handy. These examples of filters are easily understood qualitatively by noting that (1) a capacitor at low frequency is an open circuit (no current flows) and at high

frequency is a short circuit (no voltage drop), (2) an inductor at low frequency is a short circuit, and at high frequency is an open circuit. In fact these considerations make for simple rules one can use to judge the behavior of circuits. To see the high-frequency behavior, short the capacitors, and erase the inductors.

Exercise B.1 Referring to Fig. B.4, compute the transfer function for each filter, *i.e.*, compute the voltage on the right terminal, assuming that terminal is an open circuit, and assuming the voltage on the left terminal is specified,

Exercise B.2 Solve also for the response of the circuits in the *time-domain*, by considering the response to a delta-function applied voltage. Why is the low-pass circuit also called an *integrator*, and under what conditions is the output voltage faithful to the integral of the input voltage? Under what conditions on the input voltage is the high-pass filter a *differentiator*?

Exercise B.3 In steady-state, driven at angular frequency ω, what is the energy stored in the *LC*-circuit of the bandpass filter?

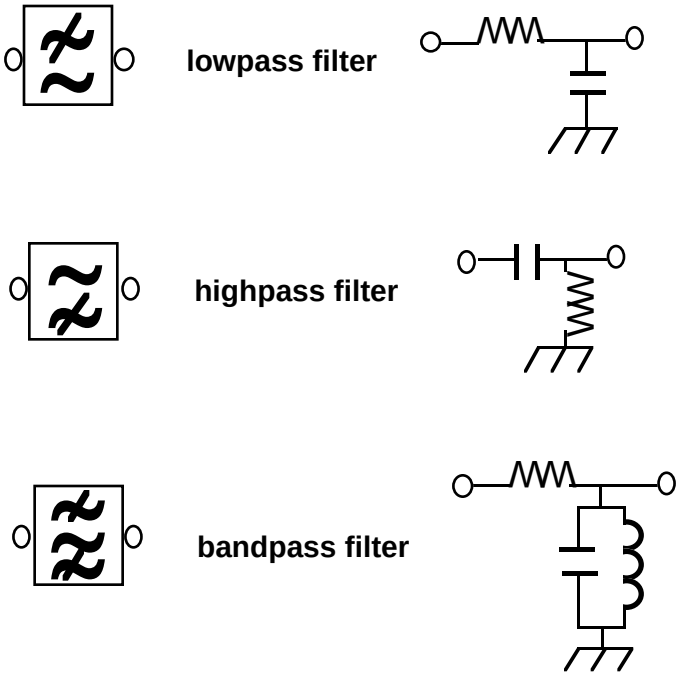

FIGURE B.4. Examples of handy items one can construct from the basic passive circuit elements.

Exercise B.4 For each of these filters, derive an exact integral expression for the voltage output. Breaking the time-axis into discrete points, and approximating the integral between points using the trapezoidal rule, devise a simple numerical (digital) algorithm for applying each filter to an input voltage specified at discrete time steps. In your algorithm, do not assume the time-step is small compared to characteristic circuit time-scales. Implement these filters as numerical subroutines in the language or with the software of your choice, and test each against an exact solution.

Exercise B.5 Making use of a standard fast-Fourier-transform package, devise an algorithm for numerical implementation of these filters, assuming an input voltage specified at discrete time-steps numbering 2^N.

Two additional circuit elements will come in handy, and they are illustrated in Fig. B.5. One encounters the diode in modulator circuits, and in a special variety of diode for microwave detection, the *crystal detector*.[41] Transformers one finds in the modulator circuit, and more importantly, we will find ourselves calling on the notion of transformer when we adopt a circuit analogy for certain microwave problems.

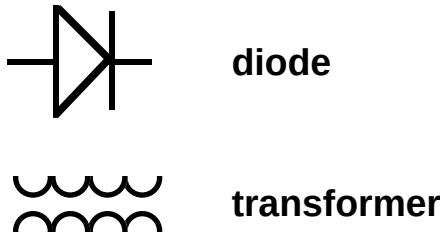

FIGURE B.5. Two very common, but not-so-elementary circuit elements.

B.4 Diodes

A diode consists of *p* and *n* type semiconductors sandwiched together as one crystal, on a mount. A *p*-type semi-conductor has positively charged holes as the majority carriers; *n*-type has negatively charged electrons as the majority carriers of current. When a positive voltage is applied to the *p*-side of the junction (forward bias), both *p* and *n* carriers flow through the junction in opposite directions. For the opposite, reverse bias, little current flows. The *I*-*V* characteristic for a diode takes the form, $I = I_s\left(e^{eV/k_BT} - 1\right)$, and the sign convention for the diode symbol is given in Fig. B.6. The saturation current $I_s \approx 10^{-8}$-10^{-14} A is a property of the junction and T is the temperature, with k_B, Boltzmann's constant. To gauge the behavior of circuits, it is often adequate to replace diodes with ideal rectifiers, for which $I>0 \rightarrow V=0$, and $V<0 \rightarrow I=0$. More precisely, $>0 \rightarrow V \approx 0.7$, $V<0.7 \rightarrow I \approx 0$ for silicon.

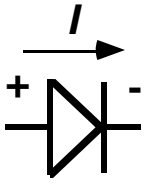

FIGURE B.6. Sign convention for a diode.

B.5 Transformers

An ideal transformer, as depicted in Fig. B.7, is characterized by the turns ratio N_1/N_2. The ratio of voltages is just

$$\frac{V_2}{V_1} = \frac{N_2}{N_1},$$

and the ratio of currents is just

$$\frac{I_2}{I_1} = -\frac{N_1}{N_2}.$$

If the voltage on the load-side (the voltage on the secondary winding) is high, this is a *step-up* transformer. Otherwise it is a *step-down* transformer.

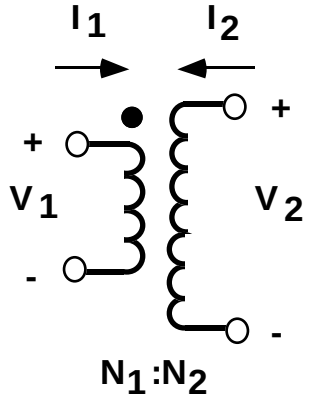

FIGURE B.7. An ideal transformer. The solid dot marks the positive terminal side. The winding on the side of the power supply is the "primary," and the winding on the load-side is the "secondary." In this drawing there is no indication of which side is the primary or the secondary.

Figure B.8 provides a glimmer of how a transformer can be devised. The application of voltage across the wire causes currents to flow and sets up a magnetic field within the magnet. The field is concentrated in the magnet due to the high μ. Thus one can control the magnetic field with the external circuit. However, this does not imply that one has direct control over the magnetic induction, for the magnet consists of many domains of magnetic dipoles, and these two respond to the applied magnetic field. The actual local magnetic induction is then the outcome of a statistical process by which atomic dipoles align themselves. By Faraday's law, the voltage drop across terminal No. 1 must be proportional to the time rate of change of magnetic flux enclosed by the circuit, and similarly for terminal No. 2,

$$V_1 = N_1 \frac{d\Phi}{dt}, \quad V_2 = N_2 \frac{d\Phi}{dt}.$$

Evidently then the voltages are transformed according to the turns ratio. As to the current transformation, the magnitude can be understood from energy conservation (neglecting losses in the magent), and the sign from Lenz's law. In connection with transformer circuits there is a notion of transferring a load to the primary circuit. The principle is illustrated in Fig. B.9. The impedance "seen" by the generator is

$$Z' = \left(\frac{N_1}{N_2} \right)^2 Z .$$

Thus a step-up transformer, lowers the impedance referred to the primary circuit.

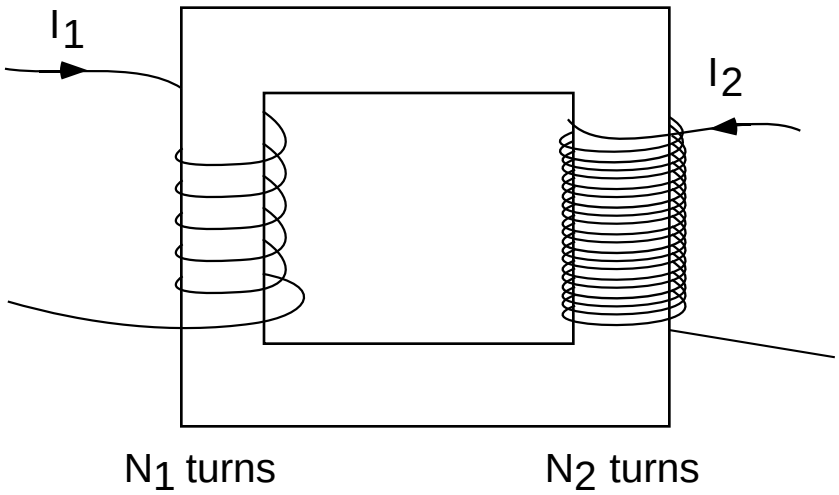

FIGURE B.8. A transformer might consist of two coils of wire, magnetically coupled through a high permeability material, such as iron.

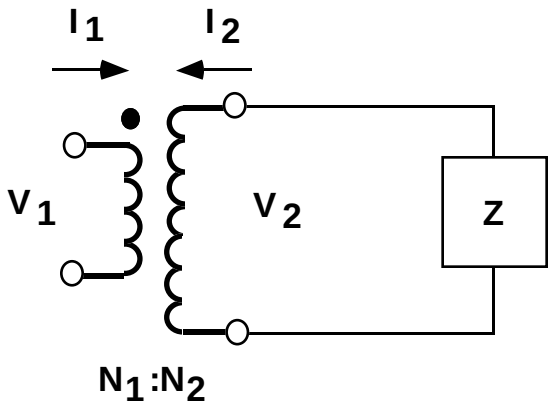

FIGURE B.9. To illustrate transformation of load impedance, when referred to the primary circuit.

Appendix C: Cavity Modes and Perturbations

The development of the theory of the accelerator cavity in Sec. 3 proceeded from an isolated resonance of a closed, lossless cavity, and considered perturbations: a beam, Eq. (3.5), wall losses, Eq. (3.6), a waveguide, Eq. (3.12), and iris-coupling to another cavity, Eq. (3.26). Since these results are central to the development of linac theory it is useful to set down a more formal treatment of these perturbations.

We consider fields and sources of the form

$$\vec{E}(\vec{r},t) = \Re\left(\tilde{E}(\vec{r},\omega)e^{j\omega t}\right),\ \ \vec{H}(\vec{r},t) = \Re\left(\tilde{H}(\vec{r},\omega)e^{j\omega t}\right),$$

$$\vec{J}(\vec{r},t) = \Re\left(\tilde{J}(\vec{r},\omega)e^{j\omega t}\right),\ \ \rho(\vec{r},t) = \Re\left(\tilde{\rho}(\vec{r},\omega)e^{j\omega t}\right),$$

and the charge density is subject to continuity,

$$\tilde{\rho}(\vec{r},\omega) = -\frac{1}{j\omega}\vec{\nabla}\bullet\tilde{J}(\vec{r},\omega).$$

Maxwell's equations reduce to the form

$$\vec{\nabla}\times\tilde{E} = -j\omega\mu\tilde{H}, \qquad \vec{\nabla}\times\tilde{H} = j\omega\varepsilon\tilde{E} + \tilde{J}.$$

Gauss's law is satisfied identically, as one can check by taking the divergence. We consider a closed cavity with perfectly conducting walls in the absence of source terms. Boundary conditions are $\hat{n}\times\tilde{E} = 0$, $\hat{n}\bullet\tilde{H} = 0$, and the fields each separately satisfy the Helmholtz equation,

$$\left(\nabla^2 + k^2\right)\tilde{E} = 0,\ \left(\nabla^2 + k^2\right)\tilde{H} = 0,$$

where $k^2 = \omega^2\mu\varepsilon$. These amount to eigenvalue equations for the mode frequencies. Let us enumerate the modes and label them with index λ. The eigenvalues we denote k_λ, and the mode frequencies, ω_λ. We select basis functions $\tilde{E}_\lambda$ to be real, and adopt the normalization

$$\int d^3\vec{r}\,\tilde{E}_\lambda\bullet\tilde{E}_{\lambda'} = \delta_{\lambda,\lambda'}.$$

To demonstrate this for $\lambda\neq\lambda'$, one employs, in the case of non-degenerate modes, the Helmholtz equation, and conducting boundary conditions:

$$\begin{aligned}\left(k_\lambda^2 - k_{\lambda'}^2\right)\int d^3\vec{r}\,\tilde{E}_\lambda\bullet\tilde{E}_{\lambda'} &= \int d^3\vec{r}\left(\tilde{E}_\lambda\nabla^2\tilde{E}_{\lambda'} - \tilde{E}_{\lambda'}\nabla^2\tilde{E}_\lambda\right)\\ &= \int d^3\vec{r}\,\vec{\nabla}\bullet\left\{\tilde{E}_\lambda\times\left(\vec{\nabla}\times\tilde{E}_{\lambda'}\right) - \tilde{E}_{\lambda'}\times\left(\vec{\nabla}\times\tilde{E}_\lambda\right)\right\}\\ &= \int d\vec{S}\bullet\left\{\tilde{E}_\lambda\times\left(\vec{\nabla}\times\tilde{E}_{\lambda'}\right) - \tilde{E}_{\lambda'}\times\left(\vec{\nabla}\times\tilde{E}_\lambda\right)\right\}\\ &= 0.\end{aligned}$$

In the case of degenerate modes, we assume Gram-Schmidt orthogonalization has been employed. We define the basis functions for the magnetic field according to

$$\vec{\nabla}\times\tilde{H}_\lambda = k_\lambda \tilde{E}_\lambda, \qquad \vec{\nabla}\times\tilde{E}_\lambda = k_\lambda \tilde{H}_\lambda,$$

and one can show that these too satisfy orthonormality. For this idealized system, a general *vacuum* oscillation may be expressed as

$$\vec{E}(\vec{r},t) = \sum_\lambda \tilde{E}_\lambda(\vec{r})\tilde{e}_\lambda(t), \qquad \vec{H}(\vec{r},t) = \sum_\lambda \tilde{H}_\lambda(\vec{r})\tilde{h}_\lambda(t),$$

where the time evolution is given by Faraday's law in the time-domain,

$$Z_0 \frac{\partial h_\lambda}{\partial t} = -\omega_\lambda e_\lambda,$$

and Ampere's law,

$$\frac{\partial e_\lambda}{\partial t} = \omega_\lambda Z_0 h_\lambda,$$

corresponding to an undamped simple harmonic oscillation in each mode,

$$\left(\frac{\partial^2}{\partial t^2} + \omega_\lambda^2\right) e_\lambda = 0.$$

On average, equal amounts of energy are stored in the electric and magnetic fields.

Next let us consider a weakly perturbed cavity, one for which the original basis functions are no longer exact solutions. Let the fields in steady-state at angular frequency ω take the form $\tilde{E}(\vec{r},\omega), \tilde{H}(\vec{r},\omega)$. We define mode amplitudes for the perturbed problem according to

$$\tilde{e}_\lambda(\omega) = \int d^3\vec{r}\, \tilde{E}(\vec{r},\omega)\bullet\tilde{E}_\lambda(\vec{r}), \qquad \tilde{h}_\lambda(\omega) = \int d^3\vec{r}\, \tilde{H}(\vec{r},\omega)\bullet\tilde{H}_\lambda(\vec{r}),$$

with integrals over the unperturbed cavity volume. To obtain equations for these mode amplitudes, we take the dot product of Faraday's law with $\tilde{H}_\lambda$, and we take the dot product of Ampere's law with $\tilde{E}_\lambda$, and we integrate each over the volume. Faraday's law takes the form

$$\begin{aligned} -j\mu\omega\tilde{h}_\lambda &= \int d^3\vec{r}\left(\vec{\nabla}\times\tilde{E}\right)\bullet\tilde{H}_\lambda = \int d^3\vec{r}\left\{\vec{\nabla}\bullet\left(\tilde{E}\times\tilde{H}_\lambda\right) + \tilde{E}\bullet\vec{\nabla}\times\tilde{H}_\lambda\right\} \\ &= \int d\vec{S}\bullet\tilde{E}\times\tilde{H}_\lambda + \int d^3\vec{r}\,\tilde{E}\bullet\left(k_\lambda\tilde{E}_\lambda\right) = k_\lambda\tilde{e}_\lambda + \int d\vec{S}\bullet\vec{E}\times\tilde{H}_\lambda. \end{aligned}$$

and Ampere's law takes the form

$$\begin{aligned} j\omega\varepsilon\tilde{e}_\lambda &= \int d^3\vec{r}\left(\vec{\nabla}\times\tilde{H}\right)\bullet\tilde{E}_\lambda - \int d^3\vec{r}\,\tilde{J}\bullet\tilde{E}_\lambda \\ &= \int d^3\vec{r}\left\{\tilde{H}\bullet\left(\vec{\nabla}\times\tilde{E}_\lambda\right) - \vec{\nabla}\bullet\left(\tilde{H}\times\tilde{E}_\lambda\right)\right\} - \int d^3\vec{r}\,\tilde{J}\bullet\tilde{E}_\lambda \\ &= k_\lambda\tilde{h}_\lambda + \int d\vec{S}\bullet\left(\tilde{E}_\lambda\times\vec{H}\right) - \int d^3\vec{r}\,\vec{J}\bullet\tilde{E}_\lambda. \end{aligned}$$

Abbreviating,

$$\tilde{J}_\lambda = \int d^3\vec{r}\; \tilde{J} \bullet \tilde{E}_\lambda ,$$

these are just

$$-j\mu\omega\tilde{h}_\lambda = k_\lambda \tilde{e}_\lambda + \int d\vec{S} \bullet \tilde{E} \times \tilde{H}_\lambda , \tag{C.1}$$

$$j\varepsilon\omega\tilde{e}_\lambda = k_\lambda \tilde{h}_\lambda + \int d\vec{S} \bullet \tilde{E}_\lambda \times \tilde{H} - \tilde{J}_\lambda . \tag{C.2}$$

The integrals are over the unperturbed cavity boundary. We consider next different kinds of perturbations.

C.1 Perturbation Due to Lossy Walls

With the addition of finite conductivity to the cavity surface, the boundary conditions on the physical fields (as opposed to our modes λ that were derived for different boundary conditions) are amended to read $\tilde{E} = -Z_s \hat{n} \times \tilde{H}$, where recall that $Z_s = R_s(1 + j\,\mathrm{sgn}\,\omega)$, with R_s the surface resistance. This permits us to compute the surface integrals. We have

$$\int_{S_w} d\vec{S} \bullet \tilde{E} \times \tilde{H}_\lambda = \int_{S_w} dS\, \hat{n} \bullet \left(-Z_s \hat{n} \times \tilde{H}\right) \times \tilde{H}_\lambda = \int_{S_w} dS\, Z_s \hat{n} \bullet \left\{ \left(\tilde{H} \bullet \tilde{H}_\lambda\right)\hat{n} - \left(\hat{n} \bullet \tilde{H}_\lambda\right)\tilde{H} \right\}$$

$$= Z_s \int_{S_w} dS\, \tilde{H} \bullet \tilde{H}_\lambda ,$$

where use is made of conducting boundary conditions on the unperturbed modal pattern, $\hat{n} \bullet \tilde{H}_\lambda = 0$; likewise, $\hat{n} \times \tilde{E}_\lambda = 0$, so that

$$\int_{S_w} d\vec{S} \bullet \left(\tilde{E}_\lambda \times \tilde{H}\right) = \int_{S_w} dS\, \hat{n} \bullet \left(\tilde{E}_\lambda \times \tilde{H}\right) = \int_{S_w} dS\, \tilde{H} \bullet \left(\hat{n} \times \tilde{E}_\lambda\right) = 0.$$

To simplify the wall loss term, we make the approximation

$$\int_{S_w} dS\, \tilde{H} \bullet \tilde{H}_\lambda \approx h_\lambda \int_{S_w} dS\, \tilde{H}_\lambda^2 ,$$

thereby discarding any *mode coupling* through the lossy wall currents. This is appropriate, for example, for an isolated resonance, one that does not overlap another mode in the frequency domain. In terms of the *wall quality factor, $Q_{w\lambda}$,*

$$\frac{1}{Q_{w\lambda}} = \frac{\delta}{2} \int_{S_w} dS\, \tilde{H}_\lambda^2 = \frac{\delta}{2} \frac{\int_{wall} dS\, \tilde{H}_\lambda^2}{\int_{volume} dV\, \tilde{H}_\lambda^2} . \tag{C.3}$$

we may write

$$\int_{S_w} d\vec{S} \bullet \tilde{E} \times \tilde{H}_\lambda = Z_s \int_{S_w} dS\, \tilde{H} \bullet \tilde{H}_\lambda = \frac{\mu}{Q_w}(1 + j\,\mathrm{sgn}\,\omega)|\omega| h_\lambda .$$

Putting the results together, we have

$$j\varepsilon\omega\tilde{e}_\lambda = k_\lambda \tilde{h}_\lambda - \tilde{J}_\lambda , \qquad -j\mu\omega\tilde{h}_\lambda = k_\lambda \tilde{e}_\lambda + \frac{\mu}{Q_w}(1 + j\,\mathrm{sgn}\,\omega)|\omega| h_\lambda . \tag{C.4}$$

We consider a weak perturbation, Q_w>>1, neglecting terms which are second-order in perturbations. In addition, we approximate $|\omega| \approx \omega_\lambda$ in the term of order $1/Q_w$. The effect of this approximation must be slight, since Q_w>>1. Note that wall-losses have produced a shift in the real part of the cavity frequency, we subsume that into a *redefinition* of ω_λ,

$$\frac{\omega_\lambda^2}{1 + 1/Q_w} \to \omega_\lambda^2 . \tag{C.5}$$

We arrive at

$$\left\{ \omega^2 - j\frac{\omega\omega_\lambda}{Q_w} - \omega_\lambda^2 \right\} \tilde{e}_\lambda = -j\omega \frac{1}{\varepsilon} \tilde{J}_\lambda ,$$

or, in the time-domain,

$$\left(\frac{d^2}{dt^2} + \frac{\omega_\lambda}{Q_w}\frac{d}{dt} + \omega_\lambda^2 \right) e_\lambda = \frac{1}{\varepsilon}\frac{d}{dt} J_\lambda . \tag{C.6}$$

C.2 Perturbation Due to Beam

Next we evalute the perturbation due to the current source in Eq. (3.6). For a ballistic "pencil" beam, the current density is

$$\vec{J} = \hat{z}\delta^2(\vec{r}_\perp) I_b\left(t - \frac{z}{V} \right), \tag{C.7}$$

where I_b is the beam current waveform. In the frequency domain,

$$\tilde{J}(\vec{r}, \omega) = \hat{z}\delta^2(\vec{r}_\perp) \int_{-\infty}^{\infty} \frac{d\omega}{\sqrt{2\pi}} e^{-j\omega t} I_b\left(t - \frac{z}{V} \right) = \hat{z}\delta^2(\vec{r}_\perp) \tilde{I}_b(\omega) e^{-j\omega z/V} .$$

With this we may compute the source term $\tilde{J}_\lambda$,

$$\begin{aligned} \tilde{J}_\lambda &= \int d^3\vec{r}\, \tilde{J} \bullet \tilde{E}_\lambda = \int d^3\vec{r} \left(\hat{z}\delta^2(\vec{r}_\perp) \tilde{I}_b(\omega) e^{-j\omega z/V} \right) \bullet \tilde{E}_\lambda \\ &= \tilde{I}_b(\omega) \int_{cavity} dz\, E_{z\lambda}(\vec{r}_\perp = 0, z) e^{-j\omega z/V} = \tilde{I}_b(\omega) w^* , \end{aligned}$$

and we abbreviate,

$$\tilde{w} = \int_{cavity} dz\, E_{z\lambda}\left(\vec{r}_\perp = 0, z\right) e^{j\omega z/v}.$$

This coefficient we may relate to the more conventional quantity, [*R/Q*], as follows. The voltage drop (or gain) experienced by a particle travelling at speed *V* in the *z*-direction, and passing *z*=0 at time $t=t_0$ is

$$V_c(t_0) = \int_{cavity} dz\, E_z\left(\vec{r}_\perp = 0, z, t_0 + \frac{z}{V}\right). \tag{C.8}$$

We may express this in terms of the modal decomposition,

$$E_z\left(\vec{r}_\perp = 0, z, t_0 + \frac{z}{V}\right) = \sum_\lambda E_{z\lambda}\left(\vec{r}_\perp = 0, z\right) e_\lambda\left(t_0 + \frac{z}{V}\right),$$

and in the frequency domain, as

$$\begin{aligned}\tilde{V}_c(\omega) &= \int_{-\infty}^{\infty} \frac{d\omega}{\sqrt{2\pi}} e^{-j\omega t_0} \tilde{V}_c(t_0) = \int_{cavity} dz \int_{-\infty}^{\infty} \frac{d\omega}{\sqrt{2\pi}} e^{-j\omega t_0}\, e_\lambda\left(t_0 + \frac{z}{V}\right) E_{z\lambda}\left(\vec{r}_\perp = 0, z\right) \\ &= \tilde{e}_\lambda(\omega) \int_{cavity} dz\, E_{z\lambda}\left(\vec{r}_\perp = 0, z\right) e^{j\omega z/V},\end{aligned}$$

and we assume for simplicity that only a single mode, λ, is excited. Evidently then $\tilde{V}_c = \tilde{e}_\lambda \tilde{w}$, and our cavity equation, Eq. (C.5), may be re-expressed in terms of the more meaningful normalizations, $\tilde{V}_c$, $\tilde{I}_b$, according to

$$\left\{\omega^2 - j\frac{\omega\omega_\lambda}{Q_w} - \omega_\lambda^2\right\} \underbrace{\tilde{V}_c}_{w\tilde{e}_\lambda} = -\frac{j\omega}{\varepsilon} \underbrace{\tilde{I}_b |w|^2}_{w\tilde{J}_\lambda},$$

or

$$\left\{\omega^2 - j\frac{\omega\omega_\lambda}{Q_w} - \omega_\lambda^2\right\} \tilde{V}_c = -j\omega\omega_\lambda \left[\frac{r}{Q}\right] \tilde{I}_b. \tag{C.9}$$

Here we introduce

$$\left[\frac{r}{Q}\right] = \frac{|w|^2}{\varepsilon_0 \omega_\lambda}.$$

The [*r/Q*] for the coupling of the beam to this mode λ may be expressed in a normalization-independent manner as

$$\left[\frac{r}{Q}\right] = \frac{\left|\int_{cavity} dz\, E_{z\lambda}\left(\vec{r}_\perp = 0, z\right) e^{j\omega_\lambda z/V}\right|^2}{\varepsilon_0 \omega_\lambda \int_{cavity} d^3\vec{r}\, \vec{E}_\lambda \bullet \vec{E}_\lambda} = \frac{\left|\tilde{V}_c\right|^2}{2\omega_\lambda U}, \tag{C.10}$$

where U is the stored energy in the cavity corresponding to cavity voltage $\tilde{V}_c$. To summarize, in the time-domain,

$$\left(\frac{d^2}{dt^2} + \frac{\omega_\lambda}{Q_w}\frac{d}{dt} + \omega_\lambda^2\right) V_c = \omega_\lambda \left[\frac{r}{Q}\right] \frac{dI_b}{dt}. \tag{C.11}$$

Let us note explicitly the relation

$$\left[\frac{R}{Q}\right] = 2\left[\frac{r}{Q}\right],$$

between circuit and accelerator notations. In these notes we have consistently distinguished between these two using upper-case and lower-case notations. In reading the literature it pays to check the definition being employed.

C.3 Cell-to-Cell Coupling

Since we are working to first order in perturbations, there is no impediment to considering each perturbation in isolation, later to return and add them all together to describe the complete system. Accordingly, let us return to the closed lossless cavity, and consider perturbation by iris-coupling to another cavity. The evolution of the mode amplitudes is governed by Faraday's law,

$$-\mu_0 \frac{\partial h_\lambda}{\partial t} = k_\lambda e_\lambda + \int_{iris} \left(\hat{n} \times \vec{E}\right) \bullet \vec{H}_\lambda \, dA,$$

and Ampere's law,

$$\varepsilon_0 \frac{\partial e_\lambda}{\partial t} = k_\lambda h_\lambda - J_\lambda + \int_{iris} \left(\hat{n} \times \vec{E}_\lambda\right) \bullet \vec{H}\, dA = k_\lambda h_\lambda .$$

In the last line we have set the current term to zero and taken account of the conducting boundary conditions satisifed by the unperturbed mode electric field. Combining these two results we obtain a single equation for the electric field amplitude,

$$\frac{\partial^2 e_\lambda}{\partial t^2} + \omega_\lambda^2 e_\lambda = -\omega_\lambda c \int_{iris} \left(\hat{n} \times \vec{E}\right) \bullet \vec{H}_\lambda \, dA. \tag{C.12}$$

Evidently the effect of the iris is known once the variation of the tangential electric field in the vicinity of the iris is known, and the integral computed. Note that if we take the variation in electric field near the iris to be just the unperturbed variation,

then the tangential field is zero, and so is the integral. Evidently then the important feature of the iris is the redistribution of electric field lines, some passing into the next cavity, but some terminating on the iris edge.

To compute this variation we should in principle solve Maxwell's equations for the new geometry. Happily however, for a *small* iris, the Helmholtz equation for the potentials reduces simply to Laplace's equation $\left(\nabla^2 + k^2\right)\varphi = 0 \approx \nabla^2\varphi$. This approximation is adequate because, near the iris, spatial variations occur on the length-scale of the iris. The rf, meanwhile, is incapable of resolving details much smaller than a wavelength. Thus our problem is considerably simplified. One has a circular aperture in a plane, and far from the aperture one has normal fields above and below, call them E_1 and E_2. One intuits that if $E_1 \neq E_2$, some field lines will terminate on the plane, and some tangential field will result. Following Jackon's derivation,[17] we simply write down the solution for this tangential field in the iris,

$$\vec{E}_\perp(\vec{r}, z=0) = \frac{(E_1 - E_2)}{\pi}\frac{\vec{r}}{\sqrt{a^2 - r^2}},$$

where z=0 locates the plane of the iris, $\vec{r}$ is the coordinate in the plane of the iris, a is the iris radius, E_1 is the asymptotic field to the left of the iris (in cavity #1), and E_2 is the asymptote to the right of the iris (in cavity #2). The basis functions and normalization for the unperturbed TM_{010} mode are

$$\vec{E}_\lambda = J_0(\beta_c r)E_{0\lambda}\hat{z}, \qquad \vec{H}_\lambda = -J_0'(\beta_c r)E_{0\lambda}\hat{\phi}, \quad E_{0\lambda} = \left(\pi L R^2 J_1^2(j_{01})\right)^{-1/2}.$$

The asymptotic field components are then $E_1 \approx e_1 E_{0\lambda}$, $E_2 \approx e_2 E_{0\lambda}$, and we amend our notation, denoting by e_1 the excitation of the fundamental mode in cavity #1, and e_2 that for cavity #2. (There is no ambiguity here, since we are not considering other modes λ, to which previously the subscripts on the e's referred.). With this it remains only to compute the port integral appearing in Eq. (C.12),

$$\begin{aligned}\int_{port}\left(\hat{n}\times\vec{E}\right)\bullet\vec{H}_\lambda\, dA &\approx \int_0^{2\pi} d\phi \int_0^a r dr \frac{(e_1 - e_0)}{\pi}\frac{J_0'(\beta_c r)}{\sqrt{a^2 - r^2}} r E_{0\lambda}^2 \\ &\approx \frac{2}{3}(e_2 - e_1)E_{0\lambda}^2 a^3 \beta_c.\end{aligned}$$

Our equation for the excitation of cavity #1 then takes the form,

$$\frac{\partial^2 e_1}{\partial t^2} + \omega_0^2 e_1 = \frac{1}{2}\kappa\omega_0^2(e_2 - e_1), \tag{C.13}$$

$$\frac{\partial^2 e_2}{\partial t^2} + \omega_0^2 e_2 = -\frac{1}{2}\kappa\omega_0^2(e_2 - e_1), \tag{C.14}$$

and the second line follows from the first, by symmetry. The coupling constant is

$$\kappa = \frac{4}{3\pi}\frac{a^3}{LR^2}\frac{1}{J_1^2(j_{01})} \approx 1.57\frac{a^3}{LR^2}. \qquad \text{(C.15)}$$

In retrospect it should be clear that the simpler, and intuitive derivation in Sec. 3, did no great injustice to this calculation, merely failing to produce an explicit result for κ.

C.4 Perturbation by Connecting Guide

To compute the coupling of a cavity to a waveguide, one again has a port-integral to compute. However, in this case it is convenient to let our unperturbed modal basis refer to the solution of the Helmholtz equation, with *open-circuit* boundary conditions at the port, and to designate the port surface, S_p, as a plane located in the smooth connecting guide. Since the waveguide modes form a complete set we may expand the electric field on S_p,

$$\tilde{E}_\perp(r_\perp) = \sum_a \tilde{E}_{\perp a}(r_\perp)V_a\ , \quad \tilde{H}_\perp(r_\perp) = \sum_a \tilde{H}_{\perp a}(r_\perp)Z_{ca}I_a\,. \qquad \text{(at port } S_p\text{)}$$

where the subscript $\perp$ denotes components lying in the transverse plane in the waveguide, *i.e.*, S_p. In a similar way we may expand the cavity modes,

$$\tilde{E}_{\perp\lambda}(r_\perp) = \sum_a \tilde{E}_{\perp a}(r_\perp)V_{a\lambda}\,, \qquad \tilde{H}_{\perp\lambda}(r_\perp) = \sum_a \tilde{H}_{\perp a}(r_\perp)Z_{ca}I_{a\lambda}\,,$$

where the mode coefficients are just the overlap integral of the unperturbed cavity fields with the waveguide mode,

$$I_{a\lambda} = Z_{ca}\int_{S_p} d^2\vec{r}_\perp \tilde{H}_\lambda(r_\perp)\bullet\tilde{H}_{\perp a}(r_\perp),\ V_{a\lambda} = \int_{S_p} d^2\vec{r}_\perp \tilde{E}_\lambda(r_\perp)\bullet\tilde{E}_{\perp a}(r_\perp).$$

Making use of the orthogonality of the waveguide modes we have then

$$\int_{S_p} d\vec{S}\bullet\tilde{E}\times\tilde{H}_\lambda = \int d^2\vec{r}_\perp\left\{\sum_a \tilde{E}_{\perp a}V_a\right\}\times\left\{\sum_b \tilde{H}_{\perp b}Z_{cb}I_{b\lambda}\right\} = \sum_a V_a I_{a\lambda}\,,$$

and similarly,

$$\int_{S_p} d\vec{S}\bullet\tilde{E}_\lambda\times\tilde{H} = \int d^2\vec{r}_\perp\left\{\sum_a \tilde{E}_{\perp a}V_{a\lambda}\right\}\times\left\{\sum_b \tilde{H}_{\perp b}Z_{cb}I_b\right\} = \sum_a V_{a\lambda}I_a.$$

Thus the mode equations take the form

$$j\varepsilon\omega\tilde{e}_\lambda = k_\lambda\tilde{h}_\lambda + \underbrace{\sum_a V_{a\lambda}I_a}_{\int_{S_p} d\vec{S}\bullet\tilde{E}_\lambda\times\tilde{H}}\ , \qquad -j\mu\omega\tilde{h}_\lambda = k_\lambda\tilde{e}_\lambda + \underbrace{\sum_a V_a I_{a\lambda}}_{\int_{S_p} d\vec{S}\bullet\tilde{E}\times\tilde{H}_\lambda} = k_\lambda\tilde{e}_\lambda,$$

and in the last equality we implemented the open-circuit boundary condition on the modal basis, $I_{a\lambda}$=0. Combining these two results, we obtain a single equation for

$\tilde{e}_\lambda$,

$$\left(\omega^2 - \omega_\lambda^2\right)\tilde{e}_\lambda = -j\omega\frac{1}{\varepsilon}\sum_a V_{a\lambda} I_a. \tag{C.16}$$

This should be augmented by one additional condition, continuity of transverse electric field at the port. The electric field at the port may be expressed in either basis,

$$\tilde{E}_\perp(r_\perp) = \sum_a \tilde{E}_{\perp a}(r_\perp) V_a \approx \sum_\lambda \tilde{E}_\lambda(r_\perp)\,\tilde{e}_\lambda,$$

and, taking the dot-product with a guide-mode, we have

$$V_a = \sum_\lambda V_{a\lambda}\,\tilde{e}_\lambda. \tag{C.17}$$

This relation closes the system of equations and permits one to solve self-consistently for the cavity fields and the forward and reverse signals in the waveguide. For example, we may compute the *impedance looking into the cavity*, from S_p, (*i.e.* in the direction in which we have taken positive current to flow)

$$Z_{11} = \frac{V_1}{I_1}.$$

Insofar as other modes are below cut-off we may solve approximately for the mode excitation in terms of the driving current in the fundamental mode,

$$\tilde{e}_\lambda = I_1 \frac{1}{\varepsilon\omega_\lambda}\frac{V_{1\lambda}}{j\left(\omega/\omega_\lambda - \omega_\lambda/\omega\right)}, \tag{C.18}$$

so that

$$V_1 = \sum_\lambda V_{1\lambda}\tilde{e}_\lambda = I_1 \sum_\lambda \frac{1}{\varepsilon\omega_\lambda}\frac{V_{1\lambda}^2}{j\left(\omega/\omega_\lambda - \omega_\lambda/\omega\right)}.$$

Next we define the *external Q*, $Q_{e\lambda}$, for mode λ coupling to the fundamental mode of the connecting guide,

$$\frac{1}{Q_{e\lambda}} = \frac{V_{1\lambda}^2}{\varepsilon\omega_\lambda Z_{c1}} = \frac{1}{\varepsilon\omega_\lambda Z_{c1}}\left(\int_{S_p} d^2\vec{r}_\perp \tilde{E}_\lambda \bullet \tilde{E}_{\perp 1}\right)^2, \tag{C.19}$$

in terms of which

$$Z_{11} = \frac{V_1}{I_1} = Z_{c1}\sum_\lambda \frac{1/Q_{e\lambda}}{j\left(\omega/\omega_\lambda - \omega_\lambda/\omega\right)}. \tag{C.20}$$

Notice that Z_{11} is large on-resonance, corresponding to an open circuit, just as we expect. Meanwhile, off-resonance, Z_{11} is small, corresponding to a short-circuit. This motivates the standard nomenclature for our choice of reference plane: the

plane of the detuned short.

To make contact with Eq. (3.12), let us define $V_F = nV_+$, $V_R = nV_-$, where *n* may be thought of as a *turns ratio*, transforming to an impedance $Z_c' = n^2 Z_{c1}$. Continuity of transverse electric field takes the form, $V_1^+ + V_1^- = V_{1\lambda}\tilde{e}_\lambda$, and this suggests defining a *cavity voltage*, $V_c = nV_{1\lambda}\tilde{e}_\lambda$, in terms of which continuity reads,

$V_c = V_F + V_R$.

The port current driving term may be expressed as, $Z_{c1}I_1 = V_1^+ - V_1^-$, and in the time domain our system takes the form

$$\left\{\frac{d^2}{dt^2} + \omega_\lambda^2\right\} e_\lambda = -\frac{1}{\varepsilon}\frac{d}{dt}\sum_a V_{a\lambda} I_a,$$

and in the transformed units,

$$\left\{\frac{d^2}{dt^2} + \omega_\lambda^2\right\} V_c = \frac{\omega_\lambda}{Q_e}\frac{d}{dt}\left(V_F - V_R\right). \tag{C.21}$$

These calculations and the results Eqs. (C.1)-(C.21) complete the formal analysis underpinning the coupled cavity model introduced in the text, having developed with some additional rigor the geometric origin of the coupled cavity circuit parameters: Q_w, κ, Q_e, n, $[R/Q]$. Historically, the formal treatment of a cavity in this way was first set down by Slater; however, there were a number of approximations in his approach that, for the pure mathematician are somewhat unsatisfying. The first complete treatment of the problem is credited, by Collin, to Kurokawa.[42] We have side-stepped the full mathematical complexity of the problem by electing to consider a single isolated, narrow-band cavity resonance. This is in fact not the totality of the problem as one can see by inspecting a measured cavity impedance. Such an impedance will indeed include narrow spikes corresponding to cavity resonances, but broadband portions as well. Thus there is a complementary problem of interest, calculation of *broadband impedance*. Such terms are important for a complete treatment of beam dynamics. They are not essential, however, for understanding the coupling of the accelerating mode, and its observational features, seen by means of couplers looking into the cavity.

There is one additional perturbation calculation that is sufficiently fundamental that it should be included, and that is Slater's theorem.

C.5 Perturbation to a Conducting Boundary (Slater's Theorem)

We consider the effect on a mode resonant frequency of indenting a cavity wall. Given the development of Sec. 1, it is most straightforward to proceed by employing two results: momentum conservation and adiabatic invariance.

We consider a lossless cavity that is ringing in one mode. Momentum conservation stipulates that if we slowly indent a cavity wall we must do work on the mode such that

$$\delta U = F^a \delta\xi_a = \int_S \left\langle T^{ab} \right\rangle dS_b \delta\xi_a,$$

where S is the region of wall being indented, F^a is the average force on the wall, $\left\langle T^{ab} \right\rangle$ is the time-averaged stress-tensor and $\delta\vec{\xi}$ is the wall displacement. Tangential wall displacements have no effect since they carry conductor into itself. Thus we may consider a displacement along the outward normal $\hat{n}$, $\delta\vec{\xi} = \hat{n}\delta\xi$, *i.e.*, $\delta\xi_a = n_a \delta\xi$. Noting that $dS_b = n_b dS$, we have simply

$$\delta U = \int_S \left\langle T^{nn} \right\rangle dS \delta\xi. \tag{C.22}$$

The diagonal element of the stress-tensor for the normal component at a conducting surface takes the simple form

$$T^{nn} = \frac{1}{2}\varepsilon_0 \vec{E}^2 - \frac{1}{2}\mu_0 \vec{H}^2,$$

and is just the electromagnetic pressure on the wall. Next we employ a mode expansion in the exact modal basis for the conducting boundaries as they are at time *t*,

$$\vec{E} = e_\lambda(t)\vec{E}_\lambda(\vec{r}),\ \vec{H} = h_\lambda(t)\vec{H}_\lambda(\vec{r}).$$

Recognizing that the mode resonant frequency may be changing in time, we choose to express the mode amplitude in terms of the cavity phase,

$$\theta(t) = \int^t dt' \omega_\lambda(t'),$$

according to

$$e_\lambda(t) = \Re\left\{\tilde{e}_\lambda(t)e^{j\theta}\right\}.$$

Maxwell's equations then take the form

$$\left\{\frac{d^2}{dt^2} + \omega_\lambda^2(t)\right\} e_\lambda(t) = 0,$$

and after some algebra this may be reduced to

$$\frac{d}{dt}\left\{\tilde{e}_\lambda(t)\sqrt{\omega_\lambda(t)}\right\} = 0,$$

in the limit of an adiabatically varying resonant frequency. Taking account of similar results for the magnetic field amplitude, and noting the expression for stored

energy,

$$U = \frac{1}{2}\int_V \left\{\mu_0 \vec{H}^2 + \varepsilon_0 \vec{E}^2\right\} dV = \int_V \left\langle \varepsilon_0 \vec{E}^2 \right\rangle dV = \frac{1}{2}\varepsilon_0 \left|\tilde{e}_\lambda(t)\right|^2$$

we find

$$\frac{\delta U}{U} = -\frac{\delta \omega_\lambda}{\omega_\lambda} \Leftrightarrow \delta\left(\frac{U}{\omega_\lambda}\right) = 0\,. \tag{C.23}$$

The adiabatic invariance of U/ω_λ ("photon number") together with momentum conservation permit us to solve for the increment in resonant frequency due to an indentation $\delta\xi$. We express the time-averaged stress on the wall as

$$\left\langle T^{nn} \right\rangle = \frac{1}{4}\varepsilon_0 \left|\tilde{e}_\lambda(t)\right|^2 \left(\vec{E}_\lambda^2 - \vec{H}_\lambda^2\right) = \frac{1}{2} U\left(\vec{E}_\lambda^2 - \vec{H}_\lambda^2\right),$$

to find

$$\frac{\delta \omega_\lambda}{\omega_\lambda} = -\frac{\delta U}{U} = -\frac{\int_S \left\langle T^{nn} \right\rangle dS}{U}\delta\xi = \frac{1}{2}\int_S \left(\vec{H}_\lambda^2 - \vec{E}_\lambda^2\right) dS\,\delta\xi\,. \tag{C.24}$$

We may integrate this formally to obtain Slater's theorem,

$$\omega_\lambda^2 = \omega_{\lambda 0}^2 \left(1 + \int_V \left(\tilde{H}_\lambda^2 - \tilde{E}_\lambda^2\right)\delta V\right), \tag{C.25}$$

for the perturbation to the resonant frequency of a mode due to an excluded volume *V*. In applying this result, it is good to keep in mind that the integration represented here employs mode profiles that vary with the surface displacement, $"\delta V" \equiv dS\,\delta\xi$.

Acknowledgments

These notes have benefited from previous US Particle Accelerator School and Stanford Applied Physics courses I have taught with Jonathan Wurtele, Alexander W. Chao, Perry B. Wilson, and Roger H. Miller. I am particularly indebted to Perry and Roger for introducing me to the subject of microwave accelerators. I have not attempted to identify in the notes their particular contributions since they are all-encompassing. The impetus for formalizing these notes came with the Japan-US-Europe Joint Accelerator School held in Shonan Village in September 1996, and was due to the encouragement of Perry Wilson, Mel Month, and Ted Wilson. These notes were then revised to accompany *Electron Linear Accelerators*, taught as Physics 412 in the US Particle Accelerator School held in Berkeley in January 1997. This was a large class consisting of some twenty students, graduate students and engineers. Many of the explanations, pictures and exercises in this version of the notes arose in connection with the numerous questions put to me during those intense two weeks, and for that I am indebted to the students. A special thanks to Steve Lidia who assisted with this course, and provided numerous helpful comments on the manuscript.

I would like to thank Prof. Shigenori Hiramatsu and Prof. Jun-ichi Kishiro of KEK for taking me into their group as a post-doc and later a staff-person, and introducing me to the practical matters of microwave work in the lab. I am indebted to Albert Menegat at SLAC for continuing this education in subsequent years. These notes owe much to helpful experiences I have had at the SLC and the help I have had over the years from the Klystron Department and Accelerator Maintenance RF. I thank Bill Gates for introducing me to Clarisworks.

Comments on these notes are appreciated and they can be directed to *whittum@slac.stanford.edu*.

References

[1] Edward L. Ginzton, "The $100 Idea: How Russell and Sigurd Varian, with the help of William Hansen and a $100 appropriation, invented the klystron", *IEEE Trans. Elec. Dev.* **ED-23** (1976) pp.714-723.

[2] E. L. Ginzton, W. W. Hansen, and W. R. Kennedy, "A Linear Electron Accelerator", *Rev. Sci. Instrum.* **19** (1948) pp. 89-108.

[3] M. Chodorow, E. L. Ginzton, W. W. Hansen, R. L. Kyhl, R. B. Neal, W. K. H. Panofsky and The Staff, "Stanford High-Energy Linear Electron Accelerator (Mark III)", *Rev. Sci. Instrum.* **26** (1955) pp. 134-204.

[4] *The Stanford Two-Mile Accelerator*, R.B. Neal, editor (W.A. Benjamin, New York, 1968).

[5] G. Caryotakis, "High Power Microwave Tubes: In the Laboratory and On-Line", *IEEE Transactions on Plasma Science* **22** (1994) pp. 683-691.

[6] Z. D. Farkas, H. A. Hogg, G. A. Loew and P. B. Wilson, "SLED: A Method of Doubling SLAC's Energy", *IX Internat'l Conference on High Energy Accelerators* (SLAC, 1974) p. 576.

[7] J. T. Seeman, "The Stanford Linear Collider", *Ann. Rev. Nucl. Part. Sci.* **41** (1991) pp. 389-428.

[8] R. B. Palmer, "Prospects for High Energy e+e- Linear Colliders", *Ann. Rev. Nucl. Part. Sci.* **40** (1990) pp.529-592.

[9] *International Linear Collider Technical Review Committee Report*, G. A. Loew and T. Weiland, eds. (July 1995) SLAC-R-95-471.

[10] Neil W. Ashcroft and N. David Mermin, *Solid State Physics* (Saunders College, Philadelphia, 1976).

[11] Alfred Price, *The History of US Electronic Warfare* (The Association of Old Crows, Westford, 1984).

[12] Merrill I. Skolnik, *Radar Applications* (IEEE Press, New York, 1988).

[13] The "WR" designation is the Electronics Industry Association (EIA) standard nomenclature.

[14] Regarding connectors, a few acronyms come up so frequently one might as well know what they mean. **APC-3.5** - Amphenol Precision Connector 3.5mm, employed into Ka Band (27-40GHz), **APC-7**-Amphenol Precision Connector 7.0mm, employed up to Ku Band, **SMA**-Sub-Miniature A - employed through Ku Band (12-18GHz), **Type N**- Navy Connector - through X-Band. The variety of connectors reflects more than just the frequency range. Type N was the predecessor for the APC series; APC connectors are intended to be used where repeated connection and disconnection will be made. SMA is normally used inside electronics boxes, or wherever a relatively static connection is intended.

[15] R. E. Collin, *Foundations for Microwave Engineering* (McGraw-Hill, Singapore, 1966).

[16] N. Marcuvitz, *Waveguide Handbook* (Boston Technical Publishers, Boston, 1964), MIT Radiation Laboratory Series.

[17] C. G. Montgomery, R. H. Dicke and E. M. Purcell, *Principles of Microwave Circuits* (McGraw-Hill, New York, 1948), MIT Radiation Laboratory Series.

[18] J.D. Jackson, *Classical Electrodynamics* (Wiley, New York, 1975).

[19] R. E. Collin, *Field Theory of Guided Waves* (IEEE Press, Piscataway, 1991).

[20] L.B. Felsen and N. Marcuvitz, *Radiation and Scattering of Waves* (IEEE Press, Piscataway, 1991).

[21] W. W. Hansen "A Type of Electrical Resonator" *J. Appl. Phys.* **9** (1938) pp. 654-663.

[22] M. Abramowitz and I. A. Stegun, *Handbook of Mathematical Functions* (Dover, New York, 1972).

[23] E. A. Knapp, "Design, Construction and Testing of RF Structures for a Proton Linear Accelerator", *IEEE Trans. Nucl. Sci.* **NS-12** (1965) pp. 118-127.

[24] D. E. Nagle, E. A. Knapp, and B. C. Knapp, "Coupled Resonator Model for Standing Wave Accelerator Tanks", *Rev. Sci. Instrum.* **38** (1967) pp. 1583 - 1587.
[25] W.H. Press, S. A. Teukolsky, W. T. Vetterling, and B. P. Flannery, *Numerical Recipes, The Art of Scientific Computing*, (Cambridge University Press, Cambridge, 1992).
[26] X. Xu, *et al.*, "RF Breakdown Studies in X-Band Klystron Cavities", *1997 Particle Accelerator Conference* (to be published).
[27] F. Villa and A. Luccio, "Test of a High-Gradient Low-Emittance Electron Gun", June 1996 (*Laser and Particle Beams*, to be published).
[28] A.E. Vlieks, *et al.*, "Breakdown Phenomena in High-Power Klystrons", SLAC-PUB-4546, presented at the *XIIIth International Symposium on Discharges and Electrical Insulation in Vacuum* (Paris, June, 1988); G. A. Loew and J. W. Wang, "RF Breakdown Studies in Room Temperature Electron Linac Structures", SLAC-PUB-4647, (ibid).
[29] D. Pritzkau, *et al.*, "Experimental Study of Pulsed Heating of Electromagnetic Cavities", *1997 Particle Accelerator Conference* (to be published).
[30] P.J. Chou, *et al.*, "Design and Fabrication of a Traveling-Wave Muffin-Tin Accelerating Structure at 91 GHz", *1997 Particle Accelerator Conference* (to be published).
[31] M. Seidel, *et al.*, "Microwave Analysis of the Damped Detuned Structure", *Proceedings of the XVIII International Linac Conference* (CERN, Geneva, to be published).
[32] S.M. Lidia, *et al.*, "W-Band Free Electron Lasers for High Gradient Structure Research", *1997 Particle Accelerator Conference* (to be published).
[33] I.S. Gradshteyn and I. M. Ryzhik, *Table of Integrals, Series and Products* (Academic Press, New York, 1980). N.B. there are known errors in these tables as of the 1980 edition.
[34] Charles K. Birdsall and A. Bruce Langdon, *Plasma Physics Via Computer Simulation* (McGraw-Hill, New York, 1985).
[35] The most recent as of this writing is Phys. Rev. D **54** (1996) pp. 7 -720. The Particle Data Group at Lawrence Berkeley Lab also publishes a pocket-size listing and helpful formularies. More information can be found at *http://pdg.lbl.gov*.
[36] R.H. Warring, *Understanding Electronics* (Tab Books, Blue Ridge Summit, 1989)
[37] S.E. Schwarz and W. G. Oldham, *Electrical Engineering* (Holt, Rinehart and Winston, New York, 1984).
[38] P. Horowitz and W. Hill, *The Art of Electronics* (Cambridge University Press, Cambridge, 1994).
[39] John H. Moore, Christopher C. Davis, and Michael A. Coplan, *Building Scientific Apparatus, A Practical Guide to Design and Construction* (Addison-Wesley, Reading, 1989).
[40] W.R. Leo, *Techniques for Nuclear and Particle Physics Experiments* (Springer-Verlag, Berlin, 1994).
[41] Frederick Seitz, "Research on silicon and germanium in World War II", *Physics Today*, January 1995, pp. 22-34.
[42] K. Kurokawa, "The expansions of electromagnetic fields in cavities", *IRE Trans. Microwave Theory Tech.*, vol. **MTT-6**, pp.178-187 (1958). See also, Kaneyuki Kurokawa, "My Personal Recollections of Microwaves", *IEEE MTT-S Newsletter* **145** (IEEE, Piscataway, 1997) pp. 57-69.